TRANSCRIPTIONAL CONTROL OF METABOLISM AND THE RESPONSE TO ISCHEMIA IN MUSCLE

THE UNIVERSITY OF OTTAWA

A DISSERTATION SUBMITTED TO
THE DEPARTMENT OF BIOCHEMISTRY
AND
THE FACULTY OF MEDICINE
IN CANDIDACY FOR THE DEGREE OF
DOCTOR OF PHILOSOPHY

COMMITTEE ON BIOCHEMISTRY (PROGRAMME OF HUMAN AND MOLECULAR GENETICS)

OTTAWA, ONTARIO
(Aug 10th, 2011)

To my beloved parents

Tien-Yin Teng and Chi Huang

and

to my utmost respectful brother

Richard C. H. Teng

ABSTRACT

Skeletal muscle is one of the largest tissues in humans and provides many pivotal functions to support life. Abnormality in skeletal muscle functions can lead to disease. For example, insulin resistance in skeletal muscle leads to type II diabetes. The underlying mechanisms that control energy balance in skeletal muscle remain largely elusive, especially at the genetic level. Here in the second chapter, I showed that MyoD mediated the transcriptional regulation of ACSL5, a mitochondrial protein, in C_2C_{12} myoblasts via two E-box elements. A SNP rs2419621 (T) created a *de novo* E-box that together with the two pre-existing proximal E-boxes strongly enhances ACSL5 expression in both CV1 and C_2C_{12} cells. In the third chapter, I identified a novel VGLL4-interacting protein IRF2BP2 and verified the interaction with co-immunoprecipitation and mammalian two-hybrid assays. Functionally, overexpression of IRF2BP2 and transcription factor TEAD1 activates mouse VEGF-A promoter in CV1 cells and enhances the biosynthesis of VEGF-A in C_2C_{12} myoblasts. *In vivo* studies showed that ischemia induced the expression of IRF2BP2 by more than three fold, suggesting that IRF2BP2 could play a pivotal role during tissue ischemia. IRF2BP2 is a nuclear protein in both mouse cardiac myocytes and C_2C_{12} myoblasts as demonstrated by immunohistochemistry and immunocytochemistry, respectively. Therefore, I sought to delineate the mechanism for the nuclear shuttling of IRF2BP2 in the fourth chapter. With various DNA alternations, I mapped the NLS to an evolutionarily conserved sequence ^{354}ARKRKPSP^{361} in IRF2BP2. Deletion of the positively charged amino acids resulted in the

abolishment of the NLS signal. Next, I showed that phosphorylation of serine 360 (S360) mediates the nuclear import of the protein. Whereas an alanine substitution (S360A) at the site resulted in perinuclear accumulation of the protein, an aspartic acid substitution (S360D) forced the nuclear accumulation. Nevertheless, the forced accumulation of the S360D mutant did not enhance the activation of VEGF-A promoter in CV1 cells as did the wild-type protein. My studies revealed two novel mechanisms by which skeletal muscle could harvest energy, thus providing new insight into the energy metabolism in skeletal muscle

ACKNOWLEDGMENTS

It is a pleasure to thank many people who made this thesis possible. It is difficult to overstate my gratitude to my Ph.D. supervisor, Dr. Alexandre F.R. Stewart. With his enthusiasm, inspiration, and great efforts to explain things concisely, he helped to make genetics and molecular biology fun for me. Throughout my Ph.D. training period, he provided encouragement, sound advice, good teaching, good company, and lots of good ideas. I would have been lost without him.

I would like to thank my thesis committee members who have taught me science:

Dr. Patrick Burgon, Dr. Ilona Skerjanc, and Dr. Alexandre Blais - for their kind assistance with writing letters, giving wise advice, helping with various applications, and so on. My special gratitude goes to Dr. Burgon for showing me different experimental techniques. Without him, a big part of this thesis would never have happened. I also wish to thank Dr. Hsiao-Huei Chen, Dr. Meng Fan, Dr. Nida Yap, and Dr. Sonny Dandona for their assistance in the preparation of manuscripts and this thesis.

I am indebted to my colleagues for providing a stimulating and fun environment in which to learn and grow. I am grateful to Lan Vo, Yanqing Wang, Tiffany Ho, Olivia Assogba, and Melanie Belanger at the John and Jennifer Cardiovascular Genetic Centre at the University of Ottawa Heart Institute (UOHI), and to Dr. Erik Suuronen and Drew Kuraitis at the Cardiovascular Tissue-engineering Department at UOHI, and Justin Caravaggio at the Vascular Biology Laboratory at UOHI. Their day-by-day technical supports made this thesis possible. I also wish to thank my best friends as graduate students, Naif Al-montashiri and Brian Cheng, for

helping me get through the difficult times, and for all the emotional support, camaraderie, entertainment, and caring they provided. I would also like to thank my entire extended facebook siblings (Asna Choundry, Cassie Roeske, Amy Martinuk, Seham Rabaa, Lara Kouri, Rumana Islam, Candice Shaw, Yuhao Shi, Bryan Marcus Raja) for providing a loving environment for me to rant and still embracing me.

My special thanks go to my soulmate Jessica Chan and her parents Willie Chan and Lilian Wong, who would never hesitate to care for me. Their emotional support is the best medication via this study.

Lastly, and most importantly, I wish to thank my family Tien-Yin Teng (dad) and Chi Huang (mum), and my dearest twin brother Richard Teng. They supported me, taught me, and loved me. To them I dedicate this thesis.

Table of Contents

LIST OF ORIGINAL COMMUNICATIONS

- Teng, A. C. T., Al-montashiri N.A.M., Cheng, B. L. M., Lou, P, Ozmizrak P, Chen, HH, and Stewart, A. F. R. (2011) *Identification of a Phosphorylation-dependent Nuclear Localization Motif in Interferon Regulatory Factor 2 Binding Protein 2*. PLoS ONE, 6(8), e24100.
- Teng, A.C.T., Kuraitis, D., Deeke, S.A., Ahmadi, A., Dugan, S.G., Cheng, B.L., Crowson, M.G., Burgon, P.G., Suuronen, E.J., Chen, H.H.*, et al.* (2010). *IRF2BP2 is a skeletal and cardiac muscle-enriched ischemia-inducible activator of VEGFA expression*. FASEB J *24*, 4825-4834.
- Teng, A.C., Adamo, K., Tesson, F., and Stewart, A.F. (2009). *Functional characterization of a promoter polymorphism that drives ACSL5 gene expression in skeletal muscle and associates with diet-induced weight loss.* FASEB J *23*, 1705-1709.

LIST OF ABBREVIATIONS

α 1 chain of type I collagen (Col1A1)

Activating protein-1 (AP-1)

Acyl-CoA synthetase long-chain (ACSL)

Adenomatous polyposis cell (APC)

Adenosine triphosphate (ATP)

Angiopoietin-2 (Ang2)

Apterous (Ap)

Atrial natriuretic peptide (ANP)

Basic fibroblast growth factor (bFGF)

Boundary enhancer (BE)

Brain natriurentic peptide (BNP)

Bromosulphophthalein (BSP)

Calcineurin 1 (RCAN1)

Calmodulin-dependent protein kinase II (CaMKII)

Casein kinase I (CKI)

Cardiac troponin T (cTNT)

Caudal type homeobox transcription factor 2 (Cdx2)

Chloramphenicol acetyltransferase (CAT)

CREB-binding protein (CBP)

Diacylglycerol (DAG)

Electromobility Shift Assays (EMSAs)

Enhanced-at-puberty 1 (EAP1)

E-twenty six (ETS)

Erythropoietin (Epo)

Extracellular signal-regulated kinase ½ (ERK1/2)

FAST kinase domain-containing protein 2 (FASTKD2)

Fatty acid binding proteins (FABPs)

Feed-forward (FF)

Fms-like kinase (Flk-1)

Fms-like tyrosine kinase (Flt-1)

Forkhead box M1 (FOXM1)

Forkhead box O1 (FOXO1)

Free fatty acids (FFAs)

Glucose-6-phosphatate (G6P)

Glucose transporter 4 protein (GLUT4)

Glycogen synthase kinase 3 (GSK3)

Green fluorescent protein (GFP)

GTP exchange factor (GEF)

Guanosine-5'-diphosphate (GDP)

Guanosine-5'-triphosphate (GTP)

High-density lipoproteins (HDLs)

Histone deacetylase (HDAC4)

Human umbilical vein endothelial cells (HUVEC)

Hydrogen peroxide (H_2O_2)

Hypoxia-inducible factor-1a (HIF-1α)

Hypoxia responsive element (HRE)

Insulin receptor substrate-1 (IRS-1)

Interferon regulatory factor 2 (IRF2)

Interferon Regulatory Factor 2 Binding Protein 2 (IRF2BP2)

Intermediate-density lipoproteins (IDLs)

Large T-antigen (T-ag)

Low-density lipoproteins (LDLs)

Low-density lipoprotein receptor-related protein 6 (LRP6)

Lysosome associated membrane protein (LAMP)

Magnetic resonance imaging (MRI)

microRNA-20b (miRNA-20b)

microRNA 23 (miR-23)

Myc-associated factor X (MAX)

Myosin heavy chain (MHC)

Myosin heavy chain-α (α-MyHC)

Myosin heavy chain-β (β-MyHC)

Myogenic enhancer factor 2 (MEF2)

Myogenic regulatory factors (MRFs)

Nicotinamide adenine dinucleotide (NAD^+)

Nuclear factor of activated T-cell (NFAT)

Nuclear localization signal (NLS)

Nuclear pore complexes (NPCs)

Nuclear receptor interacting factor 3 (NRIF3)

Oligodeoxynucleotides (ODNs)

Oxygen-dependent degradation domain (ODDD)

Per-Arnt-Sim (PAS)

Peroxiredoxin 3 (PRDX3)

Phosphatase-1b (PP1b)

Phosphatidylinositol 3-kinase (PI3K)

Platelet endothelial cell adhesion molecule-1 (PECAM-1)

Platelet-derived growth factor (PDGF)

Poly (ADP-ribose) polymerase-1 (PARP-1)

Peroxisome proliferator-activated receptor g coactivator-1α (PGC-1a)

Prolyl-4-hydroxylases (PHD)

Protein kinase A (PKA)

Protein kinase B (PKB)

Protein kinase C (PKC)

Protein kinase G (PKG)

Proprotein convertase subtilisin/kexin type 9 serine protease (PCSK9)

Quandrant enhancer (QE)

Ras-related protein 11 (Rab11)

Ribosomal S6 Kinase (RSK)

Receptor-specific enzyme-linked immunosorbent assays (ELISA)

Scalloped (Sd)

Serum response factor (SRF)

Signal transducer and activator of transcription factors (STATs)

Silent mating type information regulation (SIRT1)

Simian virus-40 (SV40)

Single nucleotide polymorphism (SNP)

Solute carrier family 2, member 4 (SLC2A4)

STAT-response element (SRE)

TATA-box binding protein (TBP)

TEA/ATTS-domain transcription factor (TEAD)

Tondu (Tdu)

TGF-β-induced factor homeobox 1 (TGIF1)

Transforming growth factor-β (TGF-β)

Transcription factor specificity protein 1 (Sp1)

Transverse aortic constriction (TAC)

Triacylglycerol (TAG)

Tumor necrosis factor-α (TNF-α)

Type II diabetes mellitus (T2DM)

Untranslated region (UTR)

Vascular endothelial-cadherin (VE-Cad)

Vascular endothelial growth factor-A (VEGF-A)

Vascular permeability factor (VPF)

VEGF receptor-1 (VEGFR-1)

VEGF receptor-2 (VEGFR-2)

Wingless (Wg)

World Health Organization (WHO)

Yes-associated protein 65 (YAP65)

Vestigial (Vg)

Vestigial-like (VGLL)

VGLL4 interacting domain (VID)

Very low-density lipoproteins (VLDLs)

LIST OF FIGURES

CHAPTER2

CHAPTER 3

CHAPTER 4

CHAPTER 5

LIST OF TABLE

CHAPTER 1

INTRODUCTION

Skeletal muscle fiber isotypes and characters

Skeletal muscle is a physiologically dynamic organ in mammals. On average, it accounts for 38.4% and 30.6% of body mass in males and females above age 18, respectively, (Janssen *et al.*, 2000). The large amount of muscle provides more functions than merely the anatomical support to the body, including physical support, biological response, and metabolism. According to the predominant myosin heavy chain (MHC) isotypes defined by immunoblotting and immunofluorescence, skeletal muscle can be classified into four sub-types (type I, IIa, IIb, and IId/x) in rodents and into three sub-types in human (type I, IIa, and IId/x). Type I is a slow-twitch oxidative fiber that is enriched with oxidative proteins, mitochondria, and microvasculature (Termin *et al.*, 1989; Tsika *et al.*, 1987). Type IIa is a fast-twitch oxidative fiber that has similar physiological and biochemical profiles as the type I fiber (Eddinger *et al.*, 1986; Eddinger and Moss, 1987; Eddinger *et al.*, 1985a, b). In comparison, type IId/x is a fast-twitch glycolytic fiber (high enzymatic activities for metabolism) and is poor in mitochondrial and capillary numbers (Prince *et al.*, 1981). Finally, type IIb is also a fast-twitch glycolytic fiber that has an even faster metabolic rate than type IId/x isotype.

The advent of genetically modified animals and molecular biology techniques continue to help demonstrating that exercise improves the reaction of skeletal muscles to external stimuli, such as insulin and weight resistance (Kahn *et al*., 2006). For instance, mice that had undergone endurance exercise had a significant increase in type IIa to type IId/x ratio, signaling an adaptation to higher oxygen demand within

fast-twitch muscles (Fitzsimons *et al.*, 1990). In contrast, the number of type I fiber in these animals remains unchanged. A study by Chin *et al.* first characterizes the underlying mechanism for such transformation between muscle fiber isotypes (Chin *et al.*, 1998). In addition, they show that a physical stretch of muscle fibers via prolonged exercise is able to enhance the intracellular calcium ion concentration that subsequently activated a calcineurin-dependent pathway. Calcineurin is a serine/threonine-specific phosphatase that, when activated, promotes downstream protein activity, including nuclear factor of activated T-cell (NFAT) in skeletal muscle. Activated NFAT heterodimerizes with myogenic enhancer factor 2 (MEF2) to activate the expression of type IIa MHC in skeletal muscle. Inhibition of the calcineurin-dependent pathway by cyclosporine reverses the process during myogenic differentiation (Chin *et al.*, 1998). Consistent with this observation, ectopic expression of regulator of calcineurin 1 (RCAN1) specifically in skeletal muscle in mice leads to a decrease in type I fibers in soleus muscle (Oh *et al.*, 2005). A similar observation that the calcineurin signaling pathway affects the development of muscle fiber isotypes is made in the transgenic mice whose calcineurin gene is deleted in skeletal muscle (Parsons *et al.*, 2004). Hence, NFAT plays an important role in the regulation of muscle fiber isotypes.

Another molecule that is also affected by the calcium concentration/calcineurine pathway is peroxisome proliferator-activated receptor γ coactivator-1α (PGC-1α). PGC-1α plays a critical role in mediating muscle fiber isotypes. Muscle-specific ectopic expression of PGC-1α leads to increases in both type I fibers and mitochondria in transgenic animals, while muscle-specific deletion of the gene show a reduction in type IIa fibers in tibialis and an increase in MHC IIb in soleus (Calvo *et al.*, 2008; Handschin *et al.*, 2007; Lin *et al.*, 2002). A recent study

shows that microRNA 23 (miR-23), which attenuates PGC-1α expression in a physiologically normal state, is downregulated in the skeletal muscle of animals that undertakes endurance exercise (Safdar *et al.*, 2009). However, the underlying mechanisms on the PGC-1α-mediated growth of oxidative muscles remain largely elusive and require further investigation.

The ability of skeletal muscle to metabolize different substrates as energy source is not only important to its survival, but is also critical for physiological homeostasis in a living organism. The energy source for skeletal muscle includes glucose, amino acids, and fatty acids. The metabolism within oxidative skeletal muscle largely utilizes fatty acids (triglycerides and phospholipids) as the source of energy. Studies of the type II diabetes mellitus (T2DM) patients in the past half-century have begun to shed light on the underlying etiopathology of the disease. In 1963, Randle *et al.* reported that various tissues that had been incubated in fatty acids had elevated intracellular concentrations of glucose-6-phosphatate (G6P) and glycogen, and a higher NADPH to $NADP^+$ ratio (Randle *et al.*, 1963). The findings amount to the hypothesis that the intake of excessive fatty acids could impair or impede glycolysis in muscle cells. However, *in vivo* studies show the opposite: the use of magnetic resonance imaging (MRI), coupled with ^{13}C-radioactive isotopes, reveals declines in the intracellular G6P and glycogen concentrations in human muscle (Dresner *et al.*, 1999). The discrepancy between two results might well be due to the differences in the tested systems. Nevertheless, the human genome project and ongoing genetic research will help to elucidate both the physiological and cellular mechanisms involved in energy partitioning.

Fatty acid metabolism, obesity, and T2DM

The survival of non-photoautotrophic living organisms depends exclusively on exogenous energy supplies (Bu and Mashek, 2010). Of all types of external energy, triacylglycerol (also known as triglyceride) harbours the highest amount of useful energy per entity to most mammals. The energy harnessed from these macromolecules is used by cells, such as cardiac and slow-twitch skeletal muscles, as an energy source or for maintaining the body temperature (thermostasis) in mammals. However, some metabolites from fatty acid oxidation are cytotoxic and genotoxic at the cellular level (Son *et al*., 2010). Accumulated side effects could amount to detrimental disease, such as T2DM and cancer (Deblon *et al.*, 2011; Nieman *et al.*, 2011). Thus, a comprehensive understanding in fatty acid metabolism is crucial for developing prophylactic treatments in individuals.

Skeletal muscle is one of the largest organs in mammals and oxidative skeletal muscle utilizes fatty acid as a main energy source for maintenance and survival. An early study by Randle *et al.* observe that free non-esterified fatty acid in plasma is statistically significantly associated with insulin-resistance in patients (Randle *et al.*, 1963). They therefore hypothesize that high plasma fatty acids may impair the insulin-mediated signaling pathways. With the use of ^{13}C-radioactive material and non-invasive magnetic resonance imaging (MRI), high plasma fatty acid is associated with both the accumulation of intracellular glucose-6-phosphate (G6P) and the reductions in both glucose uptake and glycogen synthesis in muscle in youth whose first-degree relatives were diabetic (Rothman *et al.*, 1995; Rothman *et al.*, 1992; Shulman *et al.*, 1990). To test this hypothesis, Roden and colleagues raise the plasma fatty acid level by infusing non-esterified fatty acid in healthy volunteers and observe a reduction in intracellular G6P level in skeletal myotubes and fast clearance of the infused fatty

acid. The contradicting results imply a protective mechanism that detect and then swiftly metabolize plasma fatty acid within a three-hour duration (Roden *et al.*, 1996). To discern the impact of plasma fatty acid on glucose uptake in skeletal muscle, two independent groups compare and contrast the rate of glucose metabolism in both healthy subjects and diabetic patients (Cline *et al.*, 1999; Dresner *et al.*, 1999). Their studies show that, while healthy individuals exhibit similar metabolic activities like those reported by Roden *et al.*, diabetic patients suffer from a reduction in glucose intake (as suggested by radioactive glucose analogues) rather than a hampered metabolism (as suggest by normal hexokinase activities). Roden's findings eventually lead to the discovery of glucose transporter 4 protein (GLUT4) that is important for glucose intake in skeletal muscle and adipocytes in response to insulin stimulation.

GLUT4 is also known as solute carrier family 2, member 4 (SLC2A4) and belongs to a family of thirteen members. It is first cloned from a mouse skeletal muscle library and northern blot analyses showed that GLUT4 transcript was in large abundance in heart, skeletal muscle, and adipocytes (Birnbaum, 1989). The human homolog is later cloned from a muscle biopsy (Bell *et al.*, 1990). The presence of GLUT4 level is inversely correlated with blood glucose concentration in non-diabetic mammals. Overexpression of GLUT4 in mice accelerated the rate of blood glucose clearance by one fold, while this process can increase by four-fold after exercise. In contrast, the rate of blood glucose clearance in wild type counterparts increases by merely 0.5-fold after exercise (Ikemoto *et al.*, 1995). In diabetic patients, the trafficking of GLUT4 to sarcolemma is impaired. A study by Garvey *et al.* shows a 2.8-fold increase of GLUT4 protein level in sarcolemma in healthy individuals after food consumption. Diabetic patients, on the other hand, show a substantial reduction

in sarcolemma GLUT4 protein level, signaling that glucose intake in skeletal muscle is dictated by the amount of GLUT4 (Garvey *et al.*, 1998).

In the past twenty years, the use of both molecular biology techniques and pharmacological analogues starts to shed some light on how GLUT4 is trafficked to the sarcolemma of skeletal myotubes under insulin stimulation. Generally, insulin secreted from the β-islet cells of pancreas physically binds and activates an insulin receptor that subsequently tryrosyl phosphorylates its intracellular domain. This self-modification incurs the recruitment and activation of insulin receptor substrate-1 (IRS-1), a docking protein for activating phosphatidylinositol 3-kinase (PI3K). To facilitate the transportation of GLUT4 to sarcolemma, activated PI3K physically interacts with GLUT4 in vesicles in cytoplasm (Frevert *et al.*, 1998). Therefore, disruptions at any step within the signaling cascade could reduce or completely abolish trafficking of GLUT4 in cells. This is best exemplified by the high level of diacylglycerol (DAG) in diabetic patients (Itani *et al.*, 2002) and animals (Kim *et al.*, 2004). DAG is composed of two acyl chains and a glycerol. When present in large quantity, DAG functions as ligand for protein kinase C (PKC), specifically the homologs of PKCβ, PKCδ (Griffin *et al.*, 1999), and PKCθ (Itani *et al.*, 2002). *In vitro* studies show that DAG-activated PKC phosphorylated IRS-1 at serine-307 (S307), leading to the reduction and the blockage of the tyrosine phosphorylation by insulin receptors (Aguirre *et al.*, 2002; Lewis *et al.*, 1990; Yu *et al.*, 2002). Similarly, phorbol ester-induced PKC activation also show an increase in S307 phosphorylation and an enhanced cellular resistance to insulin stimulation (Takayama *et al.*, 1988). In contrast, mice that harbour a S307A mutation in IRS-1 transgene are able to resist the DAG-induced insulin resistance in skeletal muscles (Kim *et al.*, 2004). In summary, insulin resistance in skeletal muscle is attributed to the increase of intracellular DAG

concentration and the impairment of IRS-1 tyrosine phosphorylation due to the phosphorylated S307 residue.

Fatty acid import

An inadequate uptake of excessive amounts of exogenous fatty acids in skeletal muscle has been associated with insulin resistance in humans (for a detailed review, please refer to (Samuel *et al.*, 2010)). As suggested by its name, triacylglycerol is composed of a glycerol and three acyl (long carbon) side chains. The source of triacylglycerol can be both endogenous and exogenous. While endogenous triacylglycerol is synthesized by hepatocytes, exogenous ones must come from food intake. In the past century, our understanding in fatty metabolism in organs, especially the liver, heart, and skeletal muscle, has increased drastically (for a detailed review, please refer to (Greenberg *et al.*, 2011)). Briefly, during gastrointestinal digestion in human, triacylglycerol is first chemically broken into monoacylglycerol and two free fatty acids (FFAs) by lingual and pancreatic lipases. These constituents are then reabsorbed by jejunal and ileal enterocytes and, together with cholesterol, lipid-soluble vitamins, and apolipoproteins, are assembled into chylomicrons prior to being delivered to the liver. In the liver, these chylomicros are reorganized into low-density lipoproteins (LDLs) in order to be shipped to tissues via water-based circulation. A different approach is taken by the triacylglycerol stored in adipocytes. Here, monoglycerol and FFAs are generated by hormone-sensitive lipase or adipose tissue triacylglycerol lipase. The FFAs are next packed with albumin proteins to avoid the hydrophilic circulatory condition and wait to be transported to different tissues

One protein family involved in active FFA transportation is the plasma membrane fatty acid binding proteins (FABPs) that are located at the outer leaflet of

cell membrane. FABPs are generally 14-16 kDa in size and different isoforms are identified in various tissues, including liver (Ockner *et al.*, 1979), large intestine (Levy *et al.*, 2009), brain (Bass *et al.*, 1984; Wunderlich *et al.*, 2005), heart (Bagheri *et al.*, 2010), and skeletal muscle (Claffey *et al.*, 1987). Early studies show that the quantity and functions of FABPs vary in genders and in different species. For example, the concentration of FABP per milligram of cytosolic protein was 44% greater in female liver extract than the male liver extract (Ockner *et al.*, 1979). Also, Kawashima *et al.* compared the binding affinity of liver FABPs to substrates, including oleic acid, palmitoyl-CoA, and bromosulphophthalein (BSP) – in mouse, rat, and guinea pig and found that rat FABP had a high binding affinity to all substrates. Mouse homologs, in comparison, has high affinity to oleic acid and palmitoyl-CoA, but only a third of affinity to BSP. The FABP in guinea pigs has a strong affinity to BSP, but a lower association to oleic acid and palmitoyl-CoA. In addition, FABPs from various tissues have different known functions as well. While liver-specific form of FABP is involved in fatty acid metabolism, Gerstner *et al.* show that the overexpression of brain FABP leads to a reduction in sleep time at night and an improvement in long-term memory in *D. melanogaster* (Gerstner *et al.*, 2011).

Besides FABPs, Acyl-CoA synthetase long-chain (ACSL) proteins are also involved in FFA transfer across mitochondrial membrane. As its name suggests, ACSL is responsible for catalyzing the ligation of coenzyme A and an acyl molecule at the expense of adenosine triphosphate (ATP). The newly synthesized acyl-CoA then is imported to cellular compartments for either storage or metabolism. Hence, ACSL is critical for supplying carbon sources to living cells. Many ACSL proteins have been identified in plants (Macey and Stumpf, 1968), prokaryotes (Lennarz, 1963), yeast (Knoll *et al.*, 1995), and eukaryotes (Fujino and Yamamoto, 1992;

Marcel and Suzue, 1972; Muoio *et al.*, 2000; Suzuki *et al.*, 1990; Van Horn *et al.*, 2005). The great distribution of ACSL homologs across the biology kingdom and their roles in fatty acid import imply that the proteins are important for the homeostasis of energy in species. With many studies carried out in prokaryotes or yeasts, our knowledge about the role of these proteins has advanced eminently. For example, the only ACSL structure that has ever been solved is a prokaryotic protein (Gulick *et al.*, 2003). A genetic mutation in ACSL-like gene in *Candida lipolytica* prevented the incorporation of exogenous FFA into triacylglycerol (TAG) (Kamiryo *et al.*, 1979). In yeast *S. cerevisiae*, the lethal repercussion resulted from the loss of four ACSL-like genes could be rescued by the complementation of mouse ACSL proteins (Knoll *et al.*, 1995).

There are five known ACSL homologs (ACSL1~5) in mammals and, according to the sequences and functional motifs, they can be further divided into two sub-families; ACSL1, 2, and 5 comprise one family while ACSL3 and 4 in the other. ACSL1 is present in large abundance in the organelles of microsomes in livers, heart, and adipose tissue (Muoio *et al.*, 2000). Its mRNA level significantly increases in rat livers when animals are fed with high fat or glucose diets (Suzuki *et al.*, 1990). ACSL2 is cloned from human brain extract (Abe *et al.*, 1992). A further study by Fujino *et al.* showed that rat ACSL2 transcript was equally distributed in cereberum, cerebellum, and brain stem (Fujino and Yamamoto, 1992). Bioinformatics show that ACSL1 and 2 have a high degree of peptide similarity, including two luciferase-like motifs joined by a linker region (Iijima *et al.*, 1996). Though there is great similarity in structures and the expressions in overlapping tissues, they differ in their preferences to substrates. While ACSL1 prefers palmitoleate, oleate, and linoleate, ACSL2 binds with oleate, eicosapentaenoate, and decosahexaenoate at a higher affinity *in vitro*

(Iijima *et al*., 1996). Also cloned from brain tissue, ACSL3 had the highest affinity to laurate and myristate among C_8-C_{22} saturated fatty acids, and arachidonate and eicosapentaenoate among unsaturated fatty acids. The mRNA level of ACSL3 is also detected in a lesser extent in lung, adrenal gland, kidneys, and small intestine. Interestingly, its expression increased until day 15 in the brain mouse neonates, but declined by 90% in adult brain (Fujino and Yamamoto, 1992). ACSL4 was initially identified and cloned by Kang *et al.* as part of an effort to clone ACSL3 from a rat liver library. It had the highest expression in adrenal gland and a weaker expression in ovary and testis (Kang *et al*., 1997). ACSL4 had a high affinity toward arachidonate and eicosapentaenoate, but low affinity toward palmitate (Kang *et al.*, 1997). Oikawa cloned ACSL5 from rat intestinal epithelial cells. Subsequent investigations show that ACSL5 has a greater affinity to unsaturated fatty acids and its mRNA level increases significantly in rat liver in response to fasting (Oikawa *et al.*, 1998). Similar observation was reported to show that the expression of hepatic ACSL5 is induced in rats that undertake 48 hours of fasting (Lewin *et al.*, 2001). To briefly consolidate these studies, ACSL homologs are distributed in various tissues and have different affinities to saturated and unsaturated fatty acids, suggesting that the presence of different homologs in one tissue may help to maximize energy intake. In addition, different homologs could be involved in activating different pathways for storage or metabolism.

Ischemia, Hypoxia-inducible factor-1a, and vascular endothelial growth factor

Growth and maintenance of skeletal muscle require a constant blood supply. During ischemia - a condition characterized by the deprivation of blood supply in tissues - low intracellular oxygen concentration helps to stabilize newly synthesized

hypoxia-inducible factor-1α (HIF-1α) proteins. HIF-1α is a transcription factor that is initially identified by Semenza *et al.* as a regulator for the expression of human erythropoietin in response to hypoxia in livers (Semenza *et al.*, 1991). Structurally, HIF-1α is comprised of a basic helix-loop-helix DNA-interacting domain, an oxygen-dependent degradation domain (ODDD), and a transcription activation domain (Kallio *et al.*, 1999; Wang *et al.*, 1995). The ODDD is composed of about 200 amino acids and is enriched with proline residues. In the normoxic state, these proline residues are hydroxylated by a family of prolyl-4-hydroxylases (PHD) at the expense of intracellular oxygen, therefore signaling for a proteasome-dependent degradation (Lee *et al.*, 2008). Conversely, a low intracellular oxygen concentration spares HIF-1α from being hydroxylated and, subsequently, avoiding protein degradation. In parallel with the accumulation of the peptides, HIF-1α transcript levels also increase in response to ischemia (Bergeron *et al.*, 2000). The newly synthesized HIF-1α heterodimerizes with HIF-1β in the nucleus and transactivates downstream effectors that have the hypoxia responsive element (HRE; 5'-RCGTG-3') in their promoters. Some of these targeted genes include erythropoietin (Epo) (Wang *et al.*, 1995; Wang and Semenza, 1993), VEGF-A (Liu *et al.*, 1995), basic fibroblast growth factor (bFGF) (Calvani *et al.*, 2006), and platelet-derived growth factor (PDGF) (Yamakawa *et al.*, 2003). In a recent study by Mole *et al.*, accumulation of HIF-1α in hypoxic human MCF-7 breast cancer cells promotes the expression of many proteins, of which angiogenic factors were only a small fraction. Instead, transcription factors are the biggest group of downstream target proteins, including signal transducer and activator of transcription factors (STATs), E-twenty six (ETS), and Myc (Mole *et al*., 2009). Also, HIF-1α is involved in glycolysis, oxidoreductase activity, cytoskeleton, and

regulation of cell cycle. These studies collectively demonstrate that HIF-1α plays multifaceted roles in response to tissue ischemia *in vitro* and *in vivo*.

Of all HIF-1α downstream effectors, VEGF is inarguably the most potent factor for initiating blood perfusion (Levy et al., 1995). Inadequate expression of VEGF proteins in tissues could lead to perfusion-related disease, such as retinopathy (Awata *et al.*, 2002). VEGF is also known as vascular permeability factor (VPF) that increases microvascular permeability. The functional form of the protein is a 46 kDa disulfide-linked homodimer (Ferrara and Henzel, 1989). Both homozygous and heterozygous knockouts of VEGF are embryonically lethal in mice (Carmeliet *et al.,* 1996). Immunohistochemistry analyses show the incomplete development of a cardiovascular system in the animals, suggesting the precise expression of VEGF is needed for the process. Hitherto, several splicing isoforms of this gene have been identified in human and they encode for peptides with sizes of 121, 165, 189, or 206 amino acids (for detailed review, please refer to (Carmeliet, 2003, 2005; Carmeliet and Collen, 1999; Carmeliet and Jain, 2000, 2011)). These isoforms differ by the number of heparan sulfate sites that are required to anchor insoluble VEGF to cell surface. When activated, plasminogen cleaves off and releases VEGF into the circulatory system (Houck *et al.*, 1992). VEGF is a functionally multifaceted peptide and activations of different downstream program are likely dependent on the various combinations of cell surface receptors that it activates. VEGF receptor-1 (VEGFR-1; also known as Fms-like tyrosine kinase [Flt-1]) and receptor-2 (VEGFR-2; also known as Fms-like kinase [Flk-1]) are almost expressed exclusively in endothelial cells (Carmeliet and Jain, 2011). Activation of these two receptors guides endothelial cells to the site of tissue ischemia in an incremental ascending manner prior to angiogenesis. Nevertheless, the two receptors have different functions in endothelial

cells. Taking the approaches of site-directed mutageneses and receptor-specific enzyme-linked immunosorbent (ELISA) assays, Keyt *et al.* identified the peptide sequences in VEGFR-1 and VEGFR-2 for binding the human VEGF165 isoform (Keyt *et al.*, 1996). While the negatively charged amino acids 63-67 in VEGF are required for binding VEGFR-1, the positively charged amino acids 82-86 are needed for binding VEGFR-2. Mutations of these positive residues abolish protein interactions and, therefore, the treated human endothelial cells experience a 60% reduction in proliferation when compared to their counterpart. Consistently, VEGFR-2 knockout mice show no endothelial cell differentiation while VEGFR-1 knockout mice show only blood vessels are severely impaired (Fong *et al.*, 1995; Shalaby *et al.*, 1995). Interestingly, an increase in VEGFR-2 protein level is detected in the transgenic mice that harbour a cardiac-specific overexpression of VEGF and angiopoietin-2 (Ang2). These transgenic mice develop a significant level (about 50% more) of cardiac capillary, as depicted by the immunostaining of platelet endothelial cell adhesion molecule-1 (PECAM-1), but suffer from cardiac edema and fibrosis (Visconti *et al.*, 2002). These independent studies collectively and categorically underline the importance of VEGF receptors in various developmental stages of angiogenesis and vasculogenesis in mammals.

Of all VEGF isoforms, VEGF189 is the least characterized splicing isoforms. This isoforms is found in many cancer tissues, but its role in carcinogenesis remains elusive. Recently, Yuan *et al.* showed that an increase in VEGF189 protein level is correlated with an increase in vessel density and a decline in the number of blood vessel in mouse brain tumors (Yuan *et al.*, 2011). During pregnancy, mouse stromal cells that are treated with both estradiol and progesterone induce VEGF189 expression. Similarly, *In situ* hybridization showed that female decidual cells

expressed VEGF189 at the luteal phase of pregnancy in order to promote the capillary permeability of nearby blood vessels (Ancelin *et al.*, 2002).

Other transcription regulation of VEGF expression

STAT3

As an interacting partner of HIF-1α, STAT3 is also involved in many aspects of cell physiology, including oxygen imbalance (Cascio *et al.*, 2010; Cascio *et al.*, 2009; Gray *et al.*, 2005; Jung *et al.*, 2005; Santra *et al.*, 2008; Xu *et al.*, 2005). In general, STAT3 activation requires phosphorylation at tyrosine 705 by receptor-associated tyrosine kinases, whose activities are first initiated by growth factors, including interferons (Jablonska *et al.*, 2010), epidermal growth factor (Kim *et al.*, 2010), interleukin-6 (Zhong *et al.*, 1994), hepatocyte growth factor (Schroder *et al.*, 2010), and leptin (Sierra-Honigmann *et al.*, 1998). Once activated, STAT3 homodimerize or heterodimerize with other paralogs before translocating into the nucleus to galvanize the expressions of targeted genes. Alternatively, STAT3 could be activated via phosphatidylinositol-3-kinase (PI3K)/ATK pathway. Cascio *et al.* showed that the PI3K/ATK-dependent STAT3 activation could render antagonists against epidermal growth factor ineffective in colorectal cancer patients (Cascio *et al.*, 2009).

In the nucleus, STAT3 dimers physically bind to STAT-response element (SRE) in the promoter of VEGF. In a synergistic action with HIF-1α and CREB-binding protein (CBP)/p300, STAT3 transcription complex transactivates VEGF expression (Gray *et al.*, 2005). Here, the presence of both STAT3 and HIF-1α is essential for VEGF expression; ectopic expression of dominantly negative form of either protein substantially reduces the VEGF promoter activity during hypoxia. This

observation has led to different attempts to reduce VEGF levels in cancer cells. For example, the use of guggulsterone, a plant sterol, to block STAT3 functions results in oncogenic apoptosis in human umbilical vein endothelial cells (HUVEC) (Kim *et al.*, 2008). Similarly, microRNA-20b (miRNA-20b) could effectively lower the transcripts of both HIF-1α and STAT3, and hence a reduction in a total VEGF output in MCF-7 breast cancer cells (Cascio *et al.*, 2010).

Transcription factor specificity protein 1 (Sp1)

Present in the promoter and the 5'-untranslated region (5'-UTR) of *vegf* is a stretch of GC/GT-enriched sequences that coincide with the recognition sequence for Sp1. Early works by Dynan and Tjian showed that simian virus-40 (SV40) genomic DNA was indiscriminately activated by an unknown factor for viral manifestation (Dynan and Tjian, 1983). In 1987, the same group cloned the full-length cDNA of the molecule and designated it Sp1 (Kadonaga *et al.*, 1987). The full-length protein is composed of 696 amino acids and structurally contains a DNA-interacting domain of three C_2H_2-prototypic zinc fingers. Physiologically and pathologically, Sp1 is the first line responder to extra-cellular stimuli. For example, Sp1 is involved in cell growth (Santiago *et al.*, 2007), cell differentiation and tissue maturation (Shen *et al.*, 2009; Zhang *et al.*, 2010), apoptosis (Deniaud *et al.*, 2006), and angiogenesis (Hamanaka *et al.*, 1992).

An early finding reveals that treating human omental microvascular endothelial cells with tumor necrosis factor-α (TNF- α) induced the expression of both low density lipoprotein and Sp1 (Hamanaka *et al.*, 1992). A similar observation is recapitulated when human glioma cells were substituted (Ryuto *et al.*, 1996). In addition, both the mRNA and protein levels of VEGF increase in response to TNF-α

treatments. The use of electromobility shift assays (EMSAs) and the human VEGF promoter-driven chloramphenicol acetyltransferase (CAT) assays show that Sp1 physically interacts and directly acted on VEGF promoter in response to TNF-α treatment in a dosage-dependent manner. An independent study by Novak *et al.* also shows that the human melanoma inoculated with TNF-α enhanced VEGF expression. Applying Sp1 decoy oligodeoxynucleotides (ODNs) significantly mitigates the TNF-α effect (Novak *et al.*, 2003). Thus, Sp1 is likely to function in an alternative pathway to alleviate exterior or internal stress. This is consistent with the observation that Sp1 is activated via the Ras-Raf-MEK1-ERK1/2 pathway to transactivate VEGF promoter in response to oxidative stress – initiated by hydrogen peroxide (H_2O_2) – in human gastric adenocarcinoma (Schafer *et al.*, 2003).

TEA-domain 4 (TEAD4) transcription factor

TEAD4 is a homolog in the family of TEA/ATTS-domain (TEAD) transcription factor and is commonly known as TEF1-related protein (RTEF-1). Hitherto, three splicing isoforms of this gene have been identified (Appukuttan *et al.*, 2007; Farrance and Ordahl, 1996; Stewart *et al.*, 1996). Under a normal condition, TEAD4 is expressed in pancreas, skeletal muscle, and heart, but its level increases in hypoxic endothelial cells (Appukuttan *et al.*, 2007; Shie *et al.*, 2004). Targeted deletion of TEAD4 in mice is embryonically lethal, because it is critical for the formation of trophectoderm in preimplantation embryos as well as initiating the expression of caudal type homeobox transcription factor 2 (Cdx2) during implantation (Ralston *et al.*, 2010; Yagi *et al.*, 2007). Uses of other molecular biology techniques, however, showed that TEAD4 binds to and activates the MCAT (5'-CATTCCA/T-3') *cis*-regulatory element upstream of both mouse β-MyHC and skeletal muscle α-actin genes (Karasseva *et al.*, 2003). This transactivation is further pronounced by the use of

phenylephrine in rat neonatal cardiomyocytes (Ueyama *et al.*, 2000). Phenylephrine is an agonist to α-adrenergic receptors, whose activation leads to both phosphorylation of serine 322 on TEAD4 and, subsequently, protein activation (Ueyama *et al.*, 2000). This α-adrenergic receptor-dependent TEAD4 response in cardiac myocytes is excluded in TEAD1, the other TEAD protein also found in cardiomyocytes. To investigate the role of TEAD4 in heart, Chen *et al.* generated the transgenic mice, overexpressing TEAD4 under the control of human cardiac α-actin promoter. These animals experience an increase in protein phosphatase-1b (PP1b), dephosphorylations in protein connexin40 and connexin43, and, hence, arrhythmia (Chen *et al.*, 2004a).

When experiencing hypoxia, endothelial cells increase VEGF mRNA and protein levels by raising TEAD4 protein levels (Shie *et al.*, 2004). While EMSAs show that TEAD4 physically bind to the VEGF promoter, luciferase reporter assays show that TEAD4 transactivates the promoter in bovine aortic endothelial cells in a dosage-dependent manner. This promoter activity is further pronounced by hypoxia. A similar observation is reported in human retinal endothelial cells, where a smaller sized, but functionally more potent, TEAD4 splicing isoform (447 basepairs) is identified (Appukuttan *et al.*, 2007). In addition, an ectopic expression of TEAD4 in HUVECs promotes the formation of vascular network, implying TEAD4 is important for vascular development via VEGF (Shie *et al.*, 2004). A recent study reveals that TEAD4 is involved in modulating the expression of VEGF-B both *in vivo* and *in vitro* (Xu *et al.*, 2011). The transgenic mice that harbour vascular endothelial-cadherin (VE-Cad) promoter-driven human TEAD4 have significant increases in the protein levels of atrial natriuretic peptide (ANP), brain natriurentic peptide (BNP), β-myosin heavy chain (β-MyHC), and α-actin eight days post transverse aortic construction (TAC). TAC promotes pressure overload and cardiac hypertrophy in the heart. Similar results

are obtained in rat atrial cardiac myocytes (H9C2) and human microvascular endothelial cells post hypoxia. Further investigation demonstrated that an increase in VEGF-B protein levels from endothelial cells could promote the expression of ANP, BNP, β-MyHC, and α-actin via the activated ERK1/2 signaling pathway. A blockage of the pathway with an antagonist (U0126) against ERK1/2 substantially reduces the levels of those downstream proteins.

TEAD1 is the first identified and the best characterized TEAD family protein. Initially, it is found to facilitate the expression of proteins of SV40 by binding to the GT-IIC (5'-ACATTCCACAG-3') *cis*-regulatory element on the viral plasmid (Xiao *et al.*, 1991). As a transcription factor, TEAD1 has a DNA binding TEA-domain that is composed of three α-helixes at the amino terminus (Anbanandam *et al.*, 2006). At the carboxyl terminus is the transcription activation domain that is critical for recruiting TATA-box binding protein (TBP) (Kariya *et al.*, 1993). *In vitro* studies show that a large T-antigen (T-ag) from SV40 forms a stable heterotrimeric complex with TEAD1 and TBP during viral genome coding. Based on the sequence similarity, Gupta *et al.* show that mammalian myosin heavy chain-α (α-MyHC) promoters have conserved TEAD1 binding sites (Gupta *et al.*, 1997). In addition, mammalian cardiac α-actin and troponin T (cTNT) genes also contain a functional MCAT element and the regulation of the expression of these genes is usually context dependent. For instance, TEAD1 and serum response factor (SRF) could form a transcription complex in order to transactivate skeletal α-actin promoter by 20-fold. Loss of the interaction by deleting either amino acid 144-244 in SRF or amino acid 27-113 in TEAD1 abolishes this synergistic effect (Gupta *et al.*, 2001). A similar observation is also reported by Maeda *et al.* to demonstrate that TEAD1 and MEF2, another MAD-box transcription factor, also work synergistically *in vitro* (Maeda *et al.*, 2002b).

TEAD1 is involved in multiple signaling pathways, including that of p38 MAPK and Hippo-Wart networks. A report by Ambrosino *et al.* demonstrates that homozygous knockout of p38a ($p38a^{-/-}$) in rat neonatal cardiac myocytes results in a substantial increase in both the mRNA and protein levels of α 1 chain of type I collagen (Col1A1). It appears that TEAD1 is involved in mediating the Col1A1 promoter activity in a p38a-dependent manner in proliferating rat cardiomyocytes (Ambrosino *et al.*, 2006). On the other hand, multiple studies have emphasized the importance of TEAD1 in the Hippo-wart pathway to regulate the size of organ developments (Cao *et al.*, 2008; Li *et al.*, 2010; Liu *et al.*, 2010; Ota and Sasaki, 2008; Zhang *et al.*, 2009; Zhao *et al.*, 2008). Here, Yes-associated protein 65 (YAP65), a TEAD1-interacting protein, is activated when the signaling pathway is inactivated (Li *et al.*, 2010; Vassilev *et al.*, 2001; Zhang *et al.*, 2009). Functionally active YAP65 then forms a transcription complex with TEAD1 to promote the proliferation of neural progenitors in chick embryos (Zhao *et al.*, 2008). In addition, an ectopic expression of enhanced TEAD1 proteins (TEAD1-VP16 recombinant proteins) in chicken embryos leads to an increase in the number of neural progenitor cells, whereas that of inactivated TEAD1 proteins (TEAD1-EnR fusion proteins) result in apoptosis due to the decrease in cyclin D1 transcript levels. This is in accordance with the report of Knight *et al.* that showed TEAD1 levels correlates with clinical outcome in prostate cancer (Knight *et al.*, 2008).

TEAD1 is essential for embryo development. Homozygous knockout of this gene leads to embryonic lethality on E11.5, because of the reduction of myocardium trabeculation (Sawada *et al.*, 2008). Future studies should utilize a conditional knockout technique to avoid this genotoxic effect. On the other hand, overexpression of TEAD1 in mouse hearts initiates the fetal cardiac programe, including a high level

of β-MyHC together with the α-MyHC in transgenic mice (Tsika *et al.*, 2010). On the 10-month mark, the hearts of these genetically altered mice suffer from an age-dependent cardiac remodeling, decreases in cardiac output, stroke volume, ejection fraction, fractional shortening, and an increase in the degree of fibrosis. Specifically, the ejection fraction of the hearts is reduced by nearly a half, while the left ventricle end-systolic volume increased by a fold. In a parallel study, a HA-tagged TEAD1 recombinant protein is overexpressed under the control of muscle creatine kinase in mice. These mice experienced a transition toward a slow muscle contractile protein phenotype, a slower shortening velocity, and longer contraction and relaxation times in adult fast twitch extensor digitorum longus muscle (Tsika *et al.*, 2008).

In Drosophila melanogaster, TEAD4 homolog *Scalloped* (Sd) is required for the proper development of the indirect flight muscle and the pattering of the wing primordial during the second larval instar. Sd is a functionally multifaceted transcription factor, whose preferences over different downstream effectors are guided by a few transcription co-factors, including *Vestigial* (Vg). The physical interaction between Sd and Vg is through the Vg-interacting domain in Sd and the tondu (Tdu) motif in Vg. Genetic alterations and targeted deletions of Sd or Vg amount to various wing shapes and structures (Cavicchi *et al.*, 1989).

Vg was initially identified in a screening with the use of p-element approach, in which a random insertion of a p-element led to the dysfunction of the gene and aberrant phenotypes (Williams and Bell, 1988). Vg is 453 amino acids in length and contains a conserved Tdu motif. The existence of balanced Vg expression is critical in guiding the development of wing structures, since overexpression or knockout of Vg has an adverse effect on cell proliferation, causing an improper growth of wing discs and haltere areas, and therefore a loss of the wing structure (Agrawal *et al.*, 1995).

There are two waves of Vg expression in fly embryos; the first wave is known as the Vg boundary enhancer (BE) that follows the expression of *apterous* (Ap) protein in the dorsal, but not ventral, region of the imaginal discs. Ap expression is the starting point in the wing development, since failure of its expression completely abolishes further progress. BE positive cells secret Wingless (Wg) ligand as the morphogen that, in combination with BE, induces the second wave of Vg expression along the anterior-posterior axis. The second wave of Vg divides an imaginal disc into four portions, hence the Vg quadrant enhancer (QE). This self-dependency is known as the feed-forward (FF) signaling pathway. Besides modulating its own expression, Vg also induces the expression of other genes, such as SRF and spalt, which are transcription factors also required for cell proliferation and wing tissue formation (Halder *et al.*, 1998).

In mammals, four homologs of Vg have been identified and they are termed Vestigial-like (Vgll) proteins. While Vgll1, 2, and 3 share a conserved Tdu motif, Vgll4 has two Tdu motifs (Chen *et al.*, 2004b; Chen *et al.*, 2004c; Maeda *et al.*, 2002a). Among all, Vgll2 is closest to Vg insofar as the peptide sequence similarity. Early studies identify Vgll2 as an interacting protein to both TEAD and MEF2 proteins in an evolution manner, forming transcription complexes to regulate the development of skeletal muscles (Chen *et al.*, 2004b; Gunther *et al.*, 2004; Maeda *et al.*, 2002a). An ectopic expression of mouse Vgll2 in the MyoD-transformed C3H 10T1/2 fibroblasts promoted the formation of myotubes, following myogenic differentiation (Maeda *et al.*, 2002a). In contrast, knocking down Vgll2 transcripts with a morpholino-based approach significantly reduced myotube formation in C_2C_{12} myoblasts (Chen *et al.*, 2004b; Gunther *et al.*, 2004). *In situ* hybridizations further demonstrated the presence of Vgll2 in the growing somites in mouse embryos at

embryonic day 8.5 (E8.5) and E9.5, and later in the head, trunk, and limb (Maeda *et al.*, 2002a). Similar findings are also reported in *Danio rerio* (zebrafish) (Mann *et al.*, 2007), *Xenopus tropicalis* (frog) (Faucheux *et al.*, 2010)and *Gallus gallus* (chicken) (Bonnet *et al.*, 2010).

Like Vgll2, Vgll4 also interacts with TEADs and MEF2 in African green monkey kidney cells (CV1) and murine C_2C_{12} myoblasts (Chen *et al.*, 2004c). This interaction is mediated by both Tdu motifs; loss of the functional motifs abolishes the interaction. Unlike Vgll2, Vgll4 is ubiquitously expressed in human tissues, ranging from brain, skeletal muscle, spleen, kidneys, small intestine, placenta, lung, but most intensively in heart (Chen *et al.*, 2004c). Functionally, Vgll4 is a downstream target of α-adrenergic receptor signaling. Activation of this signaling pathway by 100 mM phenylepherine results in the nuclear export of Vgll4 by chromosome regain maintenance 1 in the rat neonatal cardiac myocytes (Chen *et al.*, 2004c). Nevertheless, deleting the nuclear export signal in Vgll4 blocks the nuclear export in the treatment of phenylepherine. Future studies will need to focus on how Vgll4 is imported into the nucleus and what its role is in heart development and during cardiac stimulation.

Angiogenesis and vasculogenesis

In adult humans, new blood vessels arise mainly via angiogenesis, a process that is historically defined as endothelial sprouts from pre-existing capillary venules. More recently, the word is used to describe the development and arrangement of endothelial layers in tissues. During angiogenesis, endothelial cells move towards the source of growth factors in an increasing gradient-dependent manner. Evidently, many of these growth factors are typically affected by HIF-1α activation. When on sites, endothelial cells form a ring structure that later outlines the lumen of new blood

vessels. Here, endothelial sprouting allows the continued outgrowth of vessels, while both endothelial bridging and intussusception remodel and create new blood vessels. Endothelial linings from angiogenesis are fragile and usually require layering of smooth muscle cells and pericytes to provide protection. This process is known as vascularigenesis that endows newly synthesized endothelial linings with viscoelastic and vasomotor characters. These properties are critical to vessel dilation and contraction in response to external signals. Failure in establishing vascularigenesis amounts to deleterious diseases and is best demonstrated by blindness in T2DM patients or by leaky vessels in tumors. I hypothesized that genetic controls of energy metabolism via either genetic polymorphisms or transcription regulation could have great impacts on cellular physiology. This is best exemplified by the studies carried out in both chapter 2 and chapter 3 in the thesis.

CHAPTER 2

Functional characterization of a promoter polymorphism that drives ACSL5 gene expression in skeletal muscle and associates with diet-induced weight loss

Allen C. T. Teng[*†], Kristi Adamo[†‡§], Frédérique Tesson[*†‡1] and Alexandre F. R. Stewart[*†1]

[*]Department of Biochemistry, Microbiology, and Immunology, Program of Human and Molecular Genetics, Faculty of Medicine, University of Ottawa, Ontario, Canada

[†]The John & Jennifer Ruddy Canadian Cardiovascular Genetics Centre and

[‡]Laboratory of Genetics of Cardiac Diseases, The University of Ottawa Heart Institute, Ottawa, Ontario, Canada

[§]Healthy Active Living and Obesity (HALO) Research Group, Chalmers Research Group, Children's Hospital of Eastern Ontario (CHEO) Research Institute, Ottawa, Ontario, Canada

[1]Correspondence: University of Ottawa Heart Institute, 40 Ruskin street, Ottawa, ON, Canada, K1Y 4W7.

Short Title: rs2419621 (T) SNP enhances ACSL5 expression via MyoD.

ABSTRACT

Diet-induced weight loss is affected by a wide range of factors, including genetic variation. Identifying functional polymorphism will help to elucidate mechanisms that account for variation in dietary metabolism. Previously, we reported a strong association between a common single nucleotide polymorphism (SNP) rs2419621 (C>T) in the promoter of acyl-CoA synthetase long chain 5 (ACSL5), rapid weight loss in obese Caucasian females, and elevated ACSL5 mRNA levels in skeletal muscle biopsies. Here, we showed by electrophoretic mobility shift assay (EMSA) that the T allele creates a functional cis-regulatory E-box element (CANNTG) that is recognized by the myogenic regulatory factor MyoD. The T allele promoted MyoD-dependent activation of a 1089-base pair ACSL5 promoter fragment in nonmuscle CV1 cells. Differentiation of skeletal myoblasts significantly elevated expression of the ACSL5 promoter. The T allele sustained promoter activity 48 hours after differentiation, whereas the C allele showed a significant decline. These results reveal a mechanism for elevated transcription of ACSL5 in skeletal muscle of carriers of the rs2419621(T) allele, associated with more rapid diet-induced weight loss. Natural selection favouring promoter polymorphisms that reduced expression of catabolic genes in skeletal muscle likely accounts for the resistance of obese individuals to dietary intervention.

INTRODUCTION

Obesity is a growing global health pandemic. According to the World Health Organization (WHO), the number of overweight (BMI>25) adults will exceed 2 billion in 2015. This condition poses a global health issue, since the risk of many chronic diseases, including cerebrovascular and cardiovascular diseases (Kahn *et al.*, 2006), type II diabetes (Poirier *et al.*, 2006), musculoskeletal disorders (Poirier *et al.*, 2006), and cancers (Willig *et al.*, 1993), increases because of obesity. Although exercise and food intake modulate caloric homeostasis, differences in the response to diet-induced weight loss depend on interindividual ability to store and to partition energy.

Skeletal muscle makes up 40-50% of the body mass in an adult and utilizes free fatty acids (FFAs) as a source of energy. Generally, fatty is stored as triglycerides in adipose tissues and becomes mobilized to the sites of utilization in the form of FFA. The uptake of FFA by skeletal muscle for metabolism is initiated by transmembrane acyl-CoA synthetase long-chain (ACSL) proteins that esterify FFAs to acyl-coenzyme A (acyl-CoA) molecules. Acyl-CoA species are used mainly in both the synthesis of cellular lipids and the degradation of fatty acids via β-oxidation (please refer to **schematic 1**). Six members of ACSL family genes have been identified in humans and rodents. In humans, ACSL5 transcripts are distributed in a wide range of tissues, and a high expression has been reported in uterus and spleen (Yamashita *et al.*, 2000). In rats, ACSL5 mRNA is abundant in liver, brown adipose tissue, and duodenal mucosa (Mashek *et al.*, 2006a) and less abundant in other tissues, including skeletal muscle (Adamo *et al.*, 2007). ACSL5 overexpression in liver cell lines promotes fatty acid uptake, which results either in increased storage (Mashek *et al.*, 2006b) or increased b-oxidation (Zhou *et al.*, 2007). Thus, small increases in the expression of ACSL in skeletal muscle could have profound effects on FFA utilization.

Schematic 1. Partitioning of fatty acid in skeletal muscle cells. Intracellular fatty acids form a complex with fatty acid binding protein (FABP). Next, fatty acid is converted to acyl-CoA by acyl-coA synthetase on the mitochondrial outer membrane. Via carnitine palmitoyl transporter, acyl-CoA is transferred into mitochondria and is subsequently degraded into acetyl-CoA through β-oxidation. Finally, acetyl-CoA is fed into the TCA cycle for energy metabolism.

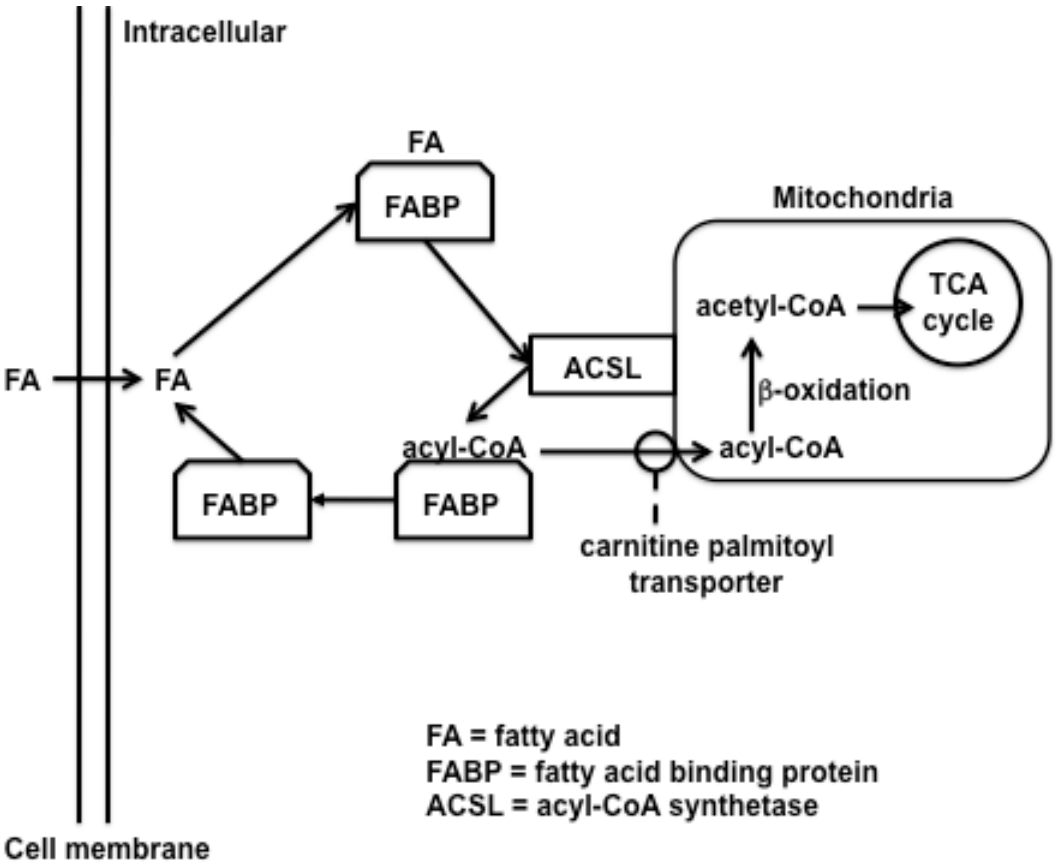
Intracellular
FA
FABP
Mitochondria
acetyl-CoA
TCA cycle
FA
FA
ACSL
β-oxidation
acyl-CoA
acyl-CoA
FABP
FABP
carnitine palmitoyl transporter
FA = fatty acid
FABP = fatty acid binding protein
ACSL = acyl-CoA synthetase
Cell membrane

Previously, we reported a strong association between the common single nucleotide polymorphism (SNP) rs2419621 and rapid weight loss in obese Caucasian females in response to restricted diet (Adamo *et al.*, 2007). The SNP located 12 nucleotides upstream of the second transcription start site of ACSL5 gene (Fig. 1A) is characterized by a cytosine [rs2419621 (C)] to thymine [rs2419621 (T)] transition (Fig. 1B). We also showed that the T allele is associated with a 2.2-fold increase of ACSL5 transcript level in skeletal muscle biopsies when compared to noncarriers (Adamo *et al.*, 2007). Here, we tested whether the T allele is functionally responsible for the upregulation of ACSL5 expression in skeletal muscle.

MATERIALS AND METHODS

Construction of vectors

Human ACSL5 promoter was amplified by PCR with the primer 5'-GAA GAG CTC GCA AAT GAC AAG TGC TCC TCC AGC C-3' (sense primer, *Sac*I) and 5'-GAA AGA TCT GAG CGT CCA TGC AGG CAG AAG GC-3' (antisense primer, *Bgl*II) and was then subcloned into a TOPO vector (Invitrogen Inc., Carlsbad, CA). The amplicon was released by *Sac*I-*Bgl*II double digestion and subcloned into pGL3-basic vector (Promega, Madison, WI) to create pGL3-ACSL5 plasmids. The T-allele was introduced in pGL3-ACSL5 plasmid using the QuikChange Site-directed Mutagenesis kit (Stratagene, La Jolla, CA) based on the manufacturer's instructions. Sequences of the sense primer (SP) and antisense primer (AP) (Operon Biotechnologies, Inc., Huntsville, AL) are 5'-CAA GTG CTC CTC CAG CTG TGA GAT GAG CCA GAG G-3' and 5'-CCT CTG GCT CAT CTC ACA GCT GGA GGA GCA CTT C-3', respectively. The CMV-promoter based pXJ40-MyoD expression vector and the

mouse myogenin-luciferase reporter were made previously (Maeda *et al.*, 2002a). For the construction of pGEX-5X-MyoD, the 1.7 kb *Mus musculus* MyoD cDNA was released from the pact-MyoD plasmid in the Matchmaker^{TM} mammalian two-hybrid system (Promega, Fitchburg, WI) by *Bam*HI digestion and was then subcloned into a *Bam*HI-digested pGEX-5X-1 vector (a gift of Dr. Heidi McBride, University of Ottawa Heart Institute, Ottawa, ON., Canada). The sequence of all plasmid constructs was checked by sequencing (Applied Biosystems, Foster City, CA).

Fusion protein purification

BL21 (DE3) competent cells competent cells (Agilent Technologies, Inc., Santa Clara, CA) transformed with pGEX-5X-MyoD were induced with 0.1 mM isopropyl-b-D-thiogalactopyranoside (IPTG) at 37^{o}C to generate glutathione S-transferase (GST)-MyoD fusion proteins. 3 hours post-induction, the cells were sonicated, and supernatants were collected. Fusion proteins were purified by absorption to glutathione-agarose beads (Sigma-Aldrich, St. Louis, MO) and were eluted with 50 mM Tri (pH8.0) and 20 mM reduced glutathione (Sigma-Aldrich). GST-MyoD fusion proteins were detected on a SDS-PAGE gel, followed by Coomassie-brilliant blue staining for verification.

Electrophoretic mobility shift assay (EMSA)

EMSA was performed as described previously (Chen *et al.*, 2004b), using double stranded oligonucleotides that carry the C allele 5'-AAA CTA AGC AAA TGA CAA GTG CTC CTC CAG C<u>C</u>G TGA GAT GAG CCA GAG GAT GGA A-3' or the T allele 5'- AAA CTA AGC AAA TGA CAA GTG CTC CTC CAG C<u>T</u>G TGA GAT GAG CCA GAG GAT GGA A-3' (rs2419621 SNP is underscored). The purified

GST-MyoD fusion protein (2mg) from bacteria was used in EMSA. Monoclonal MyoD antibody (Santa Cruz Biotechnology, Inc., Santa Cruz, CA) against mouse MyoD protein was added fro a supershift reaction. Intensity of shifted complexes was quantified on a phosphor storage screen (Amersham, NJ)

Cell culture and transient transfections

CV1 and C_2C_{12} cells were maintained in 1X minimum essential medium (MEM; Mediatech, Inc., Herndon, VA) supplemented with 10% fetal bovine serum (FBS), penicillin (100 U/ml), and streptomycin (100 mg/ml). Cells were allowed to grow until 80% confluence in 10-ml plates in a humidified incubator of 37^{o}C and 5% CO_2. One day before transfection, cells were seeded into 6-well tissue culture plates (Corning Inc., Corning, NY). Lipofectamine 2000 (Invitrogen) was used for transfection according to the manufacturer's instruction. Briefly, lipoplexes containing 0.1 mg of expression vector, 0.7 mg of reporter plasmid, and 6 ml of lipofectamine 2000 were added to wells of 80 to 90% confluent cells. After 6 hours, cells were washed with 1X phosphate-buffered saline (PBS; 80g NaCl/L, 2g KCl/L, 14.4g Na_2HPO_4/L, and 2.4g KH_2PO_4/L, pH7.4) and were incubated in 20% FBS-containing media. Differentiation in C_2C_{12} cells was initiated by adding 3% horse serum (Sigma-Aldrich) in serum-free MEM, followed by 24 and 48 hours of incubation.

Luciferase and β-galactosidase assays

Luciferase assays were performed as described previously (Maeda *et al.*, 2002a). β-galactosidase assays were performed according to the manufacturer's instruction (Promega) with modifications. Briefly, 50 ml cell lysate and 20 ml ice-cold β-gal phosphate buffer (60 mM Na_2HPO_4, 45.8 mM NaH_2PO_4•H_2O, 10 mM KCl, and 1.0

mM $MgSO_4$•7H2O) were mixed in a 96-well plate and incubated at 37°C for 10 minutes. To each sample, 50 ml ONPG buffer (200 mM Na_2HPO_4 [pH7.3], 2 mM $MgCl_2$, 100 mM β -mercaptoethanol, and 1.33 mg/ml ONPG) was added and incubated to 37oC until yellow colour developed. β-Galactosidase activity was determined on a microplate spectrophotometer (BioTek, Winooski, VT). Luciferase activities were normalized to activities in cells transfect with wild-type pGL3-ACSL5 plasmids. Mean fold activities of the rs2419621 (T allele) promoter response to mouse MyoD was considered different from the rs2419621 (C allele) at the $P<0.05$ level by independent sample *t* test. Luciferase activities were assessed on luminometer (Montreal-Biotech Inc., Montreal, QC, Canada) following the manufacturer's instructions.

Immunocytochemistry

C_2C_{12} cells were cultured in two-chambered glass plates that were first coated with 4% gelatin. Next, cells were fixed with ice-cold methanol at -20°C for 10 minutes and were permeablized with 0.1% Triton-X 100 for 10 minutes, followed by 1 hours of blocking with 5% FBS in 1X PBS. Mouse monoclonal MF-20 antibody (Cornell University Medical College, Cornell, NY) against myosin heavy chain was hybridized to the cells for 1 hour, and Alexa 488 (Invitrogen) against mouse antibodies was incubated with the cells. DAPI was used for nuclei counterstaining.

RESULTS

rs2419621 (T) allele creates a putative E-box

Consultation of HapMap identified 3 SNPs in linkage disequilibrium with rs2419621 (rs17129754, rs11195951, and rs2419627), but these polymorphisms lie within introns of ACSL5. Thus, barring the existence of other unknown functional SNPs in the promoter, the T allele was considered a good functional candidate, because it creates a *de novo* consensus E-box (CANNTG) *cis*-regulatory element (**Fig. 1**), a putative binding site for basic helix-loop-helix myogenic regulatory factors (MRFs) and E proteins (Rhodes and Konieczny, 1989; Rudnicki *et al.*, 1993; Wright *et al.*, 1989; Zhuang *et al.*, 1992). During skeletal muscle differentiation, MRFs and E proteins form transcriptional complexes that control the expression of many downstream genes, including MEF2C (Dodou *et al.*, 2003), skeletal α-actin (Skerjanc and McBurney, 1994), and muscle creatine kinase (Donoviel *et al.*, 1996). To test whether the existence of this *de novo* E box can be recognized by MRFs, ^{32}P-labeled double-stranded DNA probes carrying either the T or C allele were incubated with GST-MyoD chimeric proteins in an EMSA. MyoD interacted with the rs2419621 (T) probe (**Fig. 2**, lane 8) more strongly than the rs2419621 (C) probe (**Fig. 2**, lane 3). Supershift with antibody to MyoD confirmed its presence in the shifted complex (**Fig. 2**, lane 5 and 10). Thus, the two preexisting E-box elements are recognized by MyoD (**Fig. 2**, lane 3 and 6) *in vitro*, and the third E-box created by rs2419621 (T) recruits additional MyoD to the ACSL5 promoter.

Figure 1. The human ACSL5 promoters. (**A**) Diagram of the three human ACSL5 promoters and the location of the rs2419621 SNP, -12 basepair from the start of the second ACSL5 promoter. (**B**) Sequence of the proximal region near the second promoter carriers either two E-box elements or a third E-box created by the rs2419621 (T) allele (asterisk). The 1089 basepair promoter fragment extending from -92 basepair of the second start site to +997 basepair was cloned into the pGL3 luciferase vector.

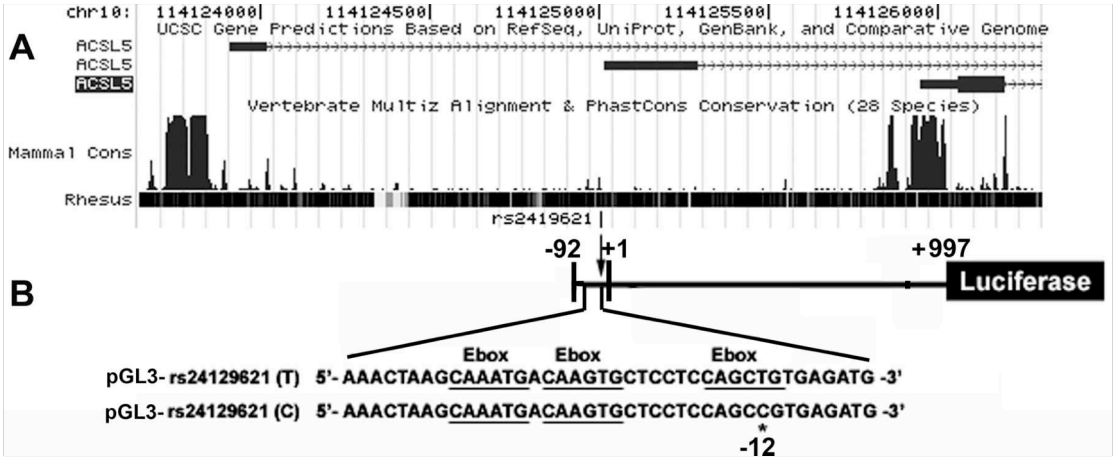
A
chr10:
114124000|
114124500|
114125000|
114125500|
114126000|
UCSC Gene Predictions Based on RefSeq, UniProt, GenBank, and Comparative Genome
ACSL5
ACSL5
ACSL5
Vertebrate Multiz Alignment & PhastCons Conservation (28 Species)
Mammal Cons
Rhesus
rs2419621
B
-92
+1
+997
Luciferase
Ebox
Ebox
Ebox
pGL3- rs24129621 (T) 5'- AAACTAAGCAAATGACAAGTGCTCCTCCAGCTGTGAGATG -3'
pGL3- rs24129621 (C) 5'- AAACTAAGCAAATGACAAGTGCTCCTCCAGCCGTGAGATG -3'
-12

Figure 2. The ACSL5 rs2419621 (T) allele is a functional MyoD binding site. Gel mobility shift assays with bacterially expressed GST-MyoD reveals a weak interaction with the rs2419621 (C) major allele (lane 3) but a strong interaction with the rs2419621 (T) allele (lane 8). Supershift (SS) with a MyoD antibody confirmed the presence of MyoD in the shifted complex (lane 5 and 10). Unprogrammed bacterial lysate produces a shift unrelated to MyoD (lane 2 and 7). The oligonucleotides are shown in **Fig. 1B**. The C-allele oligonucleotide contains 2 E-box elements, whereas the T-allele oligonucleotide contains 3 E-box elements. Gel shift with a single E-box corresponding to the T-allele was not sufficient to produce a gel shift (data not shown) due to the cooperative nature of MyoD binding.

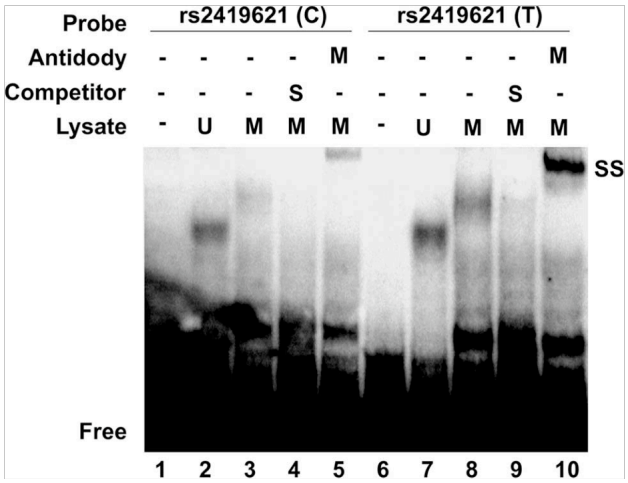
Probe
rs2419621 (C)
rs2419621 (T)
Antidody - - - - M - - - - M
Competitor - - - S - - - - S -
Lysate - U M M M - U M M M
SS
Free
1 2 3 4 5 6 7 8 9 10

The rs2419621 (T/C) ACSL5 promoter alleles are differentially activated by MyoD and during myogenic differentiation

We asked whether MyoD binding to this additional E-box site enhances ACSL5 expression, and if so, by what degree. CV1 cells were transfected with a CMV enhancer-driven MyoD expression vector and ACSL-luciferase reporter vector (carrying either the rs24196212 T or C allele) or a mouse myogenin reporter vector. All luciferase activities were expressed related to the rs2419621 (C)-allele ACSL5 reporter. MyoD activated the myogenin promoter 3-fold, the rs2419621 (T)-allele luciferase promoter 2-fold, and the rs2419621 (C)-allele luciferase promoter 1.5-fold when compared to empty expression vector in CV1 cells (**Fig. 3**). This result is consistent with the EMSA results and suggests that the third E-box element recruits more MyoD to the promoter.

Next, we asked whether the ACSL5 rs2419621 (T or C)-luciferase reporter constructs are differentially regulated in response to muscle differentiation when MRF expression is up-regulated. Prior to muscle differentiation, the rs2419621 polymorphism did not appear to affected the activity of ACSL5 promoter (**Fig. 4**). A progressive difference in the activity of ACSL5 promoter was noted during the course of muscle differentiation between the two sequence variants. The activity of ACSL5 promoter of the rs2419621 (C) allele increased then declined with muscle differentiation, whereas the activity of the rs2419621 (T) allele remained elevated. This result is consistent with our previously reported finding of elevated ACSL5 mRNA expression in patients with rs2419621 (T) variant (Adamo *et al.*, 2007).

Figure 3. MyoD differentially activates the ACSL5 promoter according to the rs2419621 genotype. The ACSL5 promoter luciferase construct bearing the C allele was weakly activated by MyoD, whereas the promoter bearing the T allele of rs2419621 was markedly activated by MyoD in transiently transfected CV1 cells. The MyoD-dependent mouse myogenin promoter served as a positive control. Luciferase activities were compared in the absence (vector) or presence of MyoD. $n = 5$ experiments.

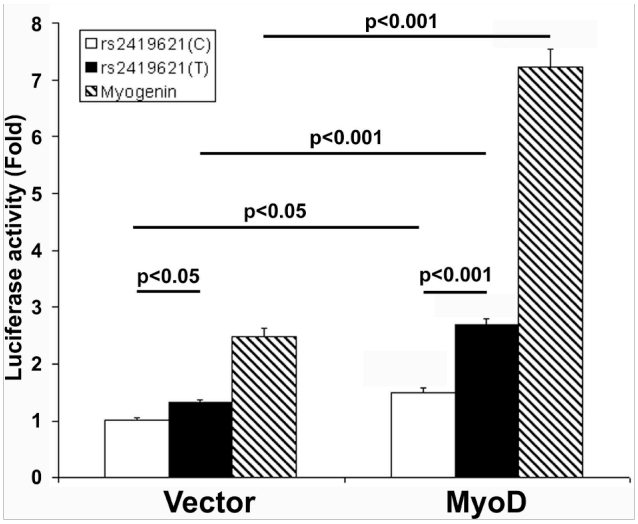
rs2419621(C)
rs2419621(T)
Myogenin
Luciferase activity (Fold)
0
1
2
3
4
5
6
7
8
p<0.001
p<0.001
p<0.05
p<0.05
p<0.001
Vector
MyoD

Figure 4. Muscle differentiation activates the ACSL5 promoter. (**A**) C_2C_{12} myogenic cells were transiently transfected with ACSL5 promoter-luciferase constructs and induced to differentiate by serum withdrawal. The rs2419621 (C) allele bearing ACSL5 promoter is activated 24 hours after muscle differentiation, but expression declines by 48 hours. In contrast, the activity of the promoter bearing rs2419621 (T) allele remains elevated. Expressed luciferase activity is standardized to the rs2419621 (C) allele in undifferentiated myoblasts. The myogenin promoter served as a positive control. *n* = 5 experiments. (**B**) Myogenic differentiation was monitored by myosin heavy chain immunofluorescence. Nuclei were stained with DAPI. Scale bar = 50 μm.

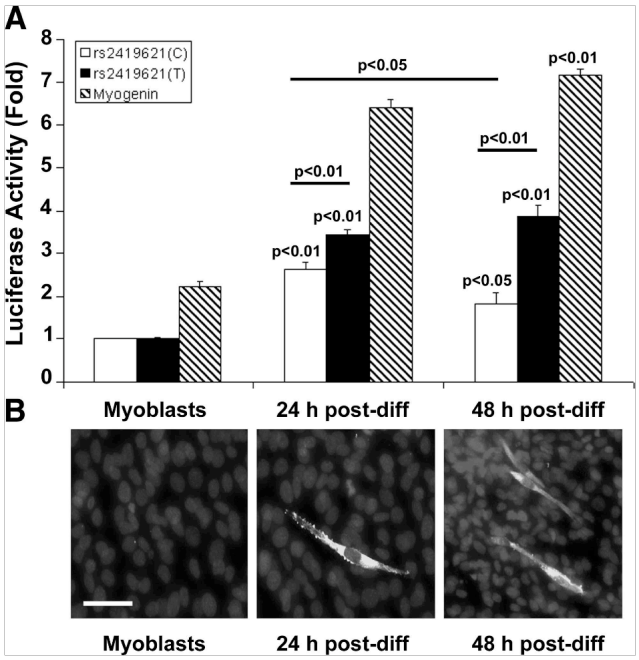
A
Luciferase Activity (Fold)
rs2419621(C)
rs2419621(T)
Myogenin
p<0.05
p<0.01
p<0.01
p<0.01
p<0.01
p<0.01
p<0.05
Myoblasts
24 h post-diff
48 h post-diff
B
Myoblasts
24 h post-diff
48 h post-diff

DISCUSSION

Our study demonstrates that the rs2419621 (T) allele forms a functional E-box element upstream of the second ACSL5 isoform transcript start site. MyoD physically and functionally interacts with this *de novo* E-box to up-regulate ACSL5 expression in muscle cells. The reference rs2419621 (C) allele lacks the third E-box element and is associated with a lower ACSL5 promoter activity in differentiating skeletal muscle. The two E-box elements make the ACSL5 promoter minimally responsive to MyoD, consistent with early work from Weintraub *et al.* that showed two or more E-boxes are required for promoter to be MyoD responsive (Weintraub *et al.*, 1990). This is the first example of a MyoD binding polymorphism conferring differential promoter activity of a metabolic gene.

The regulation of ACSL isoforms is largely unknown. The present findings represent a new molecular mechanism by which one ACSL isoform, ACSL5, is differentially regulated at the transcriptional level. Adenoviral-mediated overexpression of ACSL5 in liver cell lines produced apparently contradictory results. Mashek *et al.* showed in rat hepatoma cells that ACSL5 promotes fatty acid uptake destined for TG synthesis and storage while recently Zhou *et al.* showed in human HepG2 cells that it results in an increase of nearly 50% in b-oxidation associated with a trend toward TG reduction (Mashek *et al.*, 2006b; Zhou *et al.*, 2007). Our previous results in humans, where carriers of the rs2419621 (T) allele display higher levels of skeletal muscle ACSL5 mRNA and are better responders to diet, are consistent with the finding of Zhou *et al.* (Zhou *et al.*, 2007). Moreover, carriers of the rs2419621 (T) allele have lower total cholesterol and tend to have lower density lipoproteins and triglycerides (Adamo *et al.*, 2007). Adenovirus-mediated overexpression of ACSL5 in rat hepatoma cells leads to Ad-ACSL5 expression in both mitochondria and

endoplasmic reticulum (Mashek *et al.*, 2006b). However, because of its location 12 bp upstream of the second major transcription start site (**Fig. 1**), rs2419621 SNP is likely to influence primarily transcription from this second transcription start site. It is conceivable that transcripts from this second major transcription start site are directed mainly to the mitochondria and thus involved in fatty acid oxidation. Transcripts from the two other transcription start sites might be directed to other cellular compartments, including endoplasmic reticulum, and thus involved in lipid synthesis and storage. Taken together, these data suggest that the rs2419621 SNP influences the rate of weight loss by increasing ACSL5 levels and promoting b-oxidation over TG synthesis and storage.

Ideally, replication of the association of rs2419621 with diet-induced weight loss in other cohorts will be necessary to confirm whether it predicts dietary response. It is worth noting that rs2419621 has not been associated with obesity in genome-wide association studies, perhaps because it is not represented on commercial arrays. However, genes that predispose to weight gain may not necessarily impair the ability to lose weight. For example, several recent studies saw no association of the well-known FTO gene with diet-induced weight loss or with energy expenditure (Cecil *et al.*, 2008; Haupt *et al.*, 2008; Muller *et al.*, 2008).

The CC genotype has greater than 50% prevalence in each of four populations (67.2% in 116 CEU, 51.1% in 90 HCB, 71.4% in 84 JPT, and 71.7% in 120 YRI) sampled in the International HapMap project. Natural selection may have favored carriers of the C allele, enabling them to survive famine by promoting fatty acid storage over catabolism. Promoter polymorphisms that affect expression of metabolic genes in skeletal muscle may constitute a general mechanism underlying variation in the response to diet-induced weight loss.

CHAPTER 3

IRF2BP2 is a skeletal and cardiac muscle-enriched ischemia-inducible activator of VEGF-A expression

Allen C. T. Teng[*‡], Drew Kuraitis[*], Shelley A. Deeke[*], Ali Ahmadi[*], Stephen G. Dugan[*], Brian L. M. Cheng[*], Matthew G. Crowson[*], Patrick G. Burgon[*], Erik J. Suuronen[*], Hsiao-Heui Chen[†], and Alexandre F. R. Stewart[*‡1]

[*] University of Ottawa Heart Institute, Ottawa, Ontario, Canada

[‡] Department of Biochemistry, Microbiology, and Immunology, University of Ottawa, Ottawa, Ontario, Canada

[†] Ottawa Hospital Research Institute, Ottawa, Ontario, Canada

Short title: IRF2BP2: an ischemia-inducible activator of VEGF-A in cardiac and skeletal muscle

ABSTRACT

We sought to identify an essential component of the TEAD/VGLL4 transcription factor complex that controls vascular endothelial growth factor A (VEGF-A) expression in muscle. A yeast two-hybrid screen was used to clone a novel component of the TEAD complex from a human heart cDNA library. We identified Interferon Regulatory Factor 2 Binding Protein 2 (IRF2BP2) and confirmed its presence in the TEAD/VGLL4 complex *in vitro* by co-immunoprecipitation and mammalian two-hybrid assays. Coexpression of IRF2BP2 with TEAD4/VGLL4 or TEAD1 alone potently activated, whereas knockdown of IRF2BP2 reduced, VEGF-A expression in C_2C_{12} myoblasts. Thus, IRF2BP2 is required to activate VEGF-A expression. In mouse embryos, IRF2BP2 was ubiquitously expressed, but became progressively enriched in the fetal heart, skeletal muscles, and lung. Northern blot analysis revealed high levels of IRF2BP2 mRNA in adult human heart and skeletal muscles, but immunoblot analysis showed low levels of IRF2BP2 protein in skeletal muscle, indicating post-transcriptional regulation of IRF2BP2 expression. IRF2BP2 protein levels are markedly increased by ischemia in skeletal and cardiac muscle compared to normoxic controls. IRF2BP2 is a novel ischemia-induced coactivator of VEGF-A expression that may contribute to revascularization of ischemic cardiac and skeletal muscles.

INTRODUCTION

Muscle ischemia that results from obstruction of blood flow can occur in patients with diabetes and atherosclerosis. In skeletal muscle, ischemia produces myopathy whereas in the heart it is a major cause of myocardial infarction. In response to ischemia, the injured tissue expresses angiogenic cytokines to activate neovascularization in an attempt to restore blood flow. Many angiogenic cytokines have been described including the vascular endothelial growth factors (VEGF) (Leung *et al.*, 1989), basic fibroblast growth factor (Cao *et al.*, 2003), the angiopoietins (Holash *et al.*, 1999), and platelet-derived growth factor (Brasen *et al.*, 2001). Many laboratories are seeking to optimize protocols to promote angiogenesis. VEGFA, one of four mammalian VEGF homologues, is one of the best studied angiogenic factors, although the mechanisms controlling its expression are still not fully understood (Breen *et al.*, 2008). Muscle-specific ablation of VEGFA causes reduced vascularization of adult cardiac and skeletal muscle (Olfert *et al.*, 2009).

Transcription factors regulating VEGFA expression during tissue ischemia include hypoxia-inducible factor 1-α (HIF1-α) (Ceradini *et al.*, 2004), peroxisome proliferator-activated receptor-γ coactivator 1α (PGC1-α) (Arany *et al.*, 2008), activating protein-1 (AP-1) (Levy *et al.*, 1995) and the TEA-domain transcription factor TEAD4 (Shie *et al.*, 2004) (for a brief summary, please refer to **schematic 1**). TEAD4 is induced by hypoxia and upregulates VEGFA expression in bovine aortic endothelial cells (Shie *et al.*, 2004). TEAD4 also activates VEGFA in human ocular vascular endothelial cells and in the murine retina (Appukuttan *et al.*, 2007). Although it is not known whether other TEAD factors regulate VEGFA expression, it is noteworthy that a mutation in TEAD1 causes Sveinsson's chorioretinal atrophy (Fossdal *et al.*, 2004) associated with defects in the microvasculature of the

choriocapillaris layer (Jonasson *et al.*, 2007). Moreover, transgenic mice over-expressing TEAD1 in skeletal muscle have an excess of slow twitch oxidative fibers (Tsika *et al.*, 2008) that require enhanced vascularization.

TEAD transcription factors regulate gene expression by forming complexes with other transcription factors, including the basic helix loop helix protein MAX (Gupta *et al.*, 1997), the serum response factor (SRF) (Gupta *et al.*, 2001), myogenic enhancer factor 2 (MEF2) (Maeda *et al.*, 2002b), the YAP and TAZ transcription coactivators (Mahoney *et al.*, 2005; Vassilev *et al.*, 2001), the steroid receptor coactivator SRC1 (Belandia and Parker, 2000) and the Vestigial-like (VGLL) family of cofactors (Chen *et al.*, 2004b; Chen *et al.*, 2004c; Gunther *et al.*, 2004; Maeda *et al.*, 2002a; Vaudin *et al.*, 1999).

The *Drosophila* protein Vestigial is required for the specification of the wing primordium (Williams *et al.*, 1994) and indirect flight muscles (Sudarsan *et al.*, 2001). Four vertebrate VGLLs have been described (Chen *et al.*, 2004b; Chen *et al.*, 2004c; Gunther *et al.*, 2004; Maeda *et al.*, 2002a; Vaudin *et al.*, 1999) that have a conserved TEAD factor interacting TDU motif (Vaudin *et al.*, 1999). Interaction of VGLL proteins increases DNA binding of TEAD factors to *cis*-regulatory DNA sequences (5'-CATTCCT/A-3') (Chen *et al.*, 2004b) found in many muscle-specific genes (Yoshida, 2008). VGLL4 is expressed in the heart and contains two TDU motifs, and may serve to consolidate the interaction between TEAD factors and other transcription factors at cardiac-specific promoters (Chen *et al.*, 2004c).

Given that VEGFA expression is increased by TEAD4, we asked what effect adding VGLL4 would have and found that it conferred only a modest activation, suggesting that it may recruit additional factors. Here, we describe the identification and characterization of a novel VGLL4 interacting factor that is upregulated by

ischemia and strongly coactivates VEGFA expression in muscle.

Schematic 1. Brief summary of transcription regulation of VEGF. VEGF is the only growth factor known to mobilize endothelial cells. Transcription control of VEGF gene is modulated by many transcription factors, including, but not limited to, signaling transduction and transcription factor 3 (STAT3), hypoxia-inducible factor-1α (HIF-1α), and TEA-domain transcription factors (TEADs). However, the mechanisms to activate TEAD-dependent VEGF induction are currently unknown.

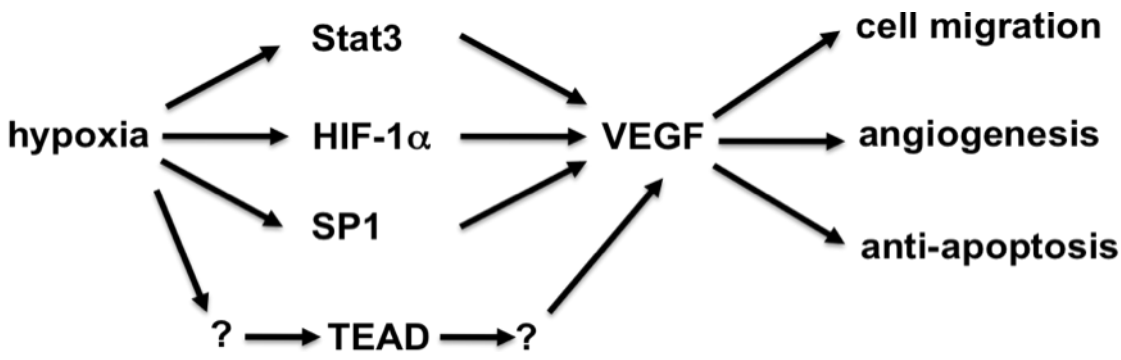
Stat3
cell migration
hypoxia
HIF-1α
VEGF
angiogenesis
SP1
anti-apoptosis
?
TEAD
?

METHODS AND MATERIALS

Animal models

Animal procedures were approved by the University of Ottawa Animal Care Committee, in accordance with the Canadian Council on Animal Care guidelines. The left femoral artery of 7-8 week old, anesthetized female Sprague-Dawley rats (Charles River) was ligated and muscle was harvested from ischemic and non-ischemic control hindlimb. In anesthetized and mechanically ventilated mice, the left anterior descending coronary artery was ligated just proximal to its main bifurcation via thoracotomy resulting in a large infarction involving the anterolateral and apical regions of the heart.

Plasmid constructs and chemicals

Many plasmid constructs were described previously (22, 24). The mouse vascular endothelial growth factor A (VEGFA) -1294 to +510 promoter was PCR amplified from genomic DNA using the primers, 5'-TTG GTA CCG GGC TAA GTG TGC AAG CAT AGA G-3' (KpnI) and 5'-AAC TCG AGG TGT CTG TCT GTC TGT CCG TCA GC-3' (XhoI) and subcloned into the pGL3-luciferase vector (Promega, Madison, WI). Human IRF2BP2a, IRF2BP2b and IRF2BP1 cDNAs (gifts of Stephen Goodbourn) (31) were ligated in-frame in the GAL4(DBD) in pM vectors. To generate pCMV-IRF2BP2-Flag 4 plasmid, full length IRF2BP2 was PCR-amplified with sense primer 5'-GAA TTC ATG GCG TCT GTG CAG GCG TCC-3' (EcoRI) and antisense primer 5'-CTC GAG GGG GTC CCG TTC TTT CTT-3' (XhoI) and cloned into the TOPO vector (Invitrogen, Inc. Carlsbad, CA). Full length of IRF2BP2 fragment was released by EcoRI/XhoI digestion and ligated in-frame with the Flag-tag sequence in the pCMV-Tag4 vector (Stratagene, La Jolla, CA). All constructs were

verified by sequencing.

Yeast two-hybrid screen. The bait vector was constructed by subcloning human VGLL4 cDNA in frame into the pGBKT7 vector. After testing for yeast toxicity, transcriptional activation, and expression, the bait vector-transformed yeast was mated with a human heart BD Matchmaker™ pretransformed library and screened according to the manufacturer's protocol (BD Biosciences Clontech, San Jose, CA).

Culture and transient DNA transfection

COS-7, CV1, and C_2C_{12} cells were maintained in Minimum Essential Medium (MEM, Mediatech, Inc., Herndon, VA) supplemented with 20% fetal bovine serum, penicillin (100U/ml) and streptomycin (100 μg/ml). Lipofectamine 2000 (Invitrogen Inc., Carlsbad, CA) was used to transfect plasmids according to the manufacturer's instructions. Differentiation of C_2C_{12} cells was initiated by switching to medium supplemented with 3% horse serum (Sigma-Aldrich, St. Louis, Missouri, MO). Luciferase assays were performed as previously described (32).

Co-immunoprecipitation

COS-7 cells transfected with pXJ40-cMyc-VGLL4 or pCMV-Tag4-IRF2BP2, or both were harvested 48 hours later in lysis buffer (20 mM Tris pH 7.5, 100 mM NaCl, 0.5% IGEPAL®CA-630 (Octylphenyl-polyethylene glycol), 0.5 mM EDTA, 0.5 mM PMSF, and 10 μg/ml each of pepstatin, aprotinin, and leupeptin) on ice for 10 minutes and clarified by centrifugation. Immunoprecipitation was carried out by adding 10 μg of cMyc-peptide (sc-13665) or OctA-peptide (sc-7787) antibodies to the lysates, mixing for 2 hours at 4°C then adding 50 μL of Protein A/G Sepharose (sc-2003, Santa Cruz Biotechnology) pre-washed lysis buffer and mixing for 1 hour at 4°C.

Immunoprecipitated proteins were released by boiling in 50 µL of 1x SDS-PAGE sample buffer and analyzed by gel electrophoresis in immunoblots.

Northern blot analyses

RNA was obtained from C_2C_{12} cells, size fractionated on formaldehyde gels, and transferred to nylon membranes as described previously (24). IRF2BP2 cDNA fragment was radiolabeled with [^{32}P]-γ-dCTP and hybridized to the C_2C_{12} mRNA blot or a human multi-tissue Northern blot (Clontech, Palo Alta, CA).

Reverse transcription-PCR (RT-PCR)

Concentration and integrity of RNA samples were assessed by NanoDrop and 2100 Bioanalyzer (Agilent Technologies, Mississauga, ON, Canada). For reverse transcription, 1µg of total RNA and Oligo(dT)$_{12-18}$ were added to SuperScript II Reverse Transcriptase master mix (Invitrogen). 2µl of each cDNA sample were subjected to a standard PCR amplification with the follow primers. 5'-CCT CCG AAA CCA TGA ACT TTC TGC TC-3' (mouse VEGFA sense primer), 5'-CAG CCT GGC TCA CCG CCT TGG CTT-3' (mouse VEGFA antisense primer), 5'-GCATCC TGA CCC TGA AGT ACC-3' (mouse β-actin sense primer) and 5'-GCT CAT AGC TCT TCT CGA GGG-3' (mouse β-actin antisense primer).

Knockdown of IRF2BP2 in C_2C_{12} myoblasts and myotubes

Mouse IRF2BP2 shRNA (V2LMM_151056) and non-silencing control shRNA (RHS4346) constructs in pGIPz lentiviral plasmids were obtained from OpenBiosystems (Thermo Scientific, Huntsville, AL) and viral particles were generated according to the manufacturer's instructions. Viral particles were further

concentrated at 20,000 rpm in a SW-28 rotor (Beckman Coulter Canada, Mississauga, ON, Canada) for 2 hours. An hour prior to transduction, C_2C_{12} myoblasts were cultured in medium containing 8μg/μl polybrene (Sigma-Aldrich, Oakville, Ontario, Canada) and viral particles were overlaid on cells. Six hours post-transduction, fresh media was added and cells were cultured overnight. Proteins were extracted and analyzed by immunoblot.

Protein lysates and immunoblot analyses

Protein lysates were prepared in RIPA buffer (4.25 mM Tris, pH8.0, 135 mM NaCl, 1% IGEPAL CA-630, 1% SDS 0.5% deoxycholate) with protease and phosphatase inhibitors (Roche Molecular Systems, Branchburg, NJ). A rabbit antibody against the IRF2BP2 epitope KLEEPPELNRQSPNPRR was obtained from OpenBiosystems, affinity purified and used in immunoblot analysis. Rabbit anti-VEGFA antibody (sc-507) and mouse anti-GAPDH antibody (sc-59540) were obtained from Santa Cruz Biotechnology (Santa Cruz, CA) whereas goat anti-mouse IgG (HAF007) was from R&D Systems (Minneapolis, MN) and goat anti-rabbit IgG (#:31460) was from Piercenet (Rockford, IL).

Immunocytochemistry

Frozen tissue sections (5 μm) were air dried, blocked in 10% horse, goat, and pre-immune serum (where appropriate) in PBS for 1 hour. IRF2BP2 antibody was detected using Regulus Red-conjugated antibody (Lake Placid Biologicals, Lake Placid, NY) in C_2C_{12} cells or with Alexa488-conjugated antibody (Invitrogen, Carlsbad, CA) for skeletal or cardiac muscle sections. Nuclei were stained with DAPI (4,6-diamidino-2-phenylindole; Sigma Chemical Co., St. Louis, MO). Fluorescent

images were captured on a Zeiss Z1 microscope. Frozen sagittal mouse embryo sections (Zyagen, San Diego, CA) probed with pre-immune or IRF2BP2 immune rabbit serum were revealed using alkaline phosphatase-conjugated goat anti-rabbit antibody.

Statistical analysis. Experimental results are shown as mean ± SEM. By independent samples *t*-test, mean fold luciferase activities relative to the negative control from triplicate assays performed in at least 5 independent transfections were considered different from control at the $p < 0.05$ significance level.

RESULTS

Identification of IRF2BP2 as a novel interacting protein to VGLL4

To search for VGLL4-interacting proteins, we interrogated a human cardiac cDNA library in a yeast-two hybrid assay. Of 180 colonies recovered and sequenced, 3 independent clones coding for the C-terminal sequence of interferon regulatory factor-2 binding protein 2 (IRF2BP2) were identified. IRF2BP2 is related to 2 other vertebrate proteins, IRF2BP1 (Childs and Goodbourn, 2003) and Enhanced-at-puberty 1 (EAP1) (Heger *et al.*, 2007) and to a Drosophila protein of unknown function. The aligned proteins bear a highly conserved N-terminal Cys4 zinc finger of unknown function and C-terminal C3HC4 RING finger motif characteristic of E3-ubiquitin ligases (**Fig. 1**). The phylogenetic relationship revealed that each paralogue arose early in vertebrate evolution (**Fig. 2**).

Physical interaction between VGLL4 and IRF2BP2 was confirmed by coimmunoprecipitation of epitope tagged proteins expressed in CV1 cells by transient transfection (**Fig. 3A**). The shortest IRF2BP2 cDNA clone isolated in the yeast two-hybrid screen identified a minimal sequence required to interact with VGLL4, between residues 423 and the C-terminus. However, in a mammalian two hybrid assay using the related protein IRF2BP1, no interaction was observed with VGLL4 (data not shown) suggesting that VGLL4 does not interact with the C-terminal RING finger motif that is highly conserved between IRF2BP2 and IRF2BP1. Thus, the VGLL4 interaction domain is likely between positions 423 and 488. To delineate the IRF2BP2 interaction domain in VGLL4, mutagenized sequences were tested in a mammalian two hydrid assay (**Fig. 3B**). Deletion of the 2 TEAD interaction motifs (pVP-VGLL4(ΔTDU)) prevented interaction with IRF2BP2, as did deletion of the

TDU1 motif (pVP-VGLL4(TDU2)) but not the TDU2 motif (pVP-VGLL4(TDU1)). This showed that TDU1

Figure 1. The IRF2BP1/2 EAP1 family of transcription cofactors. Human and zebrafish sequences were aligned to the related homologue in Drosophila by the COBALT alignment program. The cysteines of the N-terminal Cys4 Zn-finger and the C-terminal C3HC4 Ring finger motifs are highlighted in yellow. The additional sequence of the long isoform, IRF2BP2a, is in green font. The position of caspase cleavage reported in apoptosis is indicated by a red V (39). The location of the IRF2BP2 peptide epitope is highlighted in purple. The VGLL4 interaction domain in IRF2BP2 is highlighted in grey. Note that the TGFβ inhibitory factor (TGIF) interaction domain in IRF2BP1 (underlined) is more similar to EAP1 and highly divergent from IRF2BP2.

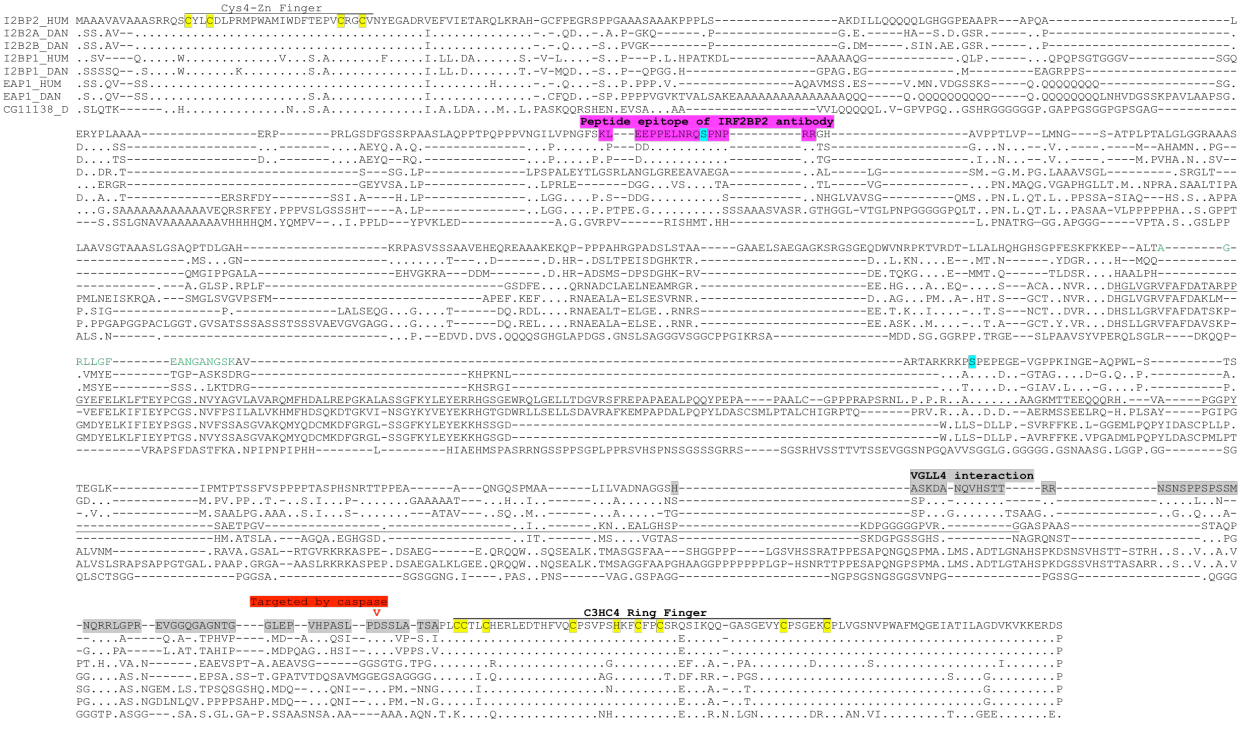
Cys4-Zn Finger
Peptide epitope of IRF2BP2 antibody
VGLL4 interaction
Targeted by caspase
C3HC4 Ring Finger

Figure 2. Phylogenetic relationship of IRF2BP2 to other members of the family. Sequences were aligned using the COBALT constraint-based alignment tool for multiple protein sequences (47). The family comprises 3 major branches corresponding to EAP1, IRF2BP1, and IRF2BP2 (zebra fish has duplicated IRF2BP2 genes). The tree was generated using the fast minimum evolution method (48). EAP1 is expressed specifically in female hypothalamic neurons controlling gonadotropin releasing hormone production. The function of the Drosophila homologue, CG11138 is unknown. Note that the divergence of the 3 family members predates the common ancestor to mammals and fishes, some 500 million years ago. Thus, these proteins are likely to have acquired unique specialized functions early in the vertebrate lineage.

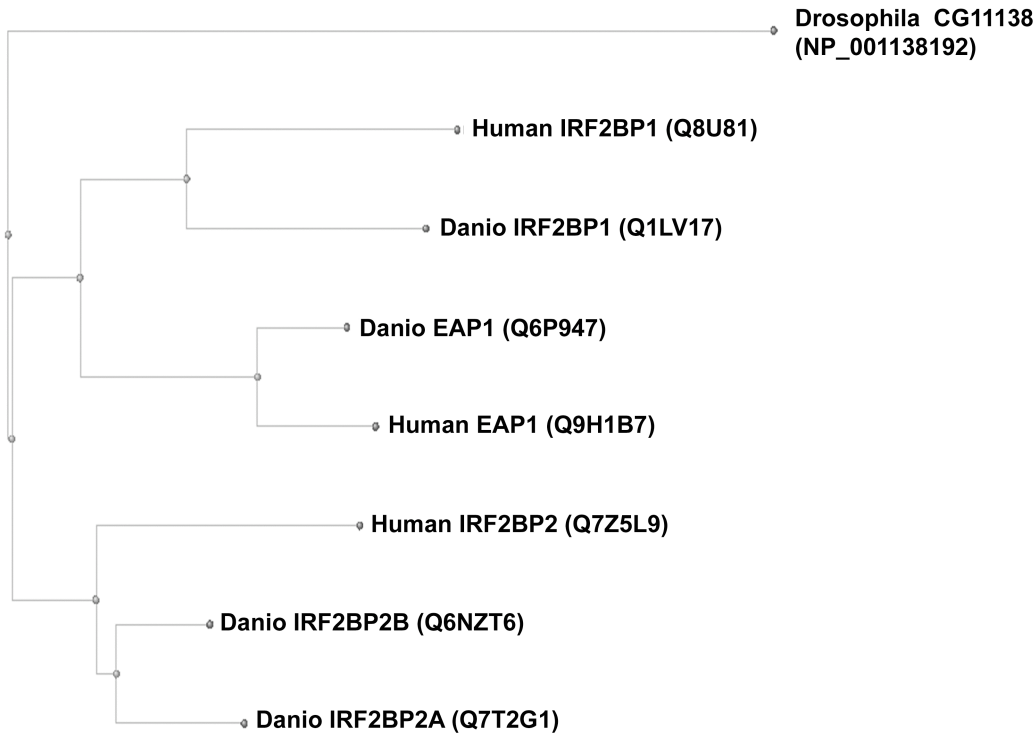
Drosophila CG11138
(NP_001138192)
Human IRF2BP1 (Q8U81)
Danio IRF2BP1 (Q1LV17)
Danio EAP1 (Q6P947)
Human EAP1 (Q9H1B7)
Human IRF2BP2 (Q7Z5L9)
Danio IRF2BP2B (Q6NZT6)
Danio IRF2BP2A (Q7T2G1)

Figure 3. Physical and functional interaction between VGLL4 and IRF2BP2. (**A**) Coimmunoprecipitation (IP) of VGLL4 and IRF2BP2 was carried out with the anti-Flag antibody and immunoblot (IB) used the HA antibody (upper panel) or vice versa (lower panel). Lanes 1 and 2 are negative controls; lane 1 is extract of cells transfected with IRF2BP2-FLAG and the HA vector, lane 2 is extract of cells transfected with the FLAG vector and HA-VGLL4. Lane 3 is extract of cells expressing IRF2BP2-FLAG and HA-VGLL4. (**B**) Mammalian 2-hybrid assay confirms VGLL4 and IRF2BP2 interaction in C_2C_{12} myoblasts and myocytes. Of the 2 TEAD interaction domains (TDU1 and TDU2) in VGLL4, only TDU1 interacts with IRF2BP2 in C_2C_{12} cells and this interaction displays a marked increase with muscle differentiation. (**C**) Schematic diagram of the interaction domains in IRF2BP2 and VGLL4. IRF2BP1 did not interact with VGLL4 (data not shown), suggesting that the highly conserved RING finger domain is not part of the VGLL4 interaction domain. The minimal domain for VGLL4 interaction in IRF2BP2 is located between residues 423 and 488 (see Figure 1).

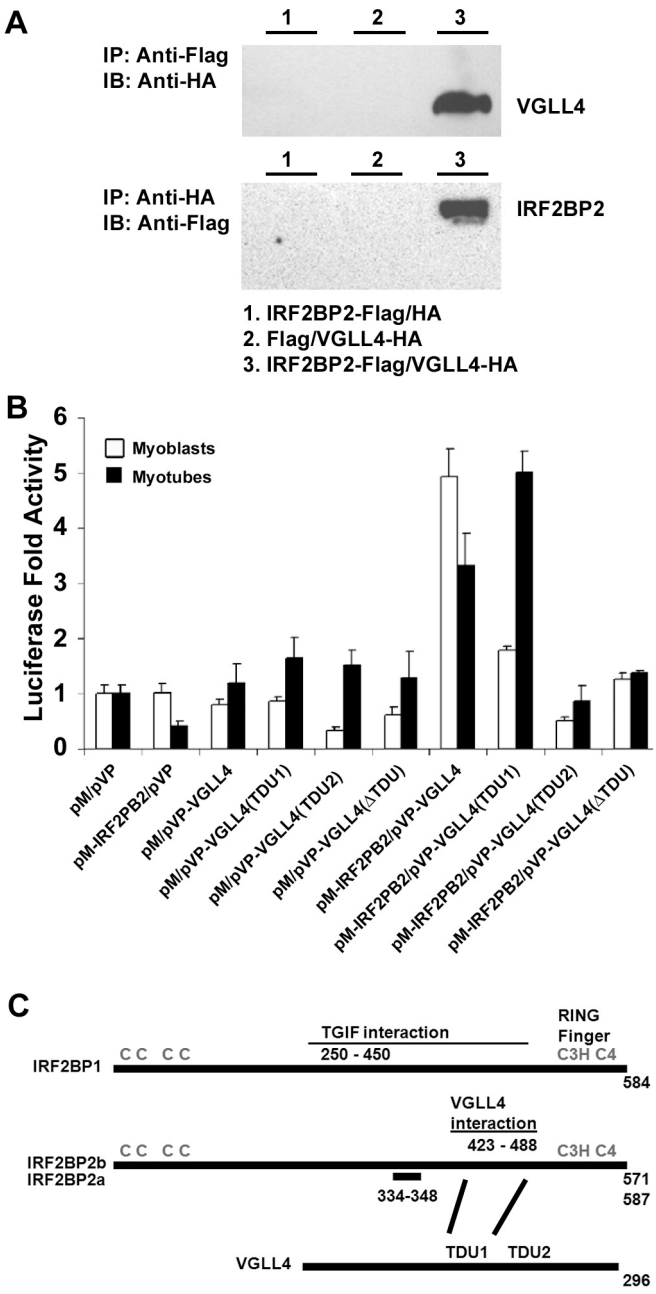
A
1
2
3
IP: Anti-Flag
IB: Anti-HA
VGLL4
1
2
3
IP: Anti-HA
IB: Anti-Flag
IRF2BP2
1. IRF2BP2-Flag/HA
2. Flag/VGLL4-HA
3. IRF2BP2-Flag/VGLL4-HA
B
Luciferase Fold Activity
0
1
2
3
4
5
6
Myoblasts
Myotubes
pM/pVP
pM-IRF2PB2/pVP
pM/pVP-VGLL4
pM/pVP-VGLL4(TDU1)
pM/pVP-VGLL4(TDU2)
pM/pVP-VGLL4(ΔTDU)
pM-IRF2PB2/pVP-VGLL4
pM-IRF2PB2/pVP-VGLL4(TDU1)
pM-IRF2PB2/pVP-VGLL4(TDU2)
pM-IRF2PB2/pVP-VGLL4(ΔTDU)
C
IRF2BP1
C C C C
TGIF interaction
250 - 450
RING
Finger
C3H C4
584
VGLL4
interaction
423 - 488
IRF2BP2b
IRF2BP2a
C C C C
C3H C4
571
587
334-348
TDU1
TDU2
VGLL4
296

is required for IRF2BP2 interaction in C_2C_{12} myoblasts. Of note, the full-length VGLL4 protein showed reduced interaction with IRF2BP2 following muscle differentiation, whereas deletion of the TDU2 motif was associated with increased interaction with IRF2BP2 upon muscle differentiation. This may represent the interaction of a factor with TDU2 that hinders IRF2BP2 interaction with the TDU1 motif during muscle differentiation is not known.

IRF2BP2 is muscle-enriched protein

IRF2BP2 mRNA levels are high in adult human cardiac and skeletal muscle, with lower levels in peripheral blood lymphocytes and low expression in other tissues (**Fig. 4A**). IRF2BP2 mRNA levels increased during differentiation of C_2C_{12} myoblasts (**Fig. 4B**). Thus, IRF2BP2 mRNA is prominently expressed in human and mouse striated muscles. Using an IRF2BP2 peptide-specific antibody that does not cross-react with IRF2BP1 (**Figs. 1, 4C**), we detected IRF2BP2 protein in adult human heart, but surprisingly only low levels in skeletal muscle (**Fig. 4D**). Given the high levels of IRF2BP2 mRNA in adult human skeletal muscle, this result suggested that IRF2BP2 undergoes post-transcriptional regulation, either by controlling mRNA translation or by rapidly degrading IRF2BP2 protein. In differentiating C_2C_{12} cells, IRF2BP2b protein levels were markedly increased at 12 hours and remained elevated at 48 hours (**Fig. 4E**). In addition, a faster migrating immunoreactive protein, likely representing a proteolytic fragment of IRF2BP2, was detected in differentiating C_2C_{12} muscle cells.

IRF2BP2 is almost exclusively localized in the nucleus of C_2C_{12} myoblasts (**Fig. 5**). Only in dividing myoblasts is IRF2BP2 excluded from the condensed DNA

Figure 4. IRF2BP2 mRNA and protein expression in cardiac and skeletal muscle. (**A**) Human multi-tissue northern blot analysis reveals IRF2BP2 mRNA is abundantly expressed in heart and skeletal muscle, with lower levels in peripheral blood lymphocytes (PBL). (**B**) IRF2BP2 mRNA is upregulated during muscle differentiation. Total RNA (10 μg per lane) from C_2C_{12} myoblasts was harvested at 0 hour and 12, 24 and 48 hours after differentiation and analyzed by northern blot. (**C**) IRF2BP2 antibody is highly specific. Lysates of CV1 cells transfected with empty vector (lane 1), IRF2BP1 (lane 2), IRF2BP2a (lane 3) and IRF2BP2b (lane 4) expression vectors show that IRF2BP1 detected by the IRF2BP1 antibody (Abcam, ab68956) is not detected by peptide-specific antibody to IRF2BP2. The IRF2BP2 antibody detects alternatively spliced isoforms of IRF2BP2 (a and b) and the presence of endogenous IRF2BP2 in CV1 cells (leftmost lane, lower panel). (**D**) Immunoblot analysis of adult human tissues reveals IRF2BP2 protein in the heart but only low levels in skeletal muscle and testis. Compare protein levels with mRNA levels in **A**. 30 μg of total protein were loaded per lane. (**E**) IRF2BP2b protein levels are markedly upregulated during C_2C_{12} skeletal muscle differentiation. At 12 hours a faster mobility band appears (since the epitope is N-terminal this is likely to be a proteolytic product, lacking C-terminal sequence).

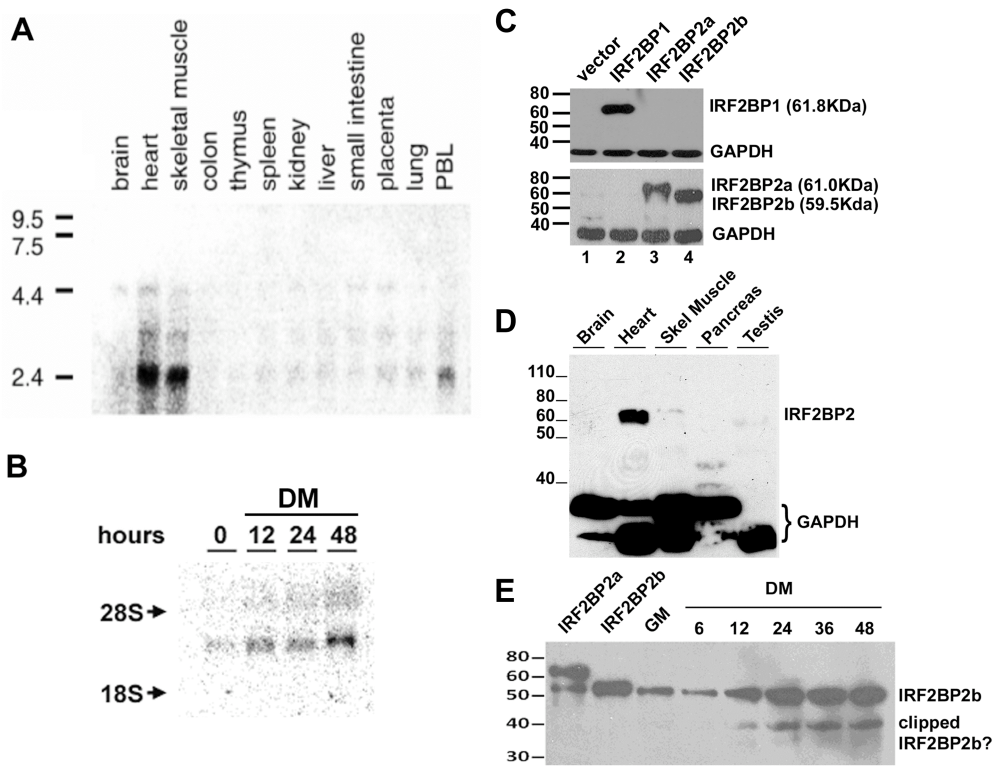
A
brain
heart
skeletal muscle
colon
thymus
spleen
kidney
liver
small intestine
placenta
lung
PBL
9.5
7.5
4.4
2.4
B
DM
hours
0
12
24
48
28S
18S
C
vector
IRF2BP1
IRF2BP2a
IRF2BP2b
80
60
50
40
IRF2BP1 (61.8KDa)
GAPDH
IRF2BP2a (61.0KDa)
IRF2BP2b (59.5Kda)
GAPDH
1
2
3
4
D
Brain
Heart
Skel Muscle
Pancreas
Testis
110
80
60
50
40
IRF2BP2
GAPDH
E
IRF2BP2a
IRF2BP2b
GM
DM
6
12
24
36
48
80
60
50
40
30
IRF2BP2b
clipped
IRF2BP2b?

Figure 5. IRF2BP2 cellular localization changes in differentiating skeletal muscle. IRF2BP2 is a nuclear protein in C_2C_{12} myoblasts but is also found in the cytoplasm 72 hours following differentiation. Note in upper panel white arrows show mitotic figures and cytosolic localization of IRF2BP2 in dividing myoblasts. Nuclei are revealed with DAPI in blue and IRF2BP2 is red. Scale bars are 50 μm.

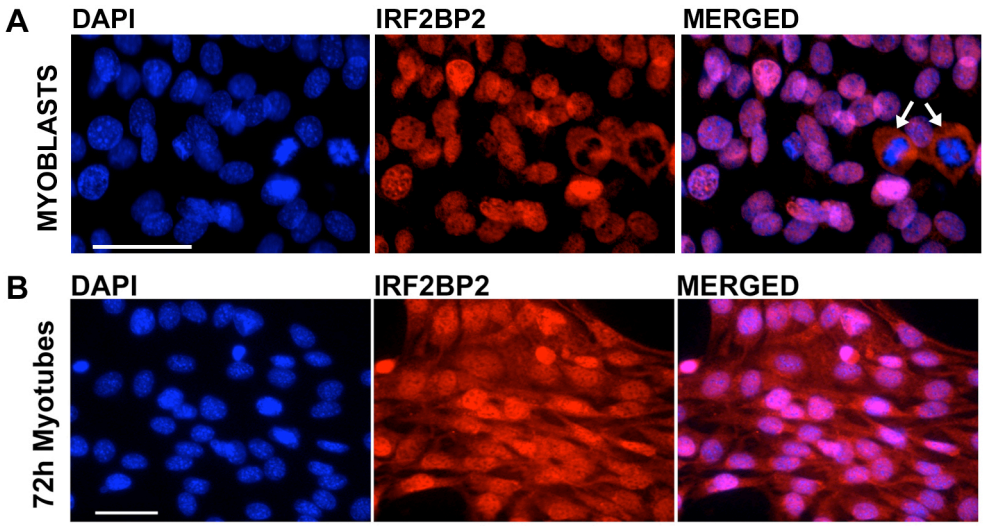
A
DAPI
IRF2BP2
MERGED
MYOBLASTS
B
DAPI
IRF2BP2
MERGED
72h Myotubes

(arrows, **Fig. 5**). However, 72 hours after skeletal muscle differentiation, IRF2BP2 is found both in the nucleus and cytoplasm of C_2C_{12} myotubes. Treatment of C_2C_{12} myotubes for 4 hours with 5 μM leptomycin B, an inhibitor of CRM1-dependent nuclear export, did not increase nuclear retention of IRF2BP2 (data not shown), indicating that translocation of IRF2BP2 to the cytoplasm is not CRM1-dependent in myotubes.

During mouse embryonic development, IRF2BP2 expression was ubiquitous at embryonic day 10.5 (E10.5) and E15.5. However, a progressive restriction of IRF2BP2 expression to the lungs, heart and skeletal muscle was apparent in the mouse fetus by E17.5 (**Fig. 6**). Expression in the E17.5 brain and liver was markedly reduced compared to E15.5.

IRF2BP2 is a transcription activator to VEGF-A expression

We next tested the effect of IRF2BP2 over-expression on the activity of the mouse VEGFA promoter (**Figs. 7A, B**). IRF2BP2 had little effect on its own, or when co-expressed with TEAD4 or VGLL4, however, when all three were co-expressed in CV1 cells, the VEGFA promoter was activated more than 6 fold above background (**Fig. 7A**). Interestingly, coexpression of IRF2BP2 with TEAD1 was sufficient to coactivate the VEGFA promoter 7 fold, without the addition of exogenous VGLL4 (**Fig. 7B**). Thus, IRF2BP2-dependent coactivation of VEGFA expression shows a differential requirement for VGLL4 in the presence of TEAD1 and TEAD4. However, unlike IRF2BP2, IRF2BP1 did not regulate the VEGFA promoter (**Fig. 7C**).

We next tested whether endogenous VEGFA expression could be upregulated by IRF2BP2/TEAD1 coexpression (**Figs. 7D, E**). Qualitative reverse transcription

PCR detected the VEGFA isoforms that are upregulated (**Figs. 7D**). Co-expression of IRF2BP2 and TEAD1 in C_2C_{12} myoblasts upregulated predominantly the expression

Figure 6. IRF2BP2 expression during mouse development. IRF2BP2 expression is ubiquitous in the developing embryo and becomes restricted to the heart, lung and skeletal muscles in late fetal development. (**A & B**), embryonic day 10.5 (E10.5), (**C & D**), E15.5 and (**E & F**), E17.5 mouse embryo sagital sections were stained with pre-immune rabbit serum (**A**, **C**, and **E**) or the IRF2BP2 immune serum (**B**, **D**, and **F**). (**G**) Note that by E17.5 IRF2BP2 remains elevated in the lung, ventricular myocardium and diaphragm (green inset in panel F). The liver (labeled **L** in panel **F**) expresses lower levels of IRF2BP2. Sections were stained with alkaline phosphatase conjugated anti-rabbit secondary antibody.

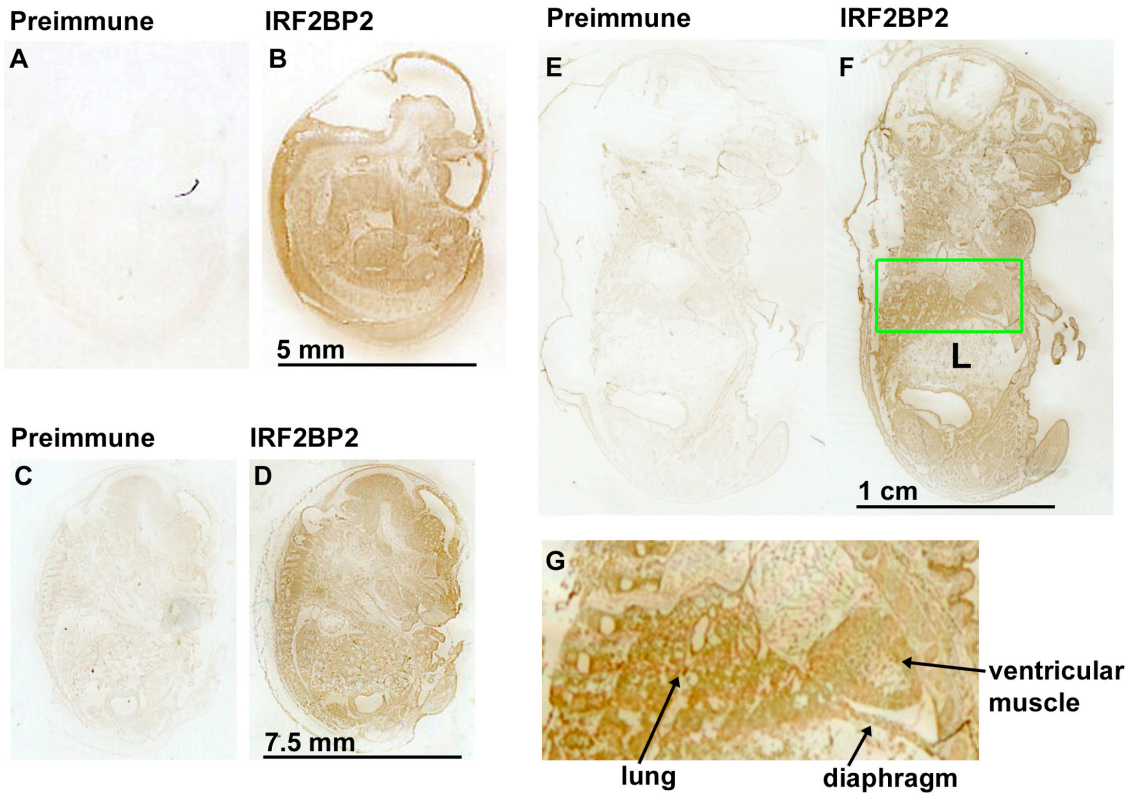
Preimmune
IRF2BP2
A
B
5 mm
Preimmune
IRF2BP2
C
D
7.5 mm
Preimmune
IRF2BP2
E
F
L
1 cm
G
ventricular muscle
lung
diaphragm

Figure 7. IRF2BP2 is a strong coactivator of the VEGFA promoter and augments endogenous VEGFA expression. (**A**) Over-expression of IRF2BP2, TEAD4 and VGLL4 strongly coactivated the VEGFA promoter in CV1 cells (n=6). (**B**) IRF2BP2 and TEAD1 co-activated the VEGFA promoter (n=6). (**C**) IRF2BP1 does not coactivate the VEGFA promoter (n=4). (**D**) Schematic diagram of VEGF-specific primers to exons 3 and 8 used to detect alternatively spliced mRNA isoforms in C_2C_{12} cells. VEGF164 and VEGF120 mRNAs are the predominant isoforms detected after induction by TEAD1/IRF2BP2. (**E**) C_2C_{12} myoblasts were transiently transfected with empty expression vector (mock), TEAD1 (TEF-1), IRF2BP2 or TEAD1/IRF2BP2. VEGFA protein expression, detected by immunoblot, was activated by IRF2BP2/TEAD1 (n=3). (**F**) IRF2BP2 protein expression was reduced by IRF2BP2-specific shRNA (+) and this also interfered with VEGFA expression in C_2C_{12} cells cultured in high serum (MB, myoblasts) or 12 and 24 houras after switching to differentiation medium. Control non-silencing shRNA (-) did not affect IRF2BP2 or VEGFA expression. GAPDH expression was not affected by IRF2BP2 knockdown (n=3).

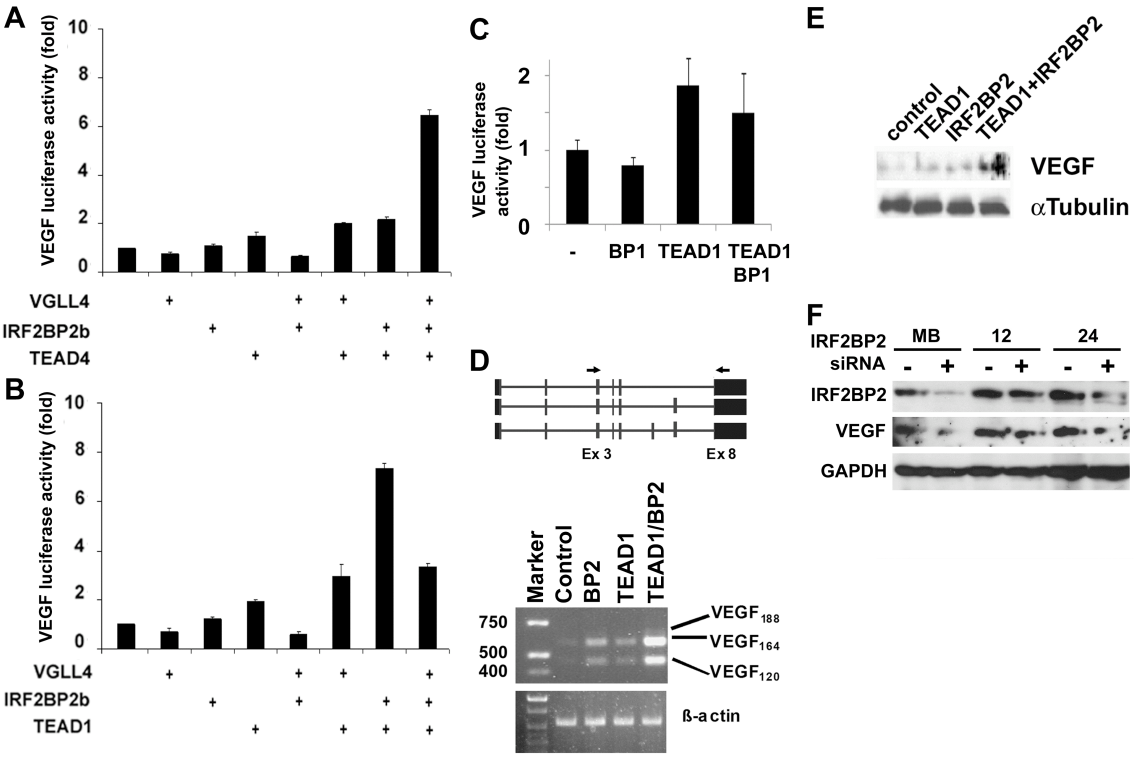
A
VEGF luciferase activity (fold)
10
8
6
4
2
0
VGLL4
IRF2BP2b
TEAD4
B
VEGF luciferase activity (fold)
10
8
6
4
2
0
VGLL4
IRF2BP2b
TEAD1
C
VEGF luciferase activity (fold)
2
1
0
-
BP1
TEAD1
TEAD1 BP1
D
Ex 3
Ex 8
Marker
Control
BP2
TEAD1
TEAD1/BP2
750
500
400
VEGF188
VEGF164
VEGF120
ß-actin
E
control
TEAD1
IRF2BP2
TEAD1+IRF2BP2
VEGF
αTubulin
F
IRF2BP2
MB
12
24
siRNA
- + - + - +
IRF2BP2
VEGF
GAPDH

of the $VEGF_{120}$ and $VEGF_{164}$ isoforms (bottom, **Fig. 7D**). In C_2C_{12} myoblasts, over-expression of IRF2BP2 or TEAD1 were sufficient to increase VEGFA protein, that was further elevated by IRF2BP2/TEAD1 co-expression (**Fig. 7E**). Given that IRF2BP2 protein expression is upregulated in C_2C_{12} cells during muscle differentiation (**Fig. 4E**), and IRF2BP2/TEAD1 could coactivate endogenous VEGFA expression in myoblasts (**Figs 7D, E**), we tested whether loss of IRF2BP2 would cause reduced VEGFA expression. Using shRNA lentiviral vector, we selectively knocked down IRF2BP2 expression in C_2C_{12} cells before and after the induction of muscle differentiation by serum withdrawal. Not only was IRF2BP2 expression reduced by the IRF2BP2 shRNA, VEGFA expression was also reduced, whereas the control protein GAPDH was not, demonstrating that the effect is specific (**Fig. 7F**). Thus, IRF2BP2 is necessary for VEGFA expression in C_2C_{12} muscle cells.

Given the coactivation of VEGFA expression by IRF2BP2 and the high levels of IRF2BP2 mRNA but not protein in adult skeletal muscle, we asked whether IRF2BP2 protein responds to muscle ischemia. Femoral artery ligation caused a 4-fold increase in IRF2BP2 protein expression in ischemic muscle (**Figs. 8A, B, C**). Similarly, myocardial infarction induced by coronary artery ligation markedly increased IRF2BP2 expression in the ischemic myocardium (**Figs 8D, E**). Of note, staining was predominantly cytoplasmic both in ischemic skeletal and cardiac muscle. Thus, our results show that IRF2BP2 protein expression is responsive to tissue ischemia.

Figure 8. Ischemia markedly upregulates IRF2BP2 protein levels in skeletal and cardiac muscle. (**A**) Immunofluorescence reveals elevated cytoplasmic expression in ischemic rat hindlimb 48 hours after ischemia. Trace levels of IRF2BP2 were detected in the normoxic contralateral muscle. n=4. Scale bar 50 μm. (**B**) Immunoblot analysis of total protein from rat normoxic contralateral control (N) and ischemic (I) muscle 48 hours after arterial occlusion. (**C**) Ischemia was associated with a 4 fold increase in IRF2BP2 levels, quantitated using ImageQuant software. GAPDH antibody verified protein loading. N=4 ($p<0.05$ by independent samples t-test). (**D**) Myocardial infarction increases IRF2BP2 protein in the ischemia myocardium 48 hours after left main coronary artery ligation (right panel). Left panel is control myocardium of a sham-operated mouse. Note especially elevated IRF2BP2 expression in the subendocardial layer. Scale bar 100 μm. (**E**) Immunoblot analysis reveals elevated IRF2BP2 levels in mouse whole ventricular myocardium after infarction (n, 24 and 48 refer to normoxic myocardium and myocardium 24 and 48 hours after infarction, respectively).

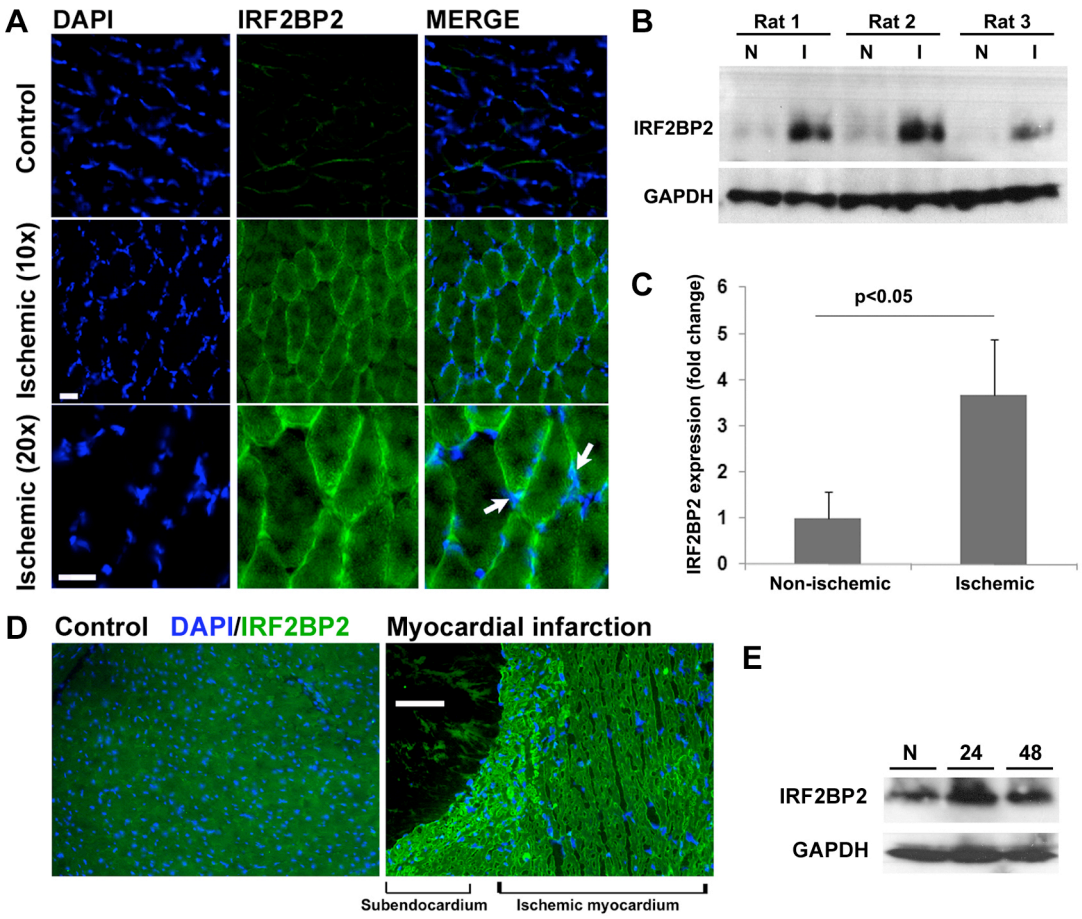
A
DAPI
IRF2BP2
MERGE
Control
Ischemic (10x)
Ischemic (20x)
B
Rat 1
Rat 2
Rat 3
N
I
N
I
N
I
IRF2BP2
GAPDH
C
p<0.05
IRF2BP2 expression (fold change)
0
1
2
3
4
5
6
Non-ischemic
Ischemic
D
Control
DAPI/IRF2BP2
Myocardial infarction
Subendocardium
Ischemic myocardium
E
N
24
48
IRF2BP2
GAPDH

DISCUSSION

Here we report the discovery of IRF2BP2 as a novel interacting partner of the TEAD4/VGLL4 transcription complex that coactivates the expression of VEGFA. IRF2BP2 knockdown reduced VEGFA expression, demonstrating that it is required for VEGFA expression in muscle. We showed that IRF2BP2 is muscle-enriched and ischemia-inducible, supporting a role for this protein in the regulation of angiogenesis.

The IRF2BP1 and IRF2BP2 proteins were initially identified by their binding and inhibition of IRF2 activity in response to interferon-β (Childs and Goodbourn, 2003). More recently, EAP1 is a third family member that was identified in hypothalamic GnRH producing neurons (Heger *et al.*, 2007). Although overall sequence similarity is approximately 50%, all members of this family share a highly conserved C-terminal C3HC4 RING finger domain and an N-terminal Cys4 zinc finger of unknown function. Our phylogenetic analysis showed that the 3 paralogues arose in a common ancestor to fish and mammals, some 420 million years ago (**Fig. 2**), suggesting that functional divergence occurred early in vertebrate evolution.

IRF2BP2, but not IRF2BP1, activated VEGFA expression. IRF2BP1 and IRF2BP2 are structurally divergent and growing evidence points to their functional divergence, as well. IRF2BP1 binds to the transforming growth factor β (TGFB β)-induced factor homeobox 1 (TGIF1) to augment TGFβ signaling (Faresse *et al.*, 2008) through a sequence (underlined in Figure 1) that is conserved in EAP1 but not in IRF2BP2. So EAP1 may interact, but IRF2BP2 is unlikely to interact, with TGIF. In addition, the putative VGLL4 interaction domain is present in IRF2BP2 but not in IRF2BP1, and this may account for the inability of IRF2BP1 to activate VEGFA expression.

Our data show that IRF2BP2 with TEAD1 can directly activate VEGFA

expression, whereas IRF2BP2 with TEAD4 is not sufficient and also requires VGLL4 to coactivate the VEGFA promoter. We do not yet understand the reason for the different requirement for VGLL4 between TEAD1 and TEAD4. Although TEAD1 and TEAD4 are highly conserved in their amino acid sequence, TEAD1 and TEAD4 regulate cardiac gene expression differently. For example, TEAD4, but not TEAD1, activates gene expression in response to α_1-adrenergic signaling in cardiac myocytes (Stewart *et al.*, 1998) through a TEAD4-specific phosphorylation site (Ueyama *et al.*, 2000). In addition, under normoxic conditions TEAD1 is 10 times more abundant in cardiac and 3 times more abundant in skeletal muscle nuclear extracts than TEAD4 (Chen *et al.*, 2004b). However, unlike TEAD1, TEAD4 expression is hypoxia-inducible (Shie *et al.*, 2004) and is likely to become functionally more important during ischemia. Also, the effect of TEAD factors on the VEGFA promoter were reported to be independent of a canonical TEAD *cis*-element (Shie *et al.*, 2004), so that the effects of IRF2BP2 could be indirect working through other *cis*-elements and transcription factors.

IRF2BP2 has been reported to be a pro-survival factor that antagonizes p53-mediated apoptosis through an unknown mechanism (Koeppel *et al.*, 2009). Interestingly, p53 upregulates the micro RNA miR34a, causing a 4-fold reduction in IRF2BP2 mRNA expression (Chang *et al.*, 2007). Proteins that are anti-apoptotic are often selectively targeted by caspases, and a large scale proteomic screen identified fragments of IRF2BP2 (Dix *et al.*, 2008) clipped at the aspartic acid residue at position 495 (**Fig. 1**). This cleavage would remove the RING finger motif and possibly an essential E3 ubiquitin ligase function of IRF2BP2. Of note, a shorter fragment of IRF2BP2 was detected during C_2C_{12} skeletal myogenesis, suggesting that IRF2BP2 processing may be targeted by caspase 3 as an intrinsic part of the myogenic

program. Caspase 3 activation is required for myogenic differentiation (Fernando *et al.*, 2002; Larsen *et al.*, 2010).

It is intriguing that adult human or rat skeletal muscles do not express high levels of IRF2BP2 protein, yet rat hindlimb muscles responded to ischemia with elevated IRF2BP2 protein. In particular, given the high levels of IRF2BP2 mRNA detected by Northern blot analysis, these observations suggest either that the IRF2BP2 mRNA is not translated in normoxic adult skeletal muscle or that the protein is highly labile and stabilized by hypoxia. Selective hypoxia-inducible mRNA translation has been described for VEGFA through an unknown mechanism (Young *et al.*, 2008). On the other hand, if IRF2BP2 protein is labile, this would be reminiscent of the degradation of the classical hypoxia-inducible factor HIF1α under normoxic conditions and its stabilization during hypoxia. These mechanisms remain to be characterized.

We found widespread expression of IRF2BP2 protein throughout the mouse embryo at E10.5. At this time, the ventricular myocardium is actually ischemic (Krishnan *et al.*, 2008). Intriguingly, this is also the time at which HIF1α levels decline in the embryonic mouse heart (Krishnan *et al.*, 2008). The fact that IRF2BP2 levels remain high throughout mouse development in the heart, skeletal muscle and lung tissues at a time when HIF1α levels have already declined suggests that IRF2BP2 may replace HIF1α in promoting VEGF expression at later development stages. IRF2BP2 likely has additional functions. Understanding the role of IRF2BP2 in development awaits the production of mice with conditional deletion of the IRF2BP2 gene.

Little is known about the function of IRF2BP2 in the heart. However, in addition to hypoxia-dependent regulation of IRF2BP2 protein levels that we reported

here, microarray-based studies suggest that transcription of the IRF2BP2 gene also responds to stress. Heart failure induced by dys-synchronous pacing reduced IRF2BP2 mRNA expression in the lateral wall of the left ventricle compared to the anterior wall (Barth *et al.*, 2009). Importantly, cardiac resynchronization therapy rescued the heart failure phenotype and restored IRF2BP2 expression in the lateral wall (Barth *et al.*, 2009). In another example, increased IRF2BP2 mRNA was detected in the interventricular septum following acute myocardial infarction (Harpster *et al.*, 2006). Mouse hearts deficient in the estrogen receptor related nuclear orphan receptor ERRα, a key regulator of mitochondrial biogenesis, show markedly elevated levels of IRF2BP2 mRNA (Dufour *et al.*, 2007). Taken with our results, IRF2BP2 mRNA and protein appear sensitive to transcriptional and post-transcriptional regulation and to the energetic status of cardiac myocytes. An intriguing feature of the myocardium is the higher levels of IRF2BP2 protein detected in our western blot analyses in the human and mouse heart than is found in skeletal muscle. Is the myocardium in a perpetual state of near-ischemia, thereby ensuring maximal vascularization? To answer this question, it will be important to identify the mechanisms that control IRF2BP2 protein levels.

In conclusion, VEGF is a critical growth factor for angiogenesis in vascular and cardiac development, involved in the regeneration of vasculature and the restoration of blood flow in ischemic tissue. Here, we identified IRF2BP2 as a novel essential coactivator of VEGFA expression in muscle cells. Moreover, IRF2BP2 protein is elevated in response to cardiac and skeletal muscle ischemia. These findings further our understanding of the mechanisms governing VEGFA expression, and may have implications in the development of therapies targeted at restoring perfusion in ischemic tissues.

Schematic 2. A brief summary of IRF2BP2-mediated VEGF expression. Muscle ischemia induces the expression of IRF2BP2, which in combination with TEAD proteins activate VEGF-A expression in C_2C_{12} myoblasts. On the other hand, myogenic differentiation also promotes IRF2BP2 protein expression that subsequently may be involved in the process.

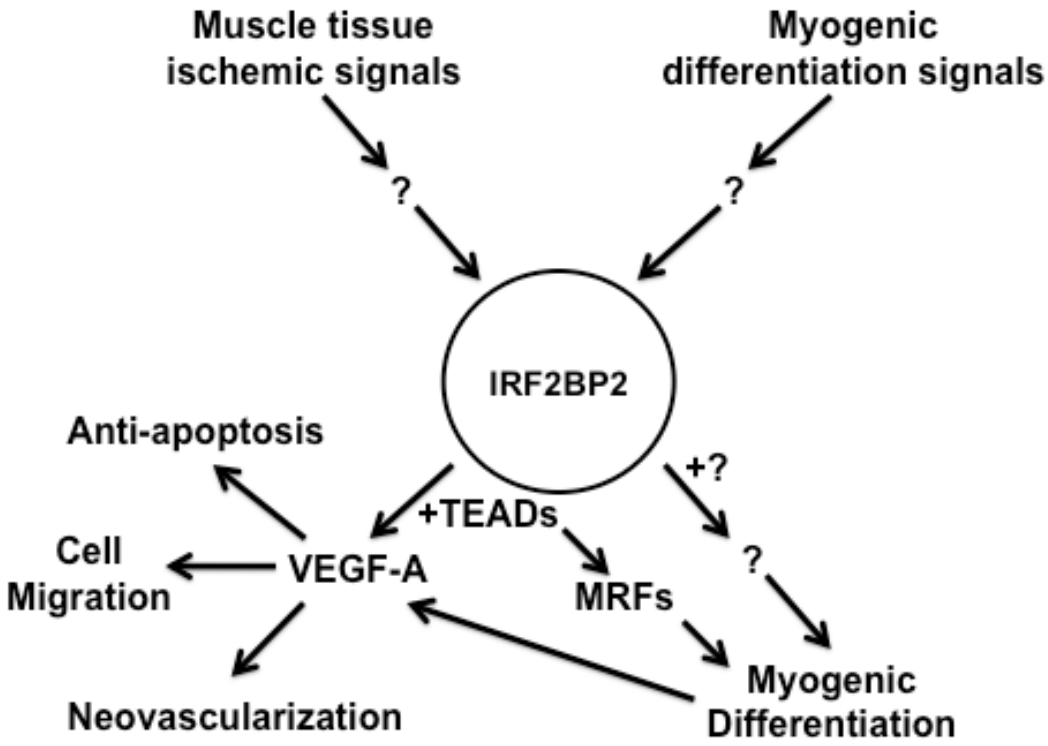
Muscle tissue
ischemic signals
Myogenic
differentiation signals
?
?
IRF2BP2
Anti-apoptosis
+?
+TEADs
Cell
Migration
VEGF-A
MRFs
?
Myogenic
Differentiation
Neovascularization

CHAPTER 4

Identification of a Phosphorylation-dependent Nuclear Localization Motif in Interferon Regulatory Factor 2 Binding Protein 2

Allen C. T. Teng[*‡], Naif A. M. Al-montashiri[*‡], Brian L. M. Cheng[*], Philip Lou[*], Pinar Ozmizrak[*], Hsiao-Huei Chen[†], and Alexandre F. R. Stewart[*‡1]

[*] University of Ottawa Heart Institute, Ottawa, Ontario, Canada

[‡] Department of Biochemistry, Microbiology, and Immunology, University of Ottawa, Ottawa, Ontario, Canada

[†] Ottawa Hospital Research Institute, Ottawa, Ontario, Canada

Short title: Phosphorylation controls IRF2BP2 nuclear import

ABSTRACT

Interferon regulatory factor 2 binding protein 2 (IRF2BP2) is a muscle-enriched transcription factor required to activate vascular endothelial growth factor-A (VEGFA) expression in muscle. IRF2BP2 is found in the nucleus of cardiac and skeletal muscle cells. During the process of skeletal muscle differentiation, some IRF2BP2 becomes relocated to the cytoplasm, although the functional significance of this relocation and the mechanisms that control nucleocytoplasmic localization of IRF2BP2 are not yet known. Here, by fusing IRF2BP2 to green fluorescent protein and testing a series of deletion and site-directed mutagenesis constructs, we mapped the nuclear localization signal (NLS) to an evolutionarily conserved sequence ^{354}ARKRKPSP^{361} in IRF2BP2. This sequence corresponds to a classical nuclear localization motif bearing positively charged arginine and lysine residues.

Substitution of arginine and lysine with negatively charged aspartic acid residues blocked nuclear localization. However, these residues were not sufficient because nuclear targeting of IRF2BP2 also required phosphorylation of serine 360 (S360). Many large-scale phosphopeptide proteomic studies had reported previously that serine 360 of IRF2BP2 is phosphorylated in numerous human cell types. Alanine substitution at this site abolished IRF2BP2 nuclear localization in C_2C_{12} myoblasts and CV1 cells. In contrast, substituting serine 360 with aspartic acid forced nuclear retention and prevented cytoplasmic redistribution in differentiated C_2C_{12} muscle cells. As for the effects of these mutations on VEGF-A promoter activity, the S360A mutation interfered with VEGF-A activation, as expected. Surprisingly, the S360D mutation also interfered with VEGFA activation, suggesting that this mutation, while enforcing nuclear entry, may disrupt an essential activation function of IRF2BP2. In summary, nuclear localization of IRF2BP2 depends on phosphorylation near a

conserved NLS. Changes in phosphorylation status likely control nucleocytoplasmic localization of IRF2BP2 during muscle differentiation.

INTRODUCTION

Interferon regulatory factor 2 binding protein 2 (IRF2BP2), together with the related protein IRF2BP1, were initially discovered as interacting partners to interferon regulatory factor 2 (IRF2) in a yeast two-hybrid screening assay (Childs and Goodbourn, 2003). A third homolog of IRF2BP2 called enhanced at puberty 1 (EAP1, formerly known as C14orf4) is expressed in the mediobasal hypothalamus and plays a critical function in regulating the female reproductive neuroendocrine axis (Heger *et al.*, 2007). All three are nuclear proteins.

Structurally, IRF2BP2 is encoded by 2 exons producing 3 alternatively spliced proteins IRF2BP2a of 587, IRF2BP2b of 561 and IRF2BP2c of 163 amino acids depending on the use of alternative donor (2a and 2b) and acceptor (2c) splice sites. IRF2BP2a and b isoforms have a Zinc-finger motif at their N-terminus, missing in the IRF2BP2c isoform, and a C3HC4 RING-finger motif at their C-terminus. The function of the Zinc-finger motif appears to enable homo- and hetero-dimerization between different members of the IRF2BP2 family (Yeung *et al.*, 2011). The RING-finger motif from amino acids 456–587 is sufficient to interact with IRF2 (Childs and Goodbourn, 2003) and also with nuclear receptor interacting factor 3 (NRIF3) (Tinnikov *et al.*, 2009). IRF2BP2 was described as a co-repressor of IRF2, inhibiting the expression of interferon-responsive genes.

The tumor suppressor p53 binds to the IRF2BP2 promoter and transactivates its expression in response to actinomycin D treatments in both cervical carcinoma (HeLa) and osteosarcoma (U2OS) (Koeppel *et al.*, 2009). Increased endogenous IRF2BP2 protein levels in turn suppress the induction of apoptosis after genotoxic stress. Specifically, IRF2BP2 suppresses the transactivation activity of p53 on both Bax and p21 promoters. Anti-apoptotic activity was also ascribed to IRF2BP2 due to

its modulation of a death domain in NRIF3 (Tinnikov *et al.*, 2009; Yeung *et al.*, 2011).

We identified IRF2BP2 as a cofactor of VGLL4 in a yeast two-hybrid screen (Teng *et al.*, 2010). VGLL4 is itself a cofactor of the TEAD transcription factors (Chen *et al.*, 2004d), that play a critical role controlling gene expression in skeletal, cardiac and smooth muscle cells (Yoshida, 2008). We showed that transient over-expression of IRF2BP2 and TEAD1 could induce the expression of vascular endothelial growth factor-A (VEGF-A) in murine C_2C_{12} myoblasts (Teng *et al.*, 2010). We also discovered that IRF2BP2 protein levels increase in response to ischemia in hindlimb and cardiac muscle. Whereas endogenous IRF2BP2 found in murine C_2C_{12} myoblasts is nuclear, following ischemia, IRF2BP2 is mostly cytoplasmic. This discrepancy suggests a potential mechanism for modulating IRF2BP2 translocation across the nuclear membrane.

Nucleocytoplasmic shuttling is a carefully regulated process controlling the import and export of both mRNA and proteins (Adam and Gerace, 1991; Germain *et al.*, 2010). To cross the nuclear membrane, polypeptides use different mechanisms for translocation; small proteins (<40kDa) diffuse through the membrane passively while large proteins (>40kDa) are actively transferred by the nuclear pore complexes (NPCs) on the nuclear membrane (Paine *et al.*, 1975). Nucleocytoplasmic transport encompasses many hierarchical steps. To initiate the process, a cargo protein heterodimerizes with karyopherin via classical nuclear localization signals (NLS; K-K/R-X-K/R, K= lysine, R= arginine, X= any amino acids) (Adam and Gerace, 1991; Zanta *et al.*, 1999). Next, physical binding of the guanosine-5'-diphosphate (GDP)-bound Ran molecule to the complex signals to cross the membrane. Once inside the nucleus, GTP exchange factor (GEF) facilitates the GDP to guanosine-5'-triphosphate

(GTP) exchange process, leading to the release of cargo protein. One of the classical examples of a nuclear shuttled protein is the T-antigen of SV40 (Miyamoto *et al.*, 1997).

In this report, we used deletion and site-directed mutagenesis to localize a conserved functional NLS in IRF2BP2. In addition, we found that phosphorylation of serine residue 360 (S360) adjacent to the NLS is also involved in controlling the nuclear entry of the protein. *In silico* database mining revealed that this serine residue is phosphorylated in IRF2BP2 and IRF2BP1, and sequence comparisons revealed that this motif is conserved in all members of the IRF2BP2 family of transcription factors. Thus, our study is the first to reveal a conserved functional domain controlling nuclear import in IRF2BP2.

METHODS AND MATERIALS

Construction of plasmids

Human IRF2BP2a (AY278023) was first amplified by PCR with the primers 5'-GGA TCC GGC TCC TCG GACATG GCC-3' (sense primer, BamHI) and 5'-TCT AGA GTC TCT CTC TTT TTT CAC TTT-3' (antisense primer, XbaI) and was then subcloned into TOPO vectors (Invitrogen, Carlsbad, CA). To generate pEGFP-IRF2BP2a, full-length IRF2BP2a was released from TOPO-IRF2BP2a plasmid by BamHI digestion and then subcloned in pEGFP-C1 (Clontech, San Jose, CA). A summary of the GFP-IRF2BP2 fusion constructs is shown in Fig. 6. To generate the GFP-TEAD4 expression construct, TEAD4 was first amplified by PCR with the following primers: 5'- GAA TTC TGG AGC CTT GGA GGG CAC GGC - 3' (EcoRI) and 5'- GGA TCC CCG AGT CTC TCA TTC TTT CAC CAG -3' (BamHI) and subcloned into pEGFP-C1 vector between EcoRI and BamHI sites. For generating mutant constructs, the IRF2BP2 mutants – 355 GAC GAC GAC GAC 358 (aspartic acids), TCT 360 TAT (S360A), and TCT 360 GAT (S360D) - flanked between the endogenous PstI and NcoI in IRF2BP2 were ordered from Integrated DNA Technologies (San Diego, CA) as pIDTSMART-IRF2BP2 and were subcloned in pEGFP-IRF2BP2a (Cloning details will be provided upon inquiry). Similarly, a pEGFP-IRF2BP2b construct was generated by swapping a PstI/NcoI fragment of IRF2BP2b into the pEGFP-IRF2BP2a clone. All plasmid constructs were purified by CsCl-banding and their reading frames were verified by sequencing. DsRed-Rab11 WT (Addgene plasmid 12679) and RFP-LAMP1 (Addgene plasmid 1817) expression vectors were obtained from Addgene (Cambridge, MA). Expression vectors for wild type IRF2BP2, S360A and S360D mutants were generated by subcloning a full-length

EcoR1 fragment from pEGFP-IRF2BP2 into the pXJ40-CMVHA vector. The mouse VEGFA promoter construct was described previously (Teng *et al.*, 2010).

Tissue culture, transient transfections and luciferase assays

C_2C_{12} myoblasts and African green monkey kidney (CV1) cells were obtained from American Type Culture Collection (Rockville, MD). Cells were maintained in high glucose DMEM with 20% FBS (or 10% FBS for CV1), 100U/ml penicillin, 100ug/ml streptomycin. Lipofectamine 2000 (Invitrogen, Carlsbad, CA) and GenJet Reagent (Cat # SL100489- C_2C_{12}, SignaGen Laboratories, Ijamsville, MD) were used to transfect CV1 and C_2C_{12} myoblasts, respectively, according to the manufacturer's instructions. Luciferase assays were conducted as described previously (Teng *et al.*, 2010) and luciferase activities were expressed as mean fold ± SEM relative to the empty pXJ40CMV vector. Differences between fold luciferase activities were compared by Student's t-test and considered significant at $p<0.05$.

Protein kinase inhibitors

The protein kinase A (PKA) inhibitor H89 (working concentration: 20 μM, Cat. #: B1427), the inhibitor of phosphoinositide 3-kinases LY294002 (10 μM, L9908), and the MEK1/MEK2 inhibitor U0126 (10 μM, #U120) were from Sigma-Aldrich (Oakville, ON., Canada). The calcium/calmodulin-dependent protein kinase II (CaMKII) inhibitor CK-59 (100 μM, #208922) and the ribosomal S6 kinase (RSK) inhibitor SL0101 (10 μM, #559285) were from Calbiochem (Gibbstown, NJ). The cyclin dependent kinase inhibitor olomoucine (10 μM, #V2372) was from Promega (Madison, WI).

Immunofluorescence

The rabbit polyclonal anti-IRF2BP2 antibody was described previously (Teng *et al.*, 2010). Rabbit polyclonal PRDX3 antibody (ab50300) was purchased from Abcam Inc., (Cambridge, MA). Alexa488-conjugated goat anti-mouse and Alexa594-conjugated goat anti-rabbit antibodies were from Santa Cruz Biotechnology Inc., (Santa Cruz, CA). 48-hours post transfection, cells were washed twice with 1x phosphate-buffered saline (PBS; 3.2 mM Na_2HPO_4, 0.5 mM KH_2PO_4, 1.3 mM KCl, 135 mM NaCl, pH 7.4), fixed in ice-cold methanol at -20°C for 10 minutes, washed thrice with 1x PBS, permeabilized by 0.5% Triton-X 100, and washed thrice with 1x PBS. Cells were then counter-stained with 4',6-diamidino-2-pheylindole (DAPI, Sigma), mounted on glass slides, and visualized on a Zeiss M1 microscope.

RESULTS

Identification of NLS in IRF2BP2

IRF2BP2b is a nuclear protein in mouse C_2C_{12} myoblasts that becomes redistributed to the cytoplasm during muscle differentiation (Teng *et al.*, 2010). The nuclear targeting sequence has not been identified in IRF2BP2 so we generated green fluorescent protein (GFP)-IRF2BP2 fusion constructs to enable the identification of sequences necessary and sufficient for this process. The GFP protein is localized to the cytoplasm of C_2C_{12} myoblasts whereas a control construct fusing GFP to the TEAD4 transcription factor is localized to the nucleus of C_2C_{12} myoblasts (**Fig. 1A**). The GFP-IRF2BP2a and GFP-IRF2BP2b fusion proteins were detected in the nucleus of C_2C_{12} myoblasts (**Fig. 1C,D**). Since the both isoforms localized to the nucleus, we chose IRF2BP2a for subsequent studies.

Using convenient restriction sites, we found that the N-terminal sequence of IRF2BP2 encoded by exon 1 (amino acids 1-333) was not imported into the nucleus, whereas a fragment encoded largely by exon 2 (amino acids 333-587) was localized in the nucleus (**Fig. 2**). A fragment containing amino acids 101-422 was also localized in the nucleus, identifying a nuclear targeting sequence between amino acids 333 and 422. The GFP-IRF2BP2 (Ex1) fusion protein was found in cytoplasmic speckles (**Fig. 2B,C**). To determine the cellular localization of this fragment, we tested for colocalization with a mitochondrial protein (peroxiredoxin 3, PRDX3), a lysosome associated membrane protein (LAMP) and a Golgi body targeted protein Ras-related protein 11 (Rab11) using specific antibodies. We found that the N-terminal fragment of IRF2BP2 is targeted to the lysosome, and is likely degraded (**Fig. 2C**).

Figure 1. Green fluorescent protein (GFP) full-length IRF2BP2 fusion constructs are targeted to the nucleus. A. GFP alone was localized in the cytoplasm of C_2C_{12} myoblasts. B. A GFP fusion construct with the nuclear-targeted transcription factor TEAD4 was nuclear localized in C_2C_{12} myoblasts. C. GFP-IRF2BP2a was localized to the nucleus of C_2C_{12} myoblasts. D. GFP-IRF2BP2b was also nuclear in C_2C_{12} myoblasts. Nuclei were revealed by DAPI in blue. Scale bar, 50 μm.

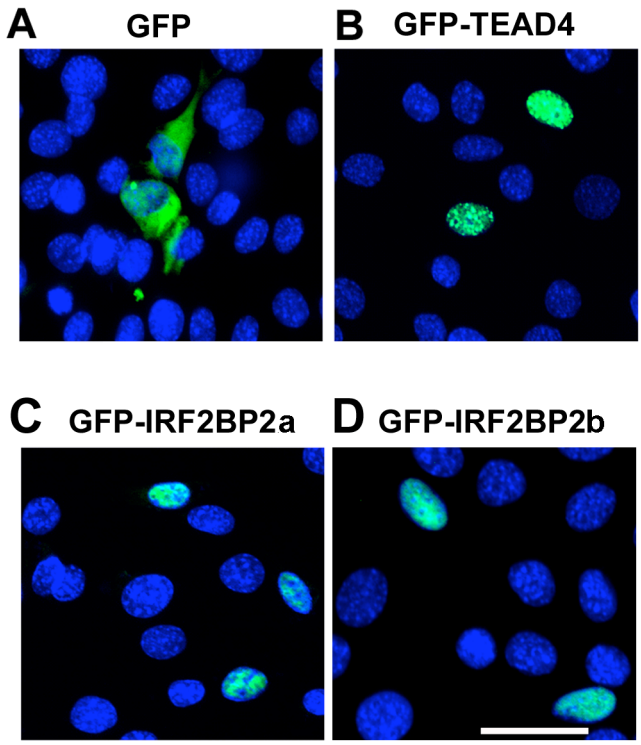
A
GFP
B
GFP-TEAD4
C
GFP-IRF2BP2a
D
GFP-IRF2BP2b

Figure 2. Nuclear localization signal is contained within the C-terminal half of IRF2BP2. A. Diagram of GFP fusion IRF2BP2 deletion contructs used to localize the NLS. B. The N-terminal fragment, GFP-IRF2BP2(Ex1) is cytoplasmic, whereas the middle, GFP-IRF2BP2(MscI), and C-terminal, GFP-IRF2BP2(Ex2P), fragments are nuclear in C_2C_{12} myoblasts. C. The N-terminal fragment is targeted to the lysosome in C_2C_{12} myoblasts. Mitochondrial-specific peroxiredoxin 3 (PRDX3) and Golgi body-sepcific Ras-related protein 11 (Rab11) did not, whereas the lysosome-associated membrane protein (LAMP) did co-localize with GFP-IRF2BP2(Ex1). Scale bars, 50 μm.

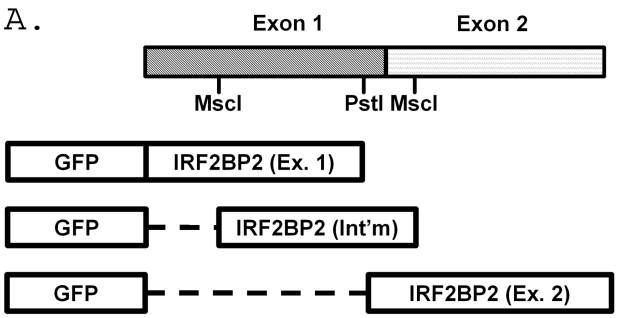
A.
Exon 1
Exon 2
MscI
PstI MscI
GFP
IRF2BP2 (Ex. 1)
GFP
IRF2BP2 (Int'm)
GFP
IRF2BP2 (Ex. 2)

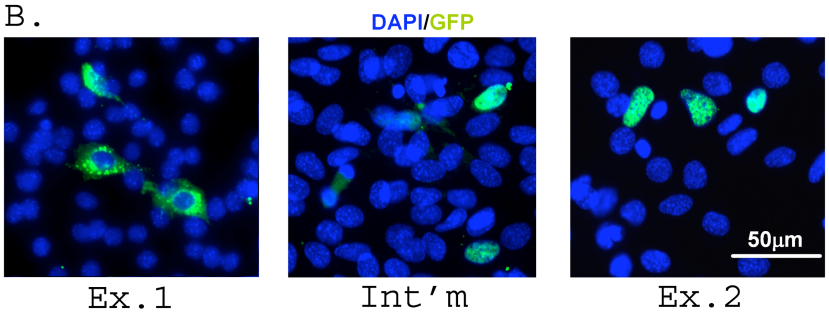
B.
DAPI/GFP
50μm
Ex.1
Int'm
Ex.2

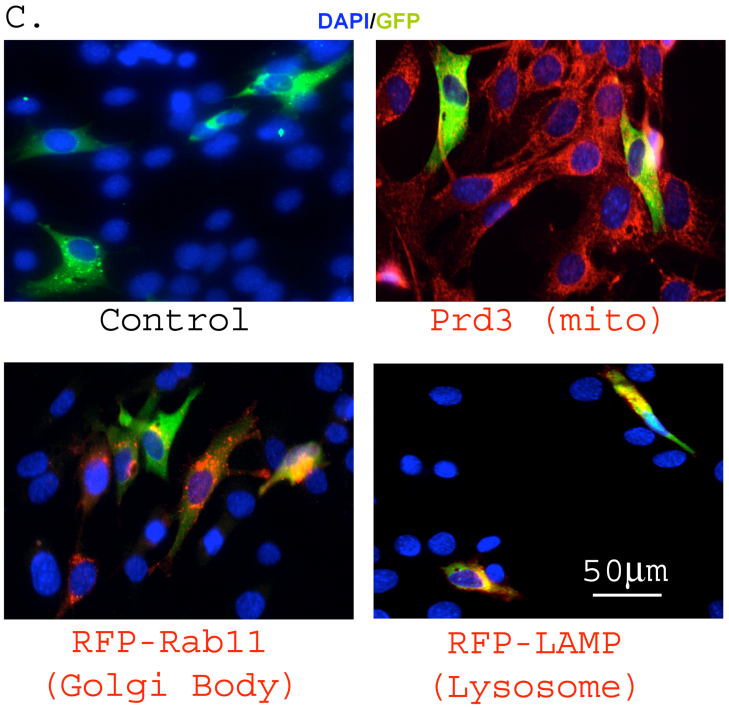
C.
DAPI/GFP
Control
Prd3 (mito)
50μm
RFP-Rab11
(Golgi Body)
RFP-LAMP
(Lysosome)

Given that the C-terminal fragment of IRF2BP2 is targeted to the nucleus, we sought to identify the minimal nuclear localization sequences (NLS) within this fragment. Bioinformatic analyses (**Fig. 3A**) suggested two putative NLS in conserved regions of IRF2BP2, one at the N-terminus of exon 2 encoded sequence we called Ex2N, ^{357}ARKRKP^{364} and the other and the C-terminus we called Ex2C, ^{579}KVKKERD^{587}. To evaluate whether these sites are functional, the second exon was further divided into three parts, namely 333-422, 422-587, and 575-587, fused with GFP, and then transiently overexpressed in C_2C_{12} myoblasts. Here, the 333-422 fragment was found in the nucleus (**Fig. 3B**), but the C-terminal Ex2C 575-587 fragment or the 422-587 fragment did not. Thus, the Ex2C sequence is not an NLS, nor is a cryptic NLS present in the sequences from amino acids 422 to 587. To authenticate the NLS at Ex.2N, positively charged amino acids were replaced by negatively charged aspartic acids (DDDD) using site-directed mutagenesis (**Fig. 3C**). When expressed in C_2C_{12} myoblasts, the aspartic acid mutant remained in the cytoplasm, confirming that the Ex2N NLS in IRF2BP2 is functional (**Fig. 3C**).

Figure 3. Identification of the NLS within the C-terminal half of IRF2BP2. A. Two putative NLS sequences were identified in conserved regions of IRF2BP2. Core arginine (R) and lysine (K) sequences are highlighted in yellow. B. GFP fusion constructs with the amino acid positions indicated were tested in C_2C_{12} myoblasts to reveal that the sequence between amino acid 333 and 422 contains the functional NLS of IRF2BP2. C. Site-directed mutagenesis converting the R and K to aspartic acid (D) residues prevented nuclear localization. Scale bar, 50 μm.

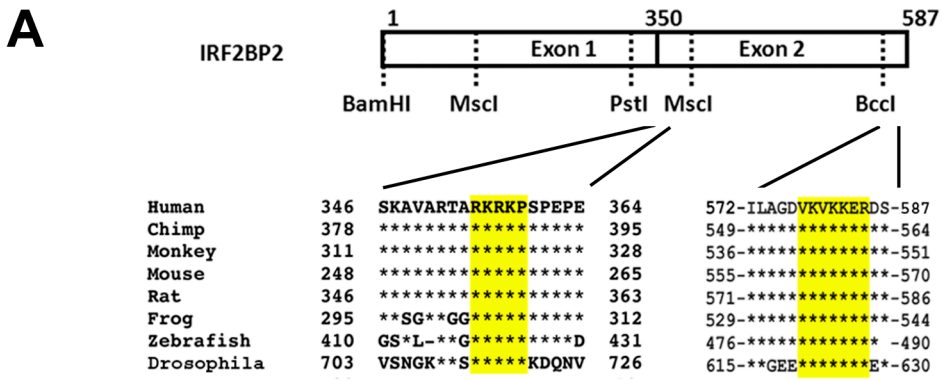
A
IRF2BP2
1
350
587
Exon 1
Exon 2
BamHI
MscI
PstI
MscI
BccI
Human 346 SKAVARTARKRKPSPEPE 364 572-ILAGDVKVKKERDS-587
Chimp 378 ********** 395 549-**********-564
Monkey 311 ********** 328 536-**********-551
Mouse 248 ********** 265 555-**********-570
Rat 346 ********** 363 571-**********-586
Frog 295 **SG**GG********** 312 529-**********-544
Zebrafish 410 GS*L-**G*********D 431 476-********** -490
Drosophila 703 VSNGK**S*****KDQNV 726 615-**GEE*******E*-630

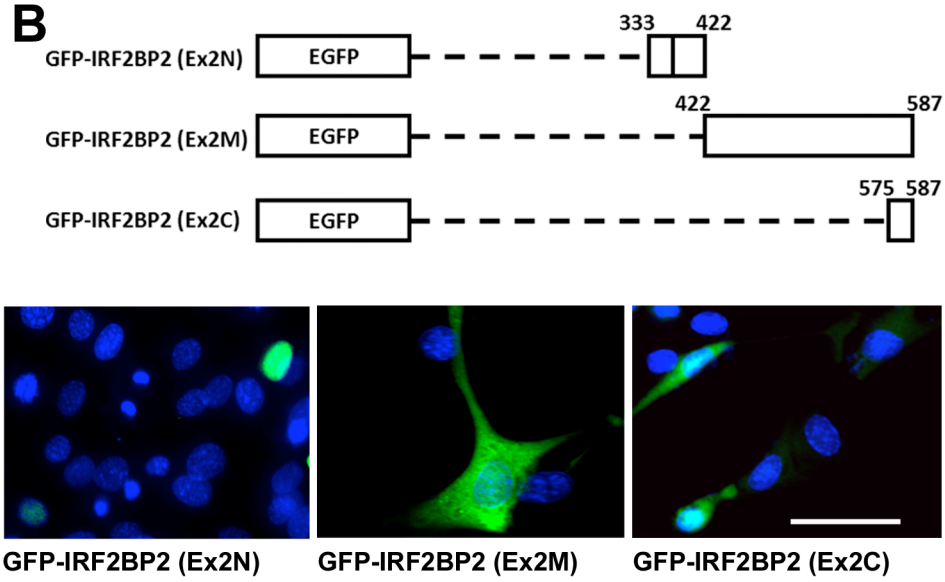
B
333
422
GFP-IRF2BP2 (Ex2N)
EGFP
422
587
GFP-IRF2BP2 (Ex2M)
EGFP
575
587
GFP-IRF2BP2 (Ex2C)
EGFP
GFP-IRF2BP2 (Ex2N)
GFP-IRF2BP2 (Ex2M)
GFP-IRF2BP2 (Ex2C)

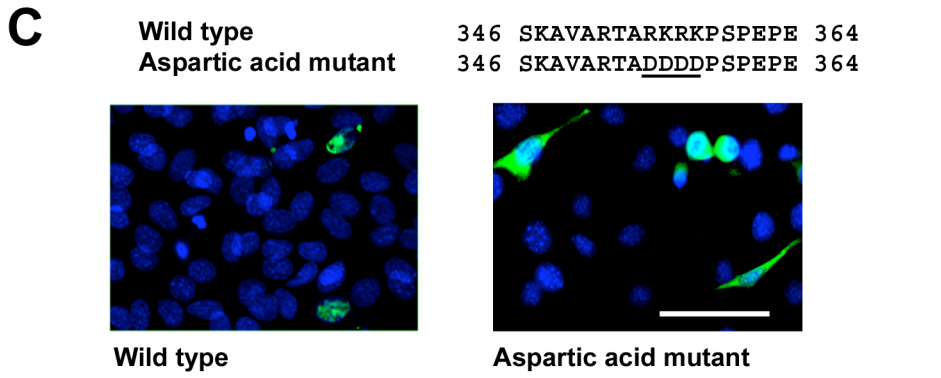
C
Wild type 346 SKAVARTARKRKPSPEPE 364
Aspartic acid mutant 346 SKAVARTADDDDPSPEPE 364
Wild type
Aspartic acid mutant

Phosphorylation of Serine 360 is critical for IRF2BP2 nuclear entry

A survey of phosphopeptide databases generated from large scale proteomic studies that employed mass spectrometry revealed that IRF2BP2 is phosphorylated at serine 360 (S360), two amino acids downstream of the newly identified Ex2N NLS, in many human cell types (**Table 1**). To test whether phosphorylation of S360 affects nuclear import of IRF2BP2, we mutagenized the serine to either an alanine (S360A) that cannot be phosphorylated or to an aspartic acid (S360D) that carries a negative charge and mimics phosphorylation. The GFP-IRF2BP2 S360A mutant was localized in the cytoplasm of C_2C_{12} myoblasts. To rule out that the S360A mutant created a cryptic nuclear export signal, leptomycin B (10 nM) was used to block CRM1-dependent nuclear export, but it did not cause nuclear retention of the GFP-IRF2BP2 S360A mutant (**supplementary data Fig. 1**). Thus, cytosolic localization of the GFP-IRF2BP2 S360A mutant likely results from failure to import rather than a CRM1-dependent nuclear export. In contrast, the GFP-IRF2BP2 S360D mutant was located in the nucleus (**Fig. 4A**). During skeletal muscle differentiation of C_2C_{12} cells, we reported previously that IRF2BP2 is partially relocated to the cytoplasm (Teng *et al.*, 2010). Thus, we asked whether the S360D mutant would enforce nuclear retention of IRF2BP2 in C_2C_{12} cells 72 hours after the induction of muscle differentiation. Both the endogenous IRF2BP2 and the GFP fusion protein bearing full-length wild type IRF2BP2 were localized in both the cytoplasm and nucleus, whereas the S360D mutant was exclusively nuclear (**Fig. 4B**).

When co-expressed with the transcription factor TEAD1, we reported previously that IRF2BP2 strongly co-activates a mouse VEGFA promoter in African green monkey kidney CV1 cells, where endogenous IRF2BP2 levels are low (Teng *et al.*, 2010).

Figure 4. Phosphorylation of serine 360 controls nuclear localization of IRF2BP2. A. Site-directed mutagenesis of serine 360 to alanine (S360A) blocked nuclear localization of IRF2BP2 whereas aspartic acid substitution (S360D) did not differ from wild type and was nuclear localized in C_2C_{12} myoblasts. B. After 72 hours in differentiation medium, the endogenous IRF2BP2 (revealed with IRF2BP2 antibody), as well as GFP-IRF2BP2 (wild type, green), are localized in both the cytoplasm and nucleus of C_2C_{12} myotubes. The S360D mutant was exclusively found in the nucleus in C_2C_{12} myotubes.

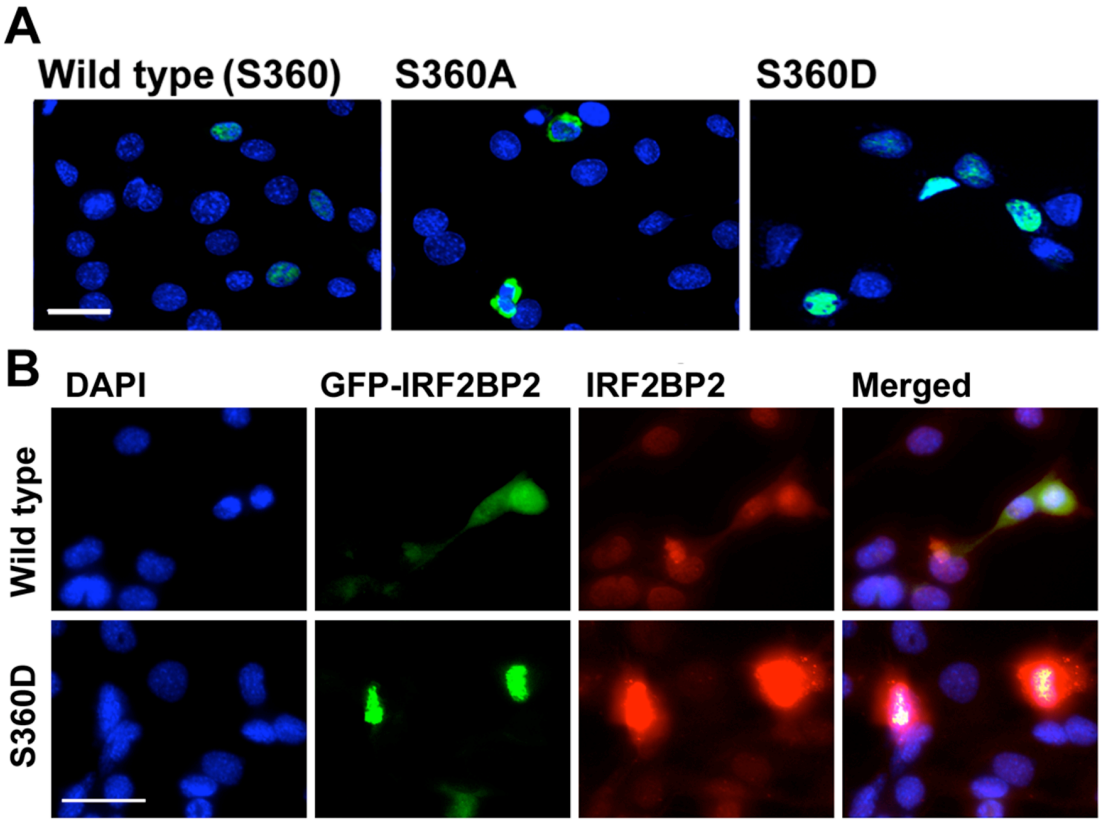
A
Wild type (S360)
S360A
S360D
B
DAPI
GFP-IRF2BP2
IRF2BP2
Merged
Wild type
S360D

We also observed nuclear exclusion of the S360A mutant of IRF2BP2 and nuclear retention of the S360D mutant in CV1 cells (**Fig. 5A**). We next tested whether nuclear exclusion of IRF2BP2 would block and whether forced nuclear retention of IRF2BP2 would enhance mouse VEGF promoter activity in the presence of TEAD1. Compared to wildtype IRF2BP2 co-expressed with TEAD1, not only did the alanine mutant fail to co-activate the VEGFA promoter, as expected, but surprisingly the aspartic acid mutant also failed to co-activate the VEGFA promoter in CV1 cells (**Fig. 5B**). We confirmed that TEAD1 and the wild type and the mutant IRF2BP2 proteins were expressed at comparable levels and were of the expected size by immunoblot analysis of transfected CV1 cells (**Fig. 5C**). Thus, although the aspartic acid substitution of serine 360 forces nuclear retention of IRF1BP2, it also appears to disrupt the co-activation function of IRF2BP2.

Currently, we do not know which kinase is responsible for the phosphorylation of S360. From a list of candidate kinases includes protein kinase A (PKA, consensus sequence R-R/K-X-S/T), kinase B (PKB), kinase C (PKC), kinase G (PKG), ribosomal S6 kinase (RSK), extracellular signal-regulated kianses 1/2 (ERK1/2, X-X-S/T-P), calmodulin-dependent protein kinase II (CaMKII, R-X-X-S/T), and Cdc2 (S/T-P-X-R/L), we tested various inhibitors against these kinases to determine whether they would cause cytoplasmic retention of IRF2BP2. However, in no case was IRF2BP2 excluded from the nucleus of C_2C_{12} myoblasts 24 hours post-treatment (**supplementary data Fig. 2**).

Figure 5. Despite forced nuclear retention the S360D mutant did not produce a dominantly active form of IRF2BP2. A. The S360A mutant of IRF2BP2 was cytoplasmic and the S360D mutant was nuclear in CV1 cells. Scale bar, 50 μm. B. The wild type IRF2BP2 augmented TEAD1-dependent activation of the mouse VEGFA promoter in CV1 cells (asterisk, $p<0.05$). The S360A and the S360D both failed to co-activate VEGFA when co-expressed with TEAD1. N=3 experiments. C. Immunoblot analysis of protein lysates from transfected CV1 cells revealed similar levels of wild type and mutant IRF2BP2 proteins.

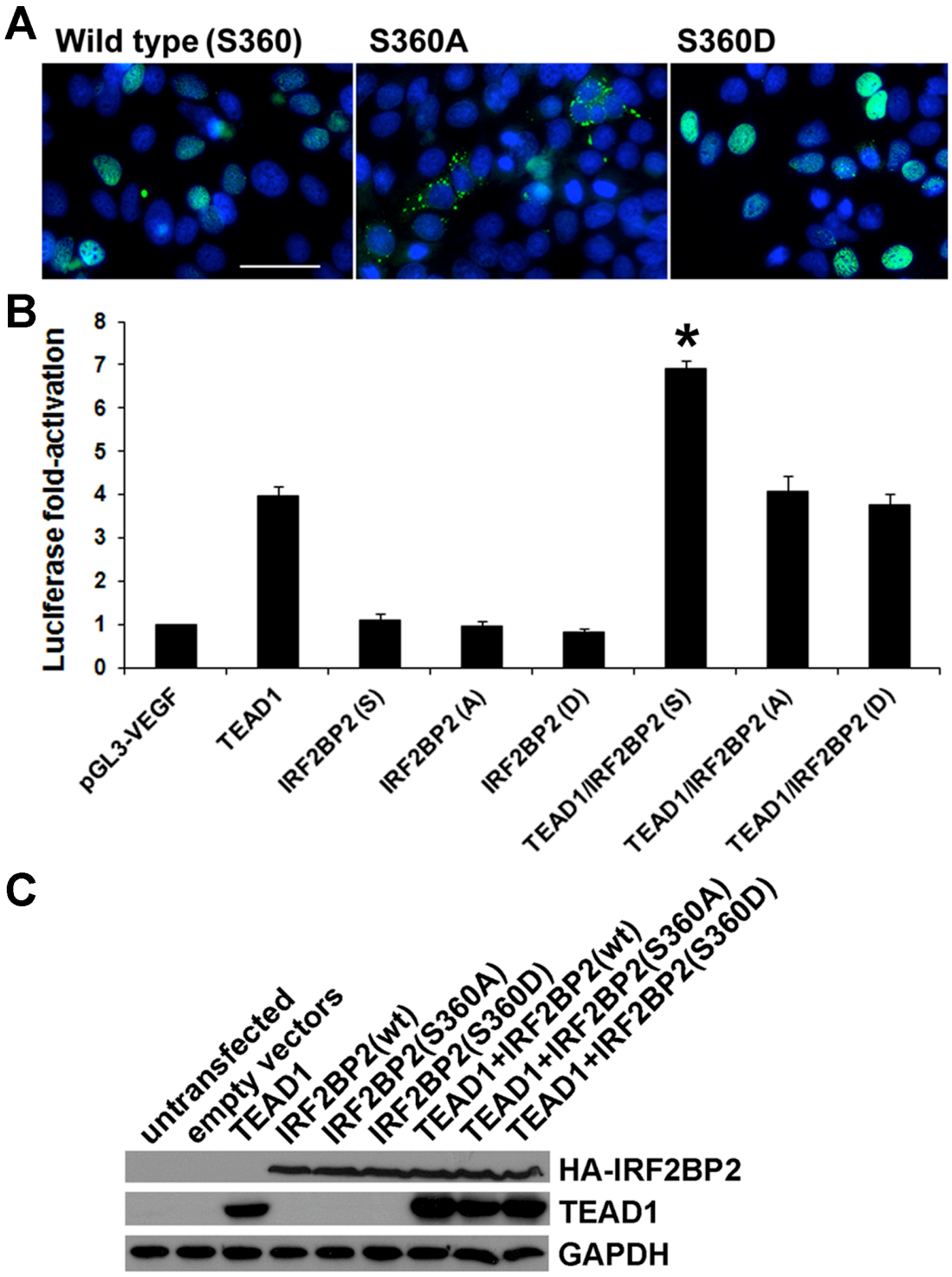
A
Wild type (S360)
S360A
S360D
B
Luciferase fold-activation
0
1
2
3
4
5
6
7
8
*
pGL3-VEGF
TEAD1
IRF2BP2 (S)
IRF2BP2 (A)
IRF2BP2 (D)
TEAD1/IRF2BP2 (S)
TEAD1/IRF2BP2 (A)
TEAD1/IRF2BP2 (D)
C
untransfected
empty vectors
TEAD1
IRF2BP2(wt)
IRF2BP2(S360A)
IRF2BP2(S360D)
TEAD1+IRF2BP2(wt)
TEAD1+IRF2BP2(S360A)
TEAD1+IRF2BP2(S360D)
HA-IRF2BP2
TEAD1
GAPDH

The diagram shown in Fig. 6A summarizes our finding of a single phosphorylation-modulated NLS in IRF2BP2. This sequence is conserved across the different paralogous homologs in both humans and zebrafish (**Fig. 6B**).

Figure 6. Identification of the phosphorylation-dependent NLS of IRF2BP2.
A. Diagram of deletion and mutagenesis constructs used to identify the phosphorylation-dependent NLS. Fusion proteins that are targeted to the nucleus are identified by a +, whereas those that are cytoplasmic are identified by -. Exes (x) represent mutagenized residues that abolish nuclear localization. B. Sequence conservation of the NLS. In all 3 paralogous genes, IRF2BP2, IRF2BP1 and EAP1 in humans (Homo sapiens) and zebrafish (Danio rerio), the NLS and the phosphorylation target sequences are conserved. Asterisks represent identical sequence.

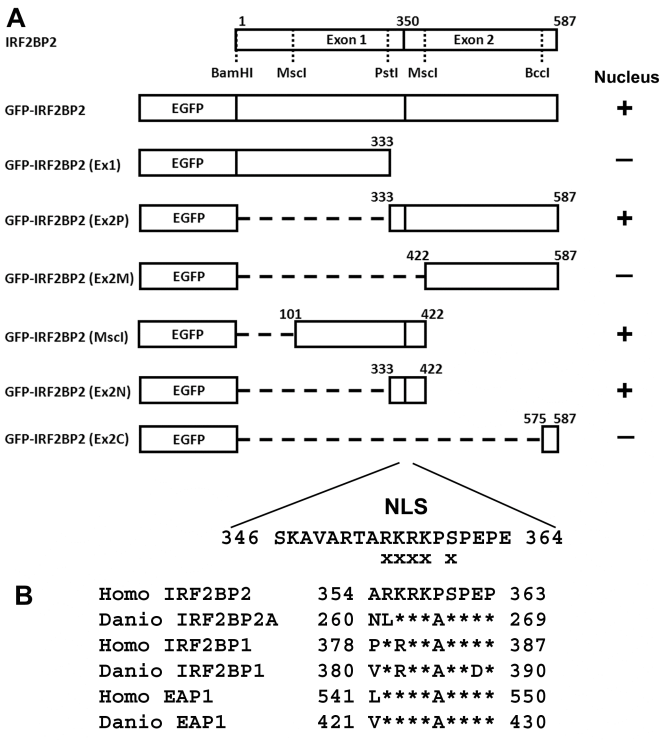

B

Homo IRF2BP2	354	ARKRKPSPEP 363
Danio IRF2BP2A	260	NL***A**** 269
Homo IRF2BP1	378	P*R**A**** 387
Danio IRF2BP1	380	V*R**A**D* 390
Homo EAP1	541	L****A**** 550
Danio EAP1	421	V****A**** 430

Online supporting Figure 1. Blocking CRM1 nuclear export did not cause retention of the S360A mutant of IRF2BP2. C_2C_{12} myoblasts transfected with GFP-IRF2BP2 (S360A) were treated with vehicle (1 μl 70% methanol in 1 ml medium, Control) or leptomycin B (10 nM, LMB). Scale bar, 10 μm.

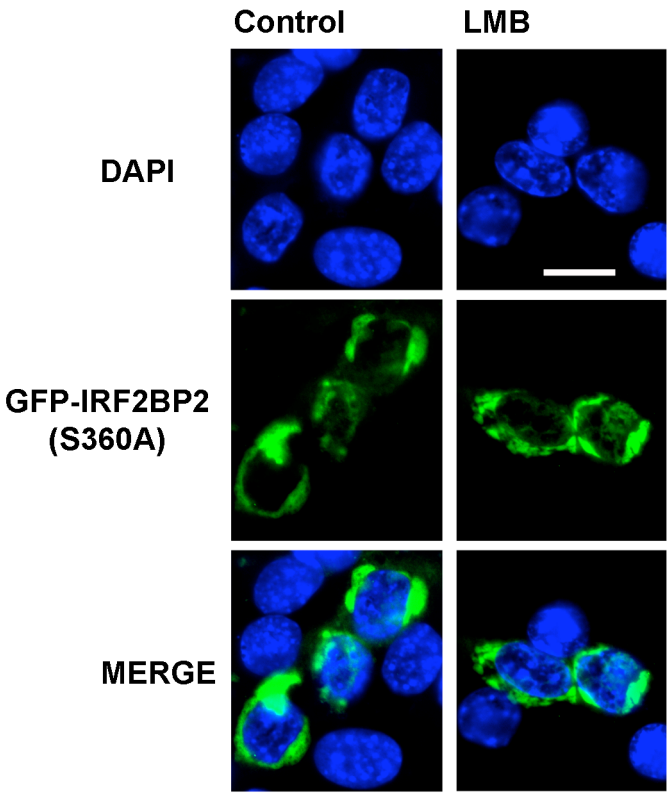
Control
LMB
DAPI
GFP-IRF2BP2
(S360A)
MERGE

Online supporting Figure 2. Various protein kinase inhibitors failed to block nuclear import of endogenous IRF2BP2. C_2C_{12} myoblasts were treated with vehicle (DMSO) or inhibitors of protein kinases for 24 hours. Scale bar, 50 μm. See Methods and Materials for descriptions and concentrations of protein kinase inhibitors.

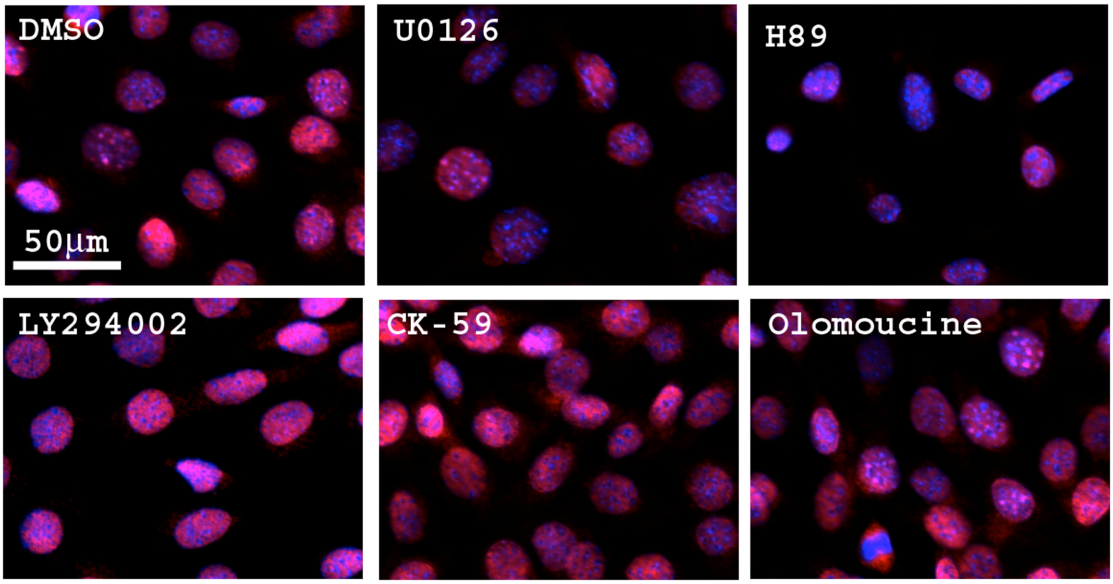
DMSO
50μm
U0126
H89
LY294002
CK-59
Olomoucine

DISCUSSION

Nuclear import of IRF2BP2 depends not only on a classical nuclear localization sequence, but also on phosphorylation of serine 360. Although our studies have not identified the protein kinase responsible for this phosphorylation event, the cytoplasmic localization of IRF2BP2 in differentiating skeletal muscle cells suggests that this protein kinase might become down-regulated or inactivated. Preventing nuclear entry of IRF2BP2 by mutating S360A was sufficient to render the protein inactive to regulate VEGFA promoter activity. Surprisingly, forced nuclear localization did not make IRF2BP2 a better transactivator of VEGFA. This result indicates that nuclear localization is not sufficient to ensure transcriptional activity of IRF2BP2 and that the S360D mutation might affect the interaction of IRF2BP2 with a putative transcription cofactor or affect a transactivation function of IRF2BP2.

Nuclear trafficking is a fundamental and essential mechanism to modulate import and export of RNA and proteins across the nuclear membranes within eukaryotes. This process depends heavily on thousands of protein complexes on the nuclear envelope and the import/export signals on cargo molecules. The classic NLS, composed of a cluster of arginine and lysine residues, has been extensively studied. X-ray crystallography shows that the positive charges from lysine and arginine enhance the binding affinity to negatively charged armadillo pockets of karyopherin-a (Fontes *et al.*, 2005). Karyopherin-a serves as an adaptor between a cargo protein and karyopherin-b. Nevertheless, other studies have shown that karyopherin-b could directly interact with a cargo protein (Lee *et al.*, 2006). Our study showed that one of two putative sequences was a functional NLS required for IRF2BP2 for nuclear entry.

Post-translational modifications are important for modulating protein structures or functions for downstream actions in response to environmental cues. One of frequently encountered examples includes phosphorylation (Baetz *et al.*, 2008; Harrison *et al.*, 2010; Kuwahara *et al.*, 2008; Sheng *et al.*, 2006). Database mining revealed that IRF2BP2 is phosphorylated at several serine residues in addition to serine 360 (data not shown). Serine 360 is located two amino acids downstream from the NLS (**Fig. 6B**) and our site-directed mutagenesis studies are consistent with phosphorylation at this site being necessary for nuclear entry, because blocking this process by mutagenesis led to perinuclear accumulation of the mutant protein (S360A), even in the presence of the NLS. A possible explanation is that phosphorylation of the serine residue is likely to alter IRF2BP2 protein structure, strengthening the stability of IRF2BP2-karyopherin complexes for crossing the nuclear membrane. Many examples for phosphorylation-dependent nuclear entry exist in eukaryotes, including import of extracellular signal-regulated kinase-1/2 (ERK1/2) (Lidke *et al.*, 2010), histone deacetylase 4 (HDAC4) (deSouza *et al.*, 2007), forkhead box M1 (FOXM1) (Ma *et al.*, 2005), and adenomatous polyposis cell (APC) protein (Zhang *et al.*, 2000). However, we were not able to identify the kinase that phosphorylates S360. This might be due to phosphorylation of S360 by more than one kinase. For example, low-density lipoprotein (LDL)-receptor-related protein 6 (LRP6) can be phosphorylated by both glycogen synthase kinase 3 (GSK3) and casein kinase I (CKI) (Zeng *et al.*, 2005).

The discovery of a single classical NLS in IRF2BP2 may help to predict the NLS in both IRF2BP1 and EAP1. The results show a striking similarity in sequence conservation, with both paralogs having a conserved NLS and a conserved phosphorylation target in an adjacent serine (**Fig. 6B**). Mass-spectrometry confirms

that both S384 of IRF2BP1 (Olsen *et al.*, 2006) and S547 of EAP1 (Mayya *et al.*, 2009) are phosphorylated in vivo. It remains to be formally proven whether both NLS signals and the serine residues provide similar functions as those observed in this study for IRF2BP2. It is worth noting that the locations of these sequences are not in currently known functional domains. This is consistent with previous studies showing that an NLS is most often away from other functional motifs to avoid interference. Our study provides important insight into the position of the nuclear targeting signals in the IRF2BP2 family of transcription factors.

Table 1 **Serine 360 of IRF2BP2 is phosphorylated in multiple human cell types**.
Fragments analyzed by mass spectrometry were identified by mining online datasets.

Human Cell line/tissues	**Identified peptides**	**Reference**
HeLa (cervical carcinoma)	RKPpSPEPEGEVGPPK	(Olsen *et al.*, 2006)
NCI-H1299 (non-small cell lung cancer)	KPpSPEPEGEVGPPK	(Tsai *et al.*, 2008)
HeLa (cervical carcinoma)	KRKRpSPEPEGEVGPPK	(Dephoure *et al.*, 2008)
Embryonic stem cells (male)	KPpSPEPEGEVGPPK	(Van Hoof *et al.*, 2009)
MV4-11 (myeloid)	RKPpSPEPEGEVGPPK	(Oppermann *et al.*, 2009)
Jurkat (T lymphocytes)	VARTARKRKPpSPEPEGEVGPP	(Mayya *et al.*, 2009)
Hepatocellular carcinoma	RKPpSPEPEGEVGPPK	(Han *et al.*, 2010)
Leukocyte-blood	RKPpSPEPEGEVGPPK	(Raijmakers *et al.*, 2010)

CHAPTER 5

GENERAL DISCUSSION

Studies of human genetic variants help to identify the roles of affected genes and to delineate the mechanisms of related human physiology. For example, a large scale screening in more than ten thousand Americans identified an association between SNPs in proprotein convertase subtilisin/kexin type 9 serine protease gene (PCSK9) and reduced plasma LDL (Cohen *et al.*, 2006). In contrast, different genetic variants found also in PCSK9 could adversely contribute to autosomal dominant hypercholesterolemia in human (Abifadel *et al.*, 2003). The significance of these findings is further magnified when similar phenotypes are recapitulated in transgenic animals or cell models (Pennacchio *et al.*, 2001). A recent study by Adamo *et al.* found that a rapid weight-loss phenotype in obese Caucasian females was associated with single nucleotide polymorphisms (SNPs) situated nearby or within PPARγ and one of its effector genes ACSL5 (Adamo *et al.*, 2007). The association was especially statistically significant with two (rs1801282 and rs2419621) of the eight tested SNPs. rs1801282 introduces a missense mutation (Pro12Ala) in the coding region of PPARγ gene and subsequently rendering study subjects more resistant to a diet-induced weight loss. Similar findings of Pro12Ala non-synonymous mutants have been repeatedly observed in human carriers (Douglas *et al.*, 2001; Lindi *et al.*, 2002; Luan *et al.*, 2001; Nicklas *et al.*, 2001; Pisabarro *et al.*, 2004; Rosado *et al.*, 2010; Stefan *et al.*, 2001).

In comparison to the well characterized Pro12Ala mutant, the genetic effect of rs2419621 and the roles of ACSL5 remain largely unknown. Previous studies in animals showed that ACSL5 was identified in tissues with a high triacylglycerol synthesis activity, such as brown adipocytes, duodenal mucosa, liver, and surprisingly,

human epidermis (Gaisa *et al.*, 2008; Mashek *et al.*, 2006a). In contrast, both soleus and gastrocnemic muscles of rats had a low level of ACSL5. Consistent with this observation, ACSL5 seems to be involved in portioning cellular triacylglycerol anabolism. Whereas ectopic expression of ACSL5 promoted the biosynthesis of triacylglycerol in human and rat hepatocytes, siRNA-dependent knockdown of ACSL5 reduced the rate of the process (Bu and Mashek, 2010; Mashek *et al.*, 2006a; Mashek *et al.*, 2006b). These results, nevertheless, do not agree with the confocal findings, in which, ACSL5 protein was localized to both mitochondria and endoplasmic reticulum, subcellular regions involved in fatty acid oxidation (Mashek *et al.*, 2006a). Despite the findings from human and rat hepatocytes, the functional significance of ACSL5 is never understood.

mRNA analyses of the muscle tissues from the carriers of the rs2419621(T) allele revealed a significantly higher ACSL5 transcript level when compared with that of non-carriers (Adamo *et al.*, 2007). This is the first study that correlates the level of ACSL5 transcripts to the rs2419621 SNP, but the exact mechanism was not described in the study. In the second chapter, we demonstrated via bioinformatics, EMSAs, and luciferase assays that SNP rs2419621 created a *de novo* E-box element immediately upstream of the human ACSL5 gene. The newly created E-box, together with two other E-box elements at the distal end, could synergize the activity of human ACSL5 promoter activity. MyoD belongs to the myogenic regulatory factor (MRF) family that recognizes an E-box element (CANNTG, N:= any nucleotides) in front of a gene. During myogenic differentiation, MyoD protein expression increases and activates downstream genes, including Myf5 and myogenin, two members of the MRF family (Armand *et al.*, 2008; Cossu *et al.*, 1996). MyoD forms homodimers or heterodimers with E-proteins, including E12 or E47, to mediate the expression of downstream

targets (Lluis *et al.*, 2005; Spinner *et al.*, 2002). Functionally, MyoD binding to two E-boxes in tandem positions could strongly enhance a promoter transactivation activity as demonstrated by the human creatine kinase promoter (Weintraub *et al.*, 1990). We had a similar observation in the human ACSL5 promoter of the carriers of rs2419621 (T-allele). A newly created E-box by the genetic variant had a strong response to the overexpression of exogenous MyoD in CV1 cells. In contrast, the C-allele variant weakly responded to the presence of MyoD. A similar observation was also made in C_2C_{12} myoblasts and differentiating myotubes. These results are consistent with others that showed the presence of E-boxes in tandem could galvanize the promoter activity.

Several transcription isoforms of ACSL5 have previously been identified, but the mechanisms that mediate the expression of these isoforms are largely unknown. Here, our study demonstrated that the expression of ACSL5 in human skeletal muscle is mediated in part by MRF members. Although the role of ACSL5 in skeletal muscle has never been studied before, studies of ACSL5 carried out in hepatoma and HepG2 cells suggest that ACSL5 may be involved the synthesis and metabolism of triacylglyceride, respectively (Mashek *et al.*, 2006a; Zhou *et al.*, 2007). These opposing observations suggest an intrinsically critical, but complicated, role of ACSL5 in mediating fatty acid levels in liver. Furthermore, the localization of ACSL5 to mitochondria in HepG2 cells is a good indication for fatty acid β-oxidation (Zhou *et al.*, 2007). Hence, an increase in mitochondrial ACSL5 proteins is likely to enhance fatty acid metabolism and, consequently, a rapid weight loss in the carriers of rs2419621 (T-allele). IRF2BP2 was initially identified as a repressor to IRF2 in a yeast two-hybrid assay (Childs and Goodbourn, 2003). Subsequent studies showed the carboxyl termini of the two proteins were required for the interaction. While the C-terminus of IRF2 is a transcription activation domain, that of IRF2BP2 is a C3HC4

RING finger motif. Besides the RING finger motif, IRF2BP2 has a N-terminal zinc-finger motif. The roles of these two domains are currently unknown, but Childs speculated that the RING finger motif was for protein interaction and the zinc-finger motif interacted with DNA (Childs and Goodbourn, 2003). Two IRF2BP2 paralogs, including IRF2BP1 and EAP1, are structurally related to IRF2BP2 in both zinc and RING motifs. Evolutionarily, the three genes are conserved in vertebrates and probably derive from the ancestral CG11138 gene in *Drosophila melanogaster*. Genetically, human IRF2BP2 is located at chromosome 1q42.3 and is composed of two exons and a long 3'-untranslated region (UTR). Once transcribed, IRF2BP2 are spliced into three isoforms, IRF2BP2a, IRF2BP2b, and IRF2BP2c. IRF2BP2a and IRF2BP2b differ by 48 nucleotides due to different donor sites at the end of the first exon. IRF2BP2c loses the entire exon one completely. This observation would imply that the second exon of the gene has a critical role in protein stability, such that no isoforms could be found without the second exon.

The role of IRF2BP2 remains largely unknown despite the first report to identify the gene in 2003 (Childs and Goodbourn, 2003). This is partially due to the lack of knowledge in known interacting proteins. My study identifies VGLL4 as a novel interacting protein to IRF2BP2. In C_2C_{12} myoblasts, VGLL4 interacts with IRF2BP2 via an evolutionarily conserved TDU1 motif, the same motif that also interacts with TEAD1. Removing this motif conversely abolishes the interaction. In a subsequent study, IRF2BP2 does not interact with other VGLL paralogs in C_2C_{12} or CV1 cells, despite the presence of conserved TDU motifs (data not shown). This implies that the interaction between VGLL4 and IRF2BP2 could be regulated by post-translational modifications or by a novel VGLL4-specific scaffold protein. Next, I mapped the VGLL4-interacting domain (VID) to 423-488 amino acids in IRF2BP2.

The VID domain is found only in IRF2BP2, but not in other vertebrate paralogs. This is the first study to demonstrate the interaction between IRF2BP2 and VGLL4 proteins, two evolutionarily conserved family proteins in mammals. Furthermore, I found that this interaction decreased during myogenic differentiation in C_2C_{12} myoblasts, suggesting either an interference of the interaction or degradation of proteins. A subsequent study using a mutant VGLL4 with only TDU1 motif showed an increase in protein interaction in differentiating C_2C_{12} myotubes. Taken together, my study helps to identify the interaction domains in both VGLL4 and IRF2BP2 and shows a decrease in interaction affinity toward IRF2BP2 during muscle differentiation.

Initially identified as a SV40 transcription enhancer factor, TEAD transcription factors have diversified roles, ranging from myogenic differentiation to organ growth, depending on the availability of transcription cofactors (Ambrosino *et al.*, 2006; Chen *et al.*, 2004a; Chen *et al.*, 2004b; Chen *et al.*, 2004c; Jablonska *et al.*, 2010; Sawada *et al.*, 2008; Xiao *et al.*, 1991). Shie's report that TEAD4 mediates the expression of VEGF-A in hypoxic endothelial cells raises two questions (Shie *et al.*, 2004). First of all, could other TEAD proteins also be involved in this process? Secondly, what is the underlying mechanism for controlling this process? My study showed that ectopic expression of exogenous TEAD1 alone had a weak activation on mouse VEGF-A promoter in CV1 cells, suggesting TEAD1 might be needed for the development of vasculature. This implication is partially supported by the observation that Tead1 and Tead2 double knockout ($Tead1^{-/-}$; $Tead2^{-/-}$) mice have an abnormal development of embryonic yolk sac vasculature organization and then embryonic lethality on embryonic day 9.5 (Sawada *et al.*, 2008). The phenotypes of these transgenic animals resemble those of VEGF-A knockout mice, suggesting that

TEAD1 and TEAD2 are critical to vasculogenesis in murine embryos (Carmeliet *et al.*, 1996). Besides blood vessel development, TEAD1 has been studied extensively *in vivo* and *in vitro* for cardiac and myogenic development. TEAD1 functions as a transcription factor to mediate the expression of contractile proteins in muscles (Farrance *et al.*, 1992; Stewart *et al.*, 1994). More specifically, TEAD1 overexpression in mouse promotes the outgrowth of slow-twitch muscle fiber isotypes of skeletal muscles (Tsika *et al.*, 2008).

The development of oxidative skeletal muscles is a complex process that requires a successful orchestration of different signaling pathways. The source of stimuli for initiating oxidative slow twitch muscles can be generally divided into two parts: exterior and interior. A conventional example for exterior stimulation is endurance exercise (Frey *et al.*, 2008). A prolonged muscle contraction motion increases the influx of calcium ions that subsequently activates NFAT in a calcineurin-dependent manner. Activated NFAT heterodimerizes with MEF2 and transactivates target genes (Calvo *et al.*, 1999; Chin *et al.*, 1998). Interior stimuli usually stem from an imbalance in cytoplasmic oxidative activity. One endogenous barometer for gauging the oxidative activity in skeletal muscle is the ratio between nicotinamide adenine dinucleotide (NAD^+) and its reduced form NADH. NAD^+ plays two important roles in contracting muscle cells: (1) it is an intermediary agent between the citric acid cycle in cytoplasm and oxidative phosphorylation in mitochondria (Pollak *et al.*, 2007). (2) It functions as part of a secondary messenger system to initiate an emergency response to activate subsequent proteins, such as the families of poly (ADP-ribose) polymerase-1 (PARP-1) and silent mating type information regulation (SIRT1) (Bai *et al.*, 2011a; Bai *et al.*, 2011b). NAD^+ is composed of a nicotinamide, an adenine, and two phosphates. An increase in cytoplasmic NAD^+

concentration signals to PARP-1 in catalyzing poly ADP-ribosylation by transferring the ADP-ribose moiety of NAD^+ to a lysine residue on a receiver protein. This reversible posttranslational modification could positively or negatively affect the functions of modified proteins. For example, while ADP-ribosylation enhances NFAT activity, the transactivation activity of TEAD1 is attenuated by this modification (Butler and Ordahl, 1999; Olabisi *et al.*, 2008). A study from Vyas *et al.* further corroborates this finding by demonstrating that a PARP-TEAD1-Myc-associated factor X (MAX) heterotrimeric complex is found in the promoters of β-MyHC and cTNT to demote the development of slow twitch muscles (Vyas *et al.*, 2001). However, a surge in intracellular NAD^+ concentration could also inactivate a certain amount of, but not all of, PARP-1 proteins through a SIRT1-dependent deacetylation of PARP-1 (Rajamohan *et al.*, 2009). This supports my finding in the synthesis of endogenous VEGF-A expression in a TEAD1-dependent manner. Consistent with this hypothesis, PARP knockout mice ($PARP^{-/-}$) or animals that are treated with PARP-antagonists show a superior muscle viability, an increase in the biosynthesis of VEGF, and greater reperfusion following ischemia in both cardiac and skeletal muscles (Bai *et al.*, 2011b; Crawford *et al.*, 2010; Hua *et al.*, 2005; Szabo *et al.*, 2002). Also, re-activation of TEAD1 via PARP-1 repression would also likely to account for the development of oxidative skeletal muscles.

SIRT-1 is a member of class III histone deacetylases (HDACs) and, like PARP-1, it also utilizes NAD^+ to catalyze deacetylation on target proteins. The activation of SIRT-1 is critical in responding to diet-induced caloric restriction *in vivo* and *in vitro*, although the degree of the physiological response is tissue-dependent. For example, while active SIRT-1 promotes the expression of PPARγ transcripts in brown adipocytes and skeletal muscle, it represses PPARγ expression in white adipocytes

(Feige *et al.*, 2008; Picard *et al.*, 2004). Consequently, a SIRT-1-mediated increase of PPARγ may possibly induce the expression of ACSL5 in skeletal muscle in individuals who undertook diet-induced weight loss (Adamo *et al.*, 2007). Recently, TEAD transcription factors are reported to mediate the expression of two MRF family members, namely Myf5 and myogenin (Benhaddou *et al.*, 2011; Ribas *et al*., 2011). In addition, via a YAP65-mediated transcription regulation, TEAD1 is capable of activating Pax3 (Gee et al., 2011), which is an positive regulator of MyoD and Myf-5 expression (Maroto et al., 1997; Tajbakhsh et al., 1997). Hence, SIRT-1 may induce the expression of skeletal muscle-specific ACSL5 through PARP-1, TEAD1 and MRFs. However, this hypothesis remains to be tested.

SIRT-1 is also involved in the immediate response to ischemia and in the process of angiogenesis via both transcription regulators and transmembrane molecules. Some of these proteins include PGC-1α, Forkhead box O1 (FOXO1), PARP-1, and Notch (Guarani *et al.*, 2011; Kelly *et al.*, 2009; Potente *et al.*, 2007; Rajamohan *et al.*, 2009). In both HT1080 primate fibrosarcoma and Hep3B human hepatoma, HIF-1α promotes the expression of SIRT-1 during hypoxia and the stabilization of transcription factor p53 (Chen *et al.*, 2011). An increase in the endogenous SIRT-1 initiates several survival pathways by activating transcription factor HIF-2a (Chen *et al.*, 2011; Rane *et al.*, 2009). While transcription factor p53 is deactivated via a SIRT-1-mediated deacetylation in several tested cancer cell lines at normoxia, stabilized p53 transcription complex at hypoxia may not offer physiological benefit to the affected cells (Langley *et al.*, 2002; Vaziri *et al.*, 2001). One possible explanation is that the function of IRF2BP2 protein is potentiated by SIRT-1; while the knockdown of SIRT-1 increases the repression activity of IRF2BP2, the use of a SIRT-1 agonist resveratrol strongly promotes a IRF2BP2-dependent repression

(Tinnikov *et al.*, 2009). Since IRF2BP2 is reported to target and to suppress p53, SIRT-1 may deactivate p53 directly via deacetylation or indirectly via IRF2BP2 in ischemic tissue (Koeppel *et al.*, 2009). Thus, activation of SIRT-1 is important for promoting neo-vascularization, because p53 activation during hypoxia inhibits angiogenesis (Ravi *et al.*, 2000; Teodoro *et al.*, 2006). My results that overexpressing both exogenous IRF2BP2 and TEAD1 could strongly transactivate mouse VEGF-A promoter in CV1 cells and induce the biosynthesis of VEGF-A in C_2C_{12} myoblasts offer another plausible mechanism to account for a SIRT-1-dependent angiogenesis.

Several reports have demonstrated the anti-apoptotic role for IRF2BP2. Koeppel *et al.* show that knocking down IRF2BP2 expression in the actinomycin D-treated HeLa cells induces apoptosis via a p53-mediated signaling pathway (Koeppel *et al.*, 2009). A similar observation is also made in MCF-7 breast cancer cells where IRF2BP2 could antagonize a putative pro-apoptotic protein FAST kinase domain-containing protein 2 (FASTKD2) (Yeung *et al.*, 2011). In my study, IRF2BP2 protein level increases in rat ischemic hindlimb tissue and, in combination with TEAD1, promotes the synthesis of VEGF-A. There are few VEGF-A splicing isoforms already identified in mammals and their roles remain as a vast interest of today's research topics. In general, these isoforms are capable of few things: (1) the induction of angiogenesis, (2) the promotion of anti-apoptosis, (3) cell polarization, and (4) cell migration (for detailed review, please refer to (Carmeliet and Jain, 2011). The activation of VEGF-A via an IRF2BP2-mediated process could likely account for the strong IRF2BP2 expression in mouse embryos and in mouse adult heart, liver, and lungs (**unpublished Fig. 1**). Thus, these studies show that IRF2BP2 is important for cell survival.

Unpublished Figure 1. Mouse multi-tissue western blot. 20 mg protein lysates extracted from different tissues from an adult mouse were analyzed in western blot. While there is a strong IRF2BP2 expression in heart (lane 1), liver (lane 4), and lung (lane 6), a milder expression was found in skeletal muscle (lane 2), brain (lane 3) and spleen (lane 5). GAPDH was used as a loading control.

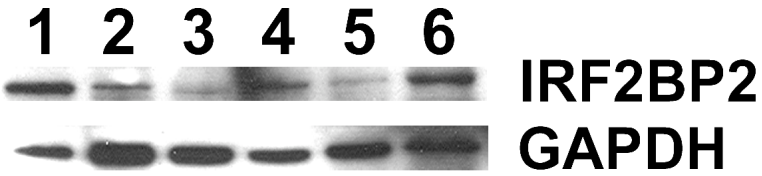

1: Heart
2: Skeletal muscle
3: Brain
4: Liver
5: Spleen
6: Lung

My study with others showed that both IRF2BP2 splicing isoforms were nuclear proteins in different cell lines, including murine C_2C_{12} myoblasts, human T-47D and MCF-7 ductal breast epithelial tumor cell line (Tinnikov *et al.*, 2009), and human HeLa cervical carcinoma (Dephoure *et al.*, 2008) and adult mouse heart (**unpublished Fig. 2**). The two isoforms use an evolutionarily conserved NLS for entering the nucleus. Deletion or alternation of this signal abolished this action. Studies employing mass spectrometry show that S360 (or S343 in IRF2BP2b) is phosphorylated *in vivo* (For a detailed summary, please refer to **Table 1** on page 95. As evidenced in our study, this post-translational modification is critical in modulating the nuclear entry of IRF2BP2 isoforms (Page 100, **Figure 5**). Although the kinase responsible for this modification remains unknown, a study by Dephoure *et al.* showed that this phosphorylation exists between the G1 to mitosis transition, but could continue after mitosis (Dephoure *et al.*, 2008). The peptid consensus has the resemblance of many kinases, including protein kinase A and calmodulin-dependent kinase II. However, treatments of C_2C_{12} myoblasts with these kinase inhibitors did not block the nuclear entry. It is likely that this modification could happen with more than one kinase. In essence, the NLS and phosphorylation serine sites are also found in two additional IRF2BP2 paralogs, IRF2BP1 and EAP1. This implies that both related proteins may utilize a similar mechanism for entering nucleus since their physical interactions with IRF2BP2 were critical for cell survival by regulating the expression of FAST domain kinase 2 (FASTKD2) in TCF-7 cells (Yeung *et al.*, 2011). Therefore, our study provides an initiative for studying the role of the IRF2BP1/IRF2BP2/EAP1 complex.

Unpublished Figure 2. IRF2BP2 is found in the nucleus of cardiac myocytes. (**A**) 20X magnification. Mouse cardiac section was labeled with IRF2BP2 antibody and developed with 3,3'-Diaminobenzidine (DAB, brown staining). Nuclear staining was performed with hematoxylin. (**B**) 60X magnification of the rectangle area in (**A**). White arrows represent IRF2BP2-free nucleus, while black arrows showed the presence of IRF2BP2 in the nuclei. Scale bar, 50 μm.

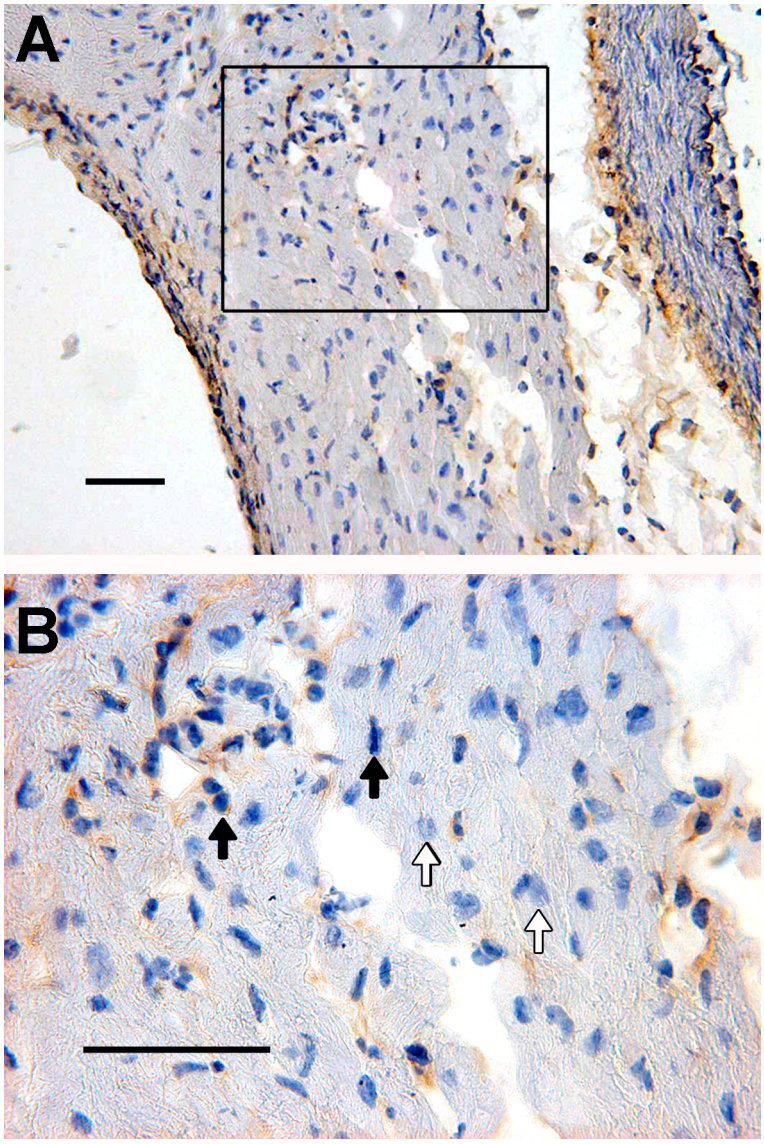
A
B

In brief conclusion, my results demonstrate that MyoD could activate the expression of ACSL5 during the myogenic differentiation of C_2C_{12} cells. In addition, the presence of rs2419621 (T) allele further enhances this activation by creating an additional E-box for MyoD binding within the vicinity of two existing E-box elements. An increase in the ACSL5 protein level strengthens the uptake of FFAs for β-oxidation in mitochondria in developing skeletal muscle. On the other hand, a surge of NAD^+ level due to energy imbalance initiates survival pathways via SIRT1. IRF2BP2 is a downstream target of an activated SIRT1 and, hence, could promote VEGF-A expression in a TEAD1-dependent manner (**unpublished Fig. 3**). These studies provide some preliminary insight in transcription regulations which skeletal muscle utilize to acquire energy.

Unpublished Figure 3. IRF2BP2 is enriched in the nucleus and cytoplasm of ischemic skeletal muscle. (**A**) 20X magnification. Rat hindlimb muscle section that underwent 48 hours of femoral artery ligation were labeled with IRF2BP2 antibody and developed with 3,3'-Diaminobenzidine (DAB, brown staining). Nuclear staining was performed with hematoxylin. Untreated (normoxic) tissue was used as a negative control.

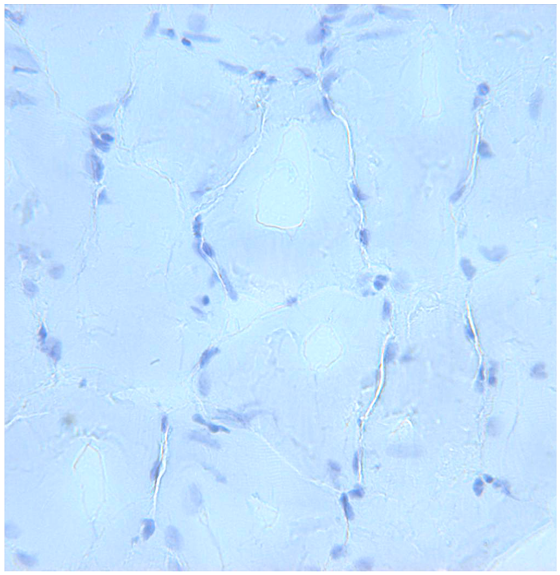

Normoxic

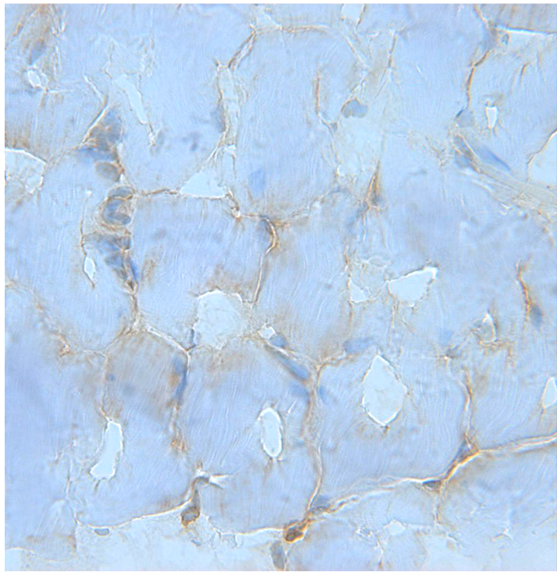

Ischemic

REFERENCES

Abe, T., Fujino, T., Fukuyama, R., Minoshima, S., Shimizu, N., Toh, H., Suzuki, H., and Yamamoto, T. (1992). Human long-chain acyl-CoA synthetase: structure and chromosomal location. J Biochem *111*, 123-128.

Abifadel, M., Varret, M., Rabes, J.P., Allard, D., Ouguerram, K., Devillers, M., Cruaud, C., Benjannet, S., Wickham, L., Erlich, D.*, et al.* (2003). Mutations in PCSK9 cause autosomal dominant hypercholesterolemia. Nat Genet *34*, 154-156.

Adam, S.A., and Gerace, L. (1991). Cytosolic proteins that specifically bind nuclear location signals are receptors for nuclear import. Cell *66*, 837-847.

Adamo, K.B., Dent, R., Langefeld, C.D., Cox, M., Williams, K., Carrick, K.M., Stuart, J.S., Sundseth, S.S., Harper, M.E., McPherson, R.*, et al.* (2007). Peroxisome proliferator-activated receptor gamma 2 and acyl-CoA synthetase 5 polymorphisms influence diet response. Obesity (Silver Spring) *15*, 1068-1075.

Agrawal, N., Joshi, S., Kango, M., Saha, D., Mishra, A., and Sinha, P. (1995). Epithelial hyperplasia of imaginal discs induced by mutations in Drosophila tumor suppressor genes: growth and pattern formation in genetic mosaics. Dev Biol *169*, 387-398.

Aguirre, V., Werner, E.D., Giraud, J., Lee, Y.H., Shoelson, S.E., and White, M.F. (2002). Phosphorylation of Ser307 in insulin receptor substrate-1 blocks interactions with the insulin receptor and inhibits insulin action. J Biol Chem *277*, 1531-1537.

Ambrosino, C., Iwata, T., Scafoglio, C., Mallardo, M., Klein, R., and Nebreda, A.R. (2006). TEF-1 and C/EBPbeta are major p38alpha MAPK-regulated transcription factors in proliferating cardiomyocytes. Biochem J *396*, 163-172.

Anbanandam, A., Albarado, D.C., Nguyen, C.T., Halder, G., Gao, X., and Veeraraghavan, S. (2006). Insights into transcription enhancer factor 1 (TEF-1) activity from the solution structure of the TEA domain. Proc Natl Acad Sci U S A *103*, 17225-17230.

Ancelin, M., Buteau-Lozano, H., Meduri, G., Osborne-Pellegrin, M., Sordello, S., Plouet, J., and Perrot-Applanat, M. (2002). A dynamic shift of VEGF isoforms with a transient and selective progesterone-induced expression of VEGF189 regulates angiogenesis and vascular permeability in human uterus. Proc Natl Acad Sci U S A *99*, 6023-6028.

Appukuttan, B., McFarland, T.J., Davies, M.H., Atchaneeyasakul, L.O., Zhang, Y., Babra, B., Pan, Y., Rosenbaum, J.T., Acott, T., Powers, M.R.*, et al.* (2007). Identification of novel alternatively spliced isoforms of RTEF-1 within human ocular vascular endothelial cells and murine retina. Invest Ophthalmol Vis Sci *48*, 3775-3782.

Arany, Z., Foo, S.Y., Ma, Y., Ruas, J.L., Bommi-Reddy, A., Girnun, G., Cooper, M., Laznik, D., Chinsomboon, J., Rangwala, S.M.*, et al.* (2008). HIF-independent regulation of VEGF and angiogenesis by the transcriptional coactivator PGC-1alpha. Nature *451*, 1008-1012.

Armand, A.S., Bourajjaj, M., Martinez-Martinez, S., el Azzouzi, H., da Costa Martins, P.A., Hatzis, P., Seidler, T., Redondo, J.M., and De Windt, L.J. (2008). Cooperative synergy between NFAT and MyoD regulates myogenin expression and myogenesis. J Biol Chem *283*, 29004-29010.

Awata, T., Inoue, K., Kurihara, S., Ohkubo, T., Watanabe, M., Inukai, K., Inoue, I., and Katayama, S. (2002). A common polymorphism in the 5'-untranslated region

of the VEGF gene is associated with diabetic retinopathy in type 2 diabetes. Diabetes *51*, 1635-1639.
Baetz, A., Koelsche, C., Strebovsky, J., Heeg, K., and Dalpke, A.H. (2008). Identification of a nuclear localization signal in suppressor of cytokine signaling 1. FASEB J *22*, 4296-4305.
Bagheri, R., Qasim, A.N., Mehta, N.N., Terembula, K., Kapoor, S., Braunstein, S., Schutta, M., Iqbal, N., Lehrke, M., and Reilly, M.P. (2010). Relation of plasma fatty acid binding proteins 4 and 5 with the metabolic syndrome, inflammation and coronary calcium in patients with type-2 diabetes mellitus. Am J Cardiol *106*, 1118-1123.
Bai, P., Canto, C., Brunyanszki, A., Huber, A., Szanto, M., Cen, Y., Yamamoto, H., Houten, S.M., Kiss, B., Oudart, H.*, et al.* (2011a). PARP-2 regulates SIRT1 expression and whole-body energy expenditure. Cell Metab *13*, 450-460.
Bai, P., Canto, C., Oudart, H., Brunyanszki, A., Cen, Y., Thomas, C., Yamamoto, H., Huber, A., Kiss, B., Houtkooper, R.H.*, et al.* (2011b). PARP-1 inhibition increases mitochondrial metabolism through SIRT1 activation. Cell Metab *13*, 461-468.
Barth, A.S., Aiba, T., Halperin, V., DiSilvestre, D., Chakir, K., Colantuoni, C., Tunin, R.S., Dimaano, V.L., Yu, W., Abraham, T.P.*, et al.* (2009). Cardiac resynchronization therapy corrects dyssynchrony-induced regional gene expression changes on a genomic level. Circ Cardiovasc Genet *2*, 371-378.
Bass, N.M., Raghupathy, E., Rhoads, D.E., Manning, J.A., and Ockner, R.K. (1984). Partial purification of molecular weight 12 000 fatty acid binding proteins from rat brain and their effect on synaptosomal Na+-dependent amino acid uptake. Biochemistry *23*, 6539-6544.
Belandia, B., and Parker, M.G. (2000). Functional interaction between the p160 coactivator proteins and the transcriptional enhancer factor family of transcription factors. J Biol Chem *275*, 30801-30805.
Bell, G.I., Kayano, T., Buse, J.B., Burant, C.F., Takeda, J., Lin, D., Fukumoto, H., and Seino, S. (1990). Molecular biology of mammalian glucose transporters. Diabetes Care *13*, 198-208.
Benhaddou, A., Keime, C., Ye, T., Morlon, A., Michel, I., Jost, B., Mengus, G., and Davidson, I. (2011). Transcription factor TEAD4 regulates expression of Myogenin and the unfolded protein response genes during C2C12 cell differentiation. Cell Death Differ.
Bergeron, M., Gidday, J.M., Yu, A.Y., Semenza, G.L., Ferriero, D.M., and Sharp, F.R. (2000). Role of hypoxia-inducible factor-1 in hypoxia-induced ischemic tolerance in neonatal rat brain. Ann Neurol *48*, 285-296.
Birnbaum, M.J. (1989). Identification of a novel gene encoding an insulin-responsive glucose transporter protein. Cell *57*, 305-315.
Bonnet, A., Dai, F., Brand-Saberi, B., and Duprez, D. (2010). Vestigial-like 2 acts downstream of MyoD activation and is associated with skeletal muscle differentiation in chick myogenesis. Mech Dev *127*, 120-136.
Brasen, J.H., Kivela, A., Roser, K., Rissanen, T.T., Niemi, M., Luft, F.C., Donath, K., and Yla-Herttuala, S. (2001). Angiogenesis, vascular endothelial growth factor and platelet-derived growth factor-BB expression, iron deposition, and oxidation-specific epitopes in stented human coronary arteries. Arterioscler Thromb Vasc Biol *21*, 1720-1726.
Breen, E., Tang, K., Olfert, M., Knapp, A., and Wagner, P. (2008). Skeletal muscle capillarity during hypoxia: VEGF and its activation. High Alt Med Biol *9*, 158-166.

Bu, S.Y., and Mashek, D.G. (2010). Hepatic long-chain acyl-CoA synthetase 5 mediates fatty acid channeling between anabolic and catabolic pathways. J Lipid Res *51*, 3270-3280.
Butler, A.J., and Ordahl, C.P. (1999). Poly(ADP-ribose) polymerase binds with transcription enhancer factor 1 to MCAT1 elements to regulate muscle-specific transcription. Mol Cell Biol *19*, 296-306.
Calvani, M., Rapisarda, A., Uranchimeg, B., Shoemaker, R.H., and Melillo, G. (2006). Hypoxic induction of an HIF-1alpha-dependent bFGF autocrine loop drives angiogenesis in human endothelial cells. Blood *107*, 2705-2712.
Calvo, J.A., Daniels, T.G., Wang, X., Paul, A., Lin, J., Spiegelman, B.M., Stevenson, S.C., and Rangwala, S.M. (2008). Muscle-specific expression of PPARgamma coactivator-1alpha improves exercise performance and increases peak oxygen uptake. J Appl Physiol *104*, 1304-1312.
Calvo, S., Venepally, P., Cheng, J., and Buonanno, A. (1999). Fiber-type-specific transcription of the troponin I slow gene is regulated by multiple elements. Mol Cell Biol *19*, 515-525.
Cao, R., Brakenhielm, E., Pawliuk, R., Wariaro, D., Post, M.J., Wahlberg, E., Leboulch, P., and Cao, Y. (2003). Angiogenic synergism, vascular stability and improvement of hind-limb ischemia by a combination of PDGF-BB and FGF-2. Nat Med *9*, 604-613.
Cao, X., Pfaff, S.L., and Gage, F.H. (2008). YAP regulates neural progenitor cell number via the TEA domain transcription factor. Genes Dev *22*, 3320-3334.
Carmeliet, P. (2003). Blood vessels and nerves: common signals, pathways and diseases. Nat Rev Genet *4*, 710-720.
Carmeliet, P. (2005). VEGF as a key mediator of angiogenesis in cancer. Oncology *69 Suppl 3*, 4-10.
Carmeliet, P., and Collen, D. (1999). Role of vascular endothelial growth factor and vascular endothelial growth factor receptors in vascular development. Curr Top Microbiol Immunol *237*, 133-158.
Carmeliet, P., Ferreira, V., Breier, G., Pollefeyt, S., Kieckens, L., Gertsenstein, M., Fahrig, M., Vandenhoeck, A., Harpal, K., Eberhardt, C.*, et al.* (1996). Abnormal blood vessel development and lethality in embryos lacking a single VEGF allele. Nature *380*, 435-439.
Carmeliet, P., and Jain, R.K. (2000). Angiogenesis in cancer and other diseases. Nature *407*, 249-257.
Carmeliet, P., and Jain, R.K. (2011). Molecular mechanisms and clinical applications of angiogenesis. Nature *473*, 298-307.
Cascio, S., D'Andrea, A., Ferla, R., Surmacz, E., Gulotta, E., Amodeo, V., Bazan, V., Gebbia, N., and Russo, A. (2010). miR-20b modulates VEGF expression by targeting HIF-1 alpha and STAT3 in MCF-7 breast cancer cells. J Cell Physiol *224*, 242-249.
Cascio, S., Ferla, R., D'Andrea, A., Gerbino, A., Bazan, V., Surmacz, E., and Russo, A. (2009). Expression of angiogenic regulators, VEGF and leptin, is regulated by the EGF/PI3K/STAT3 pathway in colorectal cancer cells. J Cell Physiol *221*, 189-194.
Cavicchi, S., Guerra, D., Natali, V., Giorgi, G., Pezzoli, C., and Villani, L. (1989). Developmental effects of modifiers of the vg mutant in Drosophila melanogaster. Dev Genet *10*, 386-392.

Cecil, J.E., Tavendale, R., Watt, P., Hetherington, M.M., and Palmer, C.N. (2008). An obesity-associated FTO gene variant and increased energy intake in children. N Engl J Med *359*, 2558-2566.
Ceradini, D.J., Kulkarni, A.R., Callaghan, M.J., Tepper, O.M., Bastidas, N., Kleinman, M.E., Capla, J.M., Galiano, R.D., Levine, J.P., and Gurtner, G.C. (2004). Progenitor cell trafficking is regulated by hypoxic gradients through HIF-1 induction of SDF-1. Nat Med *10*, 858-864.
Chang, T.C., Wentzel, E.A., Kent, O.A., Ramachandran, K., Mullendore, M., Lee, K.H., Feldmann, G., Yamakuchi, M., Ferlito, M., Lowenstein, C.J.*, et al.* (2007). Transactivation of miR-34a by p53 broadly influences gene expression and promotes apoptosis. Mol Cell *26*, 745-752.
Chen, H.H., Baty, C.J., Maeda, T., Brooks, S., Baker, L.C., Ueyama, T., Gursoy, E., Saba, S., Salama, G., London, B.*, et al.* (2004a). Transcription enhancer factor-1-related factor-transgenic mice develop cardiac conduction defects associated with altered connexin phosphorylation. Circulation *110*, 2980-2987.
Chen, H.H., Maeda, T., Mullett, S.J., and Stewart, A.F. (2004b). Transcription cofactor Vgl-2 is required for skeletal muscle differentiation. Genesis *39*, 273-279.
Chen, H.H., Mullett, S.J., and Stewart, A.F. (2004c). Vgl-4, a novel member of the vestigial-like family of transcription cofactors, regulates alpha1-adrenergic activation of gene expression in cardiac myocytes. J Biol Chem *279*, 30800-30806.
Chen, H.H., Mullett, S.J., and Stewart, A.F.R. (2004d). Vgl-4, a novel member of the vestigial-like family of transcription cofactors, regulates alpha1-adrenergic activation of gene expression in cardiac myocytes. J Biol Chem *279*, 30800-30806.
Chen, R., Dioum, E.M., Hogg, R.T., Gerard, R.D., and Garcia, J.A. (2011). Hypoxia increases sirtuin 1 expression in a hypoxia-inducible factor-dependent manner. J Biol Chem *286*, 13869-13878.
Childs, K.S., and Goodbourn, S. (2003). Identification of novel co-repressor molecules for Interferon Regulatory Factor-2. Nucleic Acids Res *31*, 3016-3026.
Chin, E.R., Olson, E.N., Richardson, J.A., Yang, Q., Humphries, C., Shelton, J.M., Wu, H., Zhu, W., Bassel-Duby, R., and Williams, R.S. (1998). A calcineurin-dependent transcriptional pathway controls skeletal muscle fiber type. Genes Dev *12*, 2499-2509.
Claffey, K.P., Herrera, V.L., Brecher, P., and Ruiz-Opazo, N. (1987). Cloning and tissue distribution of rat heart fatty acid binding protein mRNA: identical forms in heart and skeletal muscle. Biochemistry *26*, 7900-7904.
Cline, G.W., Petersen, K.F., Krssak, M., Shen, J., Hundal, R.S., Trajanoski, Z., Inzucchi, S., Dresner, A., Rothman, D.L., and Shulman, G.I. (1999). Impaired glucose transport as a cause of decreased insulin-stimulated muscle glycogen synthesis in type 2 diabetes. N Engl J Med *341*, 240-246.
Cohen, J.C., Boerwinkle, E., Mosley, T.H., Jr., and Hobbs, H.H. (2006). Sequence variations in PCSK9, low LDL, and protection against coronary heart disease. N Engl J Med *354*, 1264-1272.
Cossu, G., Kelly, R., Tajbakhsh, S., Di Donna, S., Vivarelli, E., and Buckingham, M. (1996). Activation of different myogenic pathways: myf-5 is induced by the neural tube and MyoD by the dorsal ectoderm in mouse paraxial mesoderm. Development *122*, 429-437.
Crawford, R.S., Albadawi, H., Atkins, M.D., Jones, J.E., Yoo, H.J., Conrad, M.F., Austen, W.G., Jr., and Watkins, M.T. (2010). Postischemic poly (ADP-ribose)

polymerase (PARP) inhibition reduces ischemia reperfusion injury in a hind-limb ischemia model. Surgery *148*, 110-118.
Deblon, N., Veyrat-Durebex, C., Bourgoin, L., Caillon, A., Bussier, A.L., Petrosino, S., Piscitelli, F., Legros, J.J., Geenen, V., Foti, M.*, et al.* (2011). Mechanisms of the anti-obesity effects of oxytocin in diet-induced obese rats. PLoS One *6*, e25565.
Deniaud, E., Baguet, J., Mathieu, A.L., Pages, G., Marvel, J., and Leverrier, Y. (2006). Overexpression of Sp1 transcription factor induces apoptosis. Oncogene *25*, 7096-7105.
Dephoure, N., Zhou, C., Villen, J., Beausoleil, S.A., Bakalarski, C.E., Elledge, S.J., and Gygi, S.P. (2008). A quantitative atlas of mitotic phosphorylation. Proc Natl Acad Sci U S A *105*, 10762-10767.
deSouza, N., Cui, J., Dura, M., McDonald, T.V., and Marks, A.R. (2007). A function for tyrosine phosphorylation of type 1 inositol 1,4,5-trisphosphate receptor in lymphocyte activation. J Cell Biol *179*, 923-934.
Dix, M.M., Simon, G.M., and Cravatt, B.F. (2008). Global mapping of the topography and magnitude of proteolytic events in apoptosis. Cell *134*, 679-691.
Dodou, E., Xu, S.M., and Black, B.L. (2003). mef2c is activated directly by myogenic basic helix-loop-helix proteins during skeletal muscle development in vivo. Mech Dev *120*, 1021-1032.
Donoviel, D.B., Shield, M.A., Buskin, J.N., Haugen, H.S., Clegg, C.H., and Hauschka, S.D. (1996). Analysis of muscle creatine kinase gene regulatory elements in skeletal and cardiac muscles of transgenic mice. Mol Cell Biol *16*, 1649-1658.
Douglas, J.A., Erdos, M.R., Watanabe, R.M., Braun, A., Johnston, C.L., Oeth, P., Mohlke, K.L., Valle, T.T., Ehnholm, C., Buchanan, T.A.*, et al.* (2001). The peroxisome proliferator-activated receptor-gamma2 Pro12A1a variant: association with type 2 diabetes and trait differences. Diabetes *50*, 886-890.
Dresner, A., Laurent, D., Marcucci, M., Griffin, M.E., Dufour, S., Cline, G.W., Slezak, L.A., Andersen, D.K., Hundal, R.S., Rothman, D.L.*, et al.* (1999). Effects of free fatty acids on glucose transport and IRS-1-associated phosphatidylinositol 3-kinase activity. J Clin Invest *103*, 253-259.
Dufour, C.R., Wilson, B.J., Huss, J.M., Kelly, D.P., Alaynick, W.A., Downes, M., Evans, R.M., Blanchette, M., and Giguere, V. (2007). Genome-wide orchestration of cardiac functions by the orphan nuclear receptors ERRalpha and gamma. Cell Metab *5*, 345-356.
Dynan, W.S., and Tjian, R. (1983). Isolation of transcription factors that discriminate between different promoters recognized by RNA polymerase II. Cell *32*, 669-680.
Eddinger, T.J., Cassens, R.G., and Moss, R.L. (1986). Mechanical and histochemical characterization of skeletal muscles from senescent rats. Am J Physiol *251*, C421-430.
Eddinger, T.J., and Moss, R.L. (1987). Mechanical properties of skinned single fibers of identified types from rat diaphragm. Am J Physiol *253*, C210-218.
Eddinger, T.J., Moss, R.L., and Cassens, R.G. (1985a). Fiber number and type composition in extensor digitorum longus, soleus, and diaphragm muscles with aging in Fisher 344 rats. J Histochem Cytochem *33*, 1033-1041.
Eddinger, T.J., Moss, R.L., and Cassens, R.G. (1985b). Myosin-ATPase fibre typing of chemically skinned muscle fibres. Histochem J *17*, 1021-1026.

Faresse, N., Colland, F., Ferrand, N., Prunier, C., Bourgeade, M.F., and Atfi, A. (2008). Identification of PCTA, a TGIF antagonist that promotes PML function in TGF-beta signalling. EMBO J *27*, 1804-1815.
Farrance, I.K., Mar, J.H., and Ordahl, C.P. (1992). M-CAT binding factor is related to the SV40 enhancer binding factor, TEF-1. J Biol Chem *267*, 17234-17240.
Farrance, I.K., and Ordahl, C.P. (1996). The role of transcription enhancer factor-1 (TEF-1) related proteins in the formation of M-CAT binding complexes in muscle and non-muscle tissues. J Biol Chem *271*, 8266-8274.
Farstad, M., Bremer, J., and Norum, K.R. (1967). Long-chain acyl-CoA synthetase in rat liver. A new assay procedure for the enzyme, and studies on its intracellular localization. Biochim Biophys Acta *132*, 492-502.
Faucheux, C., Naye, F., Treguer, K., Fedou, S., Thiebaud, P., and Theze, N. (2010). Vestigial like gene family expression in Xenopus: common and divergent features with other vertebrates. Int J Dev Biol *54*, 1375-1382.
Feige, J.N., Lagouge, M., Canto, C., Strehle, A., Houten, S.M., Milne, J.C., Lambert, P.D., Mataki, C., Elliott, P.J., and Auwerx, J. (2008). Specific SIRT1 activation mimics low energy levels and protects against diet-induced metabolic disorders by enhancing fat oxidation. Cell Metab *8*, 347-358.
Fernando, P., Kelly, J.F., Balazsi, K., Slack, R.S., and Megeney, L.A. (2002). Caspase 3 activity is required for skeletal muscle differentiation. Proc Natl Acad Sci U S A *99*, 11025-11030.
Ferrara, N., and Henzel, W.J. (1989). Pituitary follicular cells secrete a novel heparin-binding growth factor specific for vascular endothelial cells. Biochem Biophys Res Commun *161*, 851-858.
Fitzsimons, D.P., Diffee, G.M., Herrick, R.E., and Baldwin, K.M. (1990). Effects of endurance exercise on isomyosin patterns in fast- and slow-twitch skeletal muscles. J Appl Physiol *68*, 1950-1955.
Fong, G.H., Rossant, J., Gertsenstein, M., and Breitman, M.L. (1995). Role of the Flt-1 receptor tyrosine kinase in regulating the assembly of vascular endothelium. Nature *376*, 66-70.
Fontes, M.R., Teh, T., Riell, R.D., Park, S.B., Standaert, R.F., and Kobe, B. (2005). Crystallization and preliminary X-ray diffraction analysis of importin-alpha complexed with NLS peptidomimetics. Biochim Biophys Acta *1750*, 9-13.
Fossdal, R., Jonasson, F., Kristjansdottir, G.T., Kong, A., Stefansson, H., Gosh, S., Gulcher, J.R., and Stefansson, K. (2004). A novel TEAD1 mutation is the causative allele in Sveinsson's chorioretinal atrophy (helicoid peripapillary chorioretinal degeneration). Hum Mol Genet *13*, 975-981.
Frevert, E.U., Bjorbaek, C., Venable, C.L., Keller, S.R., and Kahn, B.B. (1998). Targeting of constitutively active phosphoinositide 3-kinase to GLUT4-containing vesicles in 3T3-L1 adipocytes. J Biol Chem *273*, 25480-25487.
Frey, N., Frank, D., Lippl, S., Kuhn, C., Kogler, H., Barrientos, T., Rohr, C., Will, R., Muller, O.J., Weiler, H.*, et al.* (2008). Calsarcin-2 deficiency increases exercise capacity in mice through calcineurin/NFAT activation. J Clin Invest *118*, 3598-3608.
Fujino, T., and Yamamoto, T. (1992). Cloning and functional expression of a novel long-chain acyl-CoA synthetase expressed in brain. J Biochem *111*, 197-203.
Gaisa, N.T., Koster, J., Reinartz, A., Ertmer, K., Ehling, J., Raupach, K., Perez-Bouza, A., Knuchel, R., and Gassler, N. (2008). Expression of acyl-CoA synthetase 5 in human epidermis. Histol Histopathol *23*, 451-458.

Garvey, W.T., Maianu, L., Zhu, J.H., Brechtel-Hook, G., Wallace, P., and Baron, A.D. (1998). Evidence for defects in the trafficking and translocation of GLUT4 glucose transporters in skeletal muscle as a cause of human insulin resistance. J Clin Invest *101*, 2377-2386.
Gee, S.T., Milgram, S.L., Kramer, K.L., Conlon, F.L., and Moody, S.A. (2011). Yes-Associated Protein 65 (YAP) Expands Neural Progenitors and Regulates Pax3 Expression in the Neural Plate Border Zone. PLoS One *6*, e20309.
Germain, H., Qu, N., Cheng, Y.T., Lee, E., Huang, Y., Dong, O.X., Gannon, P., Huang, S., Ding, P., Li, Y.*, et al.* (2010). MOS11: A New Component in the mRNA Export Pathway. PLoS Genet *6*, e1001250.
Gerstner, J.R., Vanderheyden, W.M., Shaw, P.J., Landry, C.F., and Yin, J.C. (2011). Fatty-Acid binding proteins modulate sleep and enhance long-term memory consolidation in Drosophila. PLoS One *6*, e15890.
Gray, M.J., Zhang, J., Ellis, L.M., Semenza, G.L., Evans, D.B., Watowich, S.S., and Gallick, G.E. (2005). HIF-1alpha, STAT3, CBP/p300 and Ref-1/APE are components of a transcriptional complex that regulates Src-dependent hypoxia-induced expression of VEGF in pancreatic and prostate carcinomas. Oncogene *24*, 3110-3120.
Greenberg, A.S., Coleman, R.A., Kraemer, F.B., McManaman, J.L., Obin, M.S., Puri, V., Yan, Q.W., Miyoshi, H., and Mashek, D.G. (2011). The role of lipid droplets in metabolic disease in rodents and humans. J Clin Invest *121*, 2102-2110.
Griffin, M.E., Marcucci, M.J., Cline, G.W., Bell, K., Barucci, N., Lee, D., Goodyear, L.J., Kraegen, E.W., White, M.F., and Shulman, G.I. (1999). Free fatty acid-induced insulin resistance is associated with activation of protein kinase C theta and alterations in the insulin signaling cascade. Diabetes *48*, 1270-1274.
Guarani, V., Deflorian, G., Franco, C.A., Kruger, M., Phng, L.K., Bentley, K., Toussaint, L., Dequiedt, F., Mostoslavsky, R., Schmidt, M.H.*, et al.* (2011). Acetylation-dependent regulation of endothelial Notch signalling by the SIRT1 deacetylase. Nature *473*, 234-238.
Gulick, A.M., Starai, V.J., Horswill, A.R., Homick, K.M., and Escalante-Semerena, J.C. (2003). The 1.75 A crystal structure of acetyl-CoA synthetase bound to adenosine-5'-propylphosphate and coenzyme A. Biochemistry *42*, 2866-2873.
Gunther, S., Mielcarek, M., Kruger, M., and Braun, T. (2004). VITO-1 is an essential cofactor of TEF1-dependent muscle-specific gene regulation. Nucleic Acids Res *32*, 791-802.
Gupta, M., Kogut, P., Davis, F.J., Belaguli, N.S., Schwartz, R.J., and Gupta, M.P. (2001). Physical interaction between the MADS box of serum response factor and the TEA/ATTS DNA-binding domain of transcription enhancer factor-1. J Biol Chem *276*, 10413-10422.
Gupta, M.P., Amin, C.S., Gupta, M., Hay, N., and Zak, R. (1997). Transcription enhancer factor 1 interacts with a basic helix-loop-helix zipper protein, Max, for positive regulation of cardiac alpha-myosin heavy-chain gene expression. Mol Cell Biol *17*, 3924-3936.
Halder, G., Polaczyk, P., Kraus, M.E., Hudson, A., Kim, J., Laughon, A., and Carroll, S. (1998). The Vestigial and Scalloped proteins act together to directly regulate wing-specific gene expression in Drosophila. Genes Dev *12*, 3900-3909.
Hamanaka, R., Kohno, K., Seguchi, T., Okamura, K., Morimoto, A., Ono, M., Ogata, J., and Kuwano, M. (1992). Induction of low density lipoprotein receptor and a

transcription factor SP-1 by tumor necrosis factor in human microvascular endothelial cells. J Biol Chem *267*, 13160-13165.
Han, G., Ye, M., Liu, H., Song, C., Sun, D., Wu, Y., Jiang, X., Chen, R., Wang, C., Wang, L.*, et al.* (2010). Phosphoproteome analysis of human liver tissue by long-gradient nanoflow LC coupled with multiple stage MS analysis. Electrophoresis *31*, 1080-1089.
Handschin, C., Chin, S., Li, P., Liu, F., Maratos-Flier, E., Lebrasseur, N.K., Yan, Z., and Spiegelman, B.M. (2007). Skeletal muscle fiber-type switching, exercise intolerance, and myopathy in PGC-1alpha muscle-specific knock-out animals. J Biol Chem *282*, 30014-30021.
Harpster, M.H., Bandyopadhyay, S., Thomas, D.P., Ivanov, P.S., Keele, J.A., Pineguina, N., Gao, B., Amarendran, V., Gomelsky, M., McCormick, R.J.*, et al.* (2006). Earliest changes in the left ventricular transcriptome postmyocardial infarction. Mamm Genome *17*, 701-715.
Harrison, B.C., Huynh, K., Lundgaard, G.L., Helmke, S.M., Perryman, M.B., and McKinsey, T.A. (2010). Protein kinase C-related kinase targets nuclear localization signals in a subset of class IIa histone deacetylases. FEBS Lett *584*, 1103-1110.
Haupt, A., Thamer, C., Machann, J., Kirchhoff, K., Stefan, N., Tschritter, O., Machicao, F., Schick, F., Haring, H.U., and Fritsche, A. (2008). Impact of variation in the FTO gene on whole body fat distribution, ectopic fat, and weight loss. Obesity (Silver Spring) *16*, 1969-1972.
Heger, S., Mastronardi, C., Dissen, G.A., Lomniczi, A., Cabrera, R., Roth, C.L., Jung, H., Galimi, F., Sippell, W., and Ojeda, S.R. (2007). Enhanced at puberty 1 (EAP1) is a new transcriptional regulator of the female neuroendocrine reproductive axis. J Clin Invest *117*, 2145-2154.
Holash, J., Maisonpierre, P.C., Compton, D., Boland, P., Alexander, C.R., Zagzag, D., Yancopoulos, G.D., and Wiegand, S.J. (1999). Vessel cooption, regression, and growth in tumors mediated by angiopoietins and VEGF. Science *284*, 1994-1998.
Houck, K.A., Leung, D.W., Rowland, A.M., Winer, J., and Ferrara, N. (1992). Dual regulation of vascular endothelial growth factor bioavailability by genetic and proteolytic mechanisms. J Biol Chem *267*, 26031-26037.
Hua, H.T., Albadawi, H., Entabi, F., Conrad, M., Stoner, M.C., Meriam, B.T., Sroufe, R., Houser, S., Lamuraglia, G.M., and Watkins, M.T. (2005). Polyadenosine diphosphate-ribose polymerase inhibition modulates skeletal muscle injury following ischemia reperfusion. Arch Surg *140*, 344-351; discussion 351-342.
Iijima, H., Fujino, T., Minekura, H., Suzuki, H., Kang, M.J., and Yamamoto, T. (1996). Biochemical studies of two rat acyl-CoA synthetases, ACS1 and ACS2. Eur J Biochem *242*, 186-190.
Ikemoto, S., Thompson, K.S., Itakura, H., Lane, M.D., and Ezaki, O. (1995). Expression of an insulin-responsive glucose transporter (GLUT4) minigene in transgenic mice: effect of exercise and role in glucose homeostasis. Proc Natl Acad Sci U S A *92*, 865-869.
Itani, S.I., Ruderman, N.B., Schmieder, F., and Boden, G. (2002). Lipid-induced insulin resistance in human muscle is associated with changes in diacylglycerol, protein kinase C, and IkappaB-alpha. Diabetes *51*, 2005-2011.
Jablonska, J., Leschner, S., Westphal, K., Lienenklaus, S., and Weiss, S. (2010). Neutrophils responsive to endogenous IFN-beta regulate tumor angiogenesis and growth in a mouse tumor model. J Clin Invest *120*, 1151-1164.

Janssen, I., Heymsfield, S.B., Wang, Z.M., and Ross, R. (2000). Skeletal muscle mass and distribution in 468 men and women aged 18-88 yr. J Appl Physiol *89*, 81-88.
Jonasson, F., Sander, B., Eysteinsson, T., Jorgensen, T., and Klintworth, G.K. (2007). Sveinsson chorioretinal atrophy: the mildest changes are located in the photoreceptor outer segment/retinal pigment epithelium junction. Acta Ophthalmol Scand *85*, 862-867.
Jung, J.E., Lee, H.G., Cho, I.H., Chung, D.H., Yoon, S.H., Yang, Y.M., Lee, J.W., Choi, S., Park, J.W., Ye, S.K.*, et al.* (2005). STAT3 is a potential modulator of HIF-1-mediated VEGF expression in human renal carcinoma cells. FASEB J *19*, 1296-1298.
Kadonaga, J.T., Carner, K.R., Masiarz, F.R., and Tjian, R. (1987). Isolation of cDNA encoding transcription factor Sp1 and functional analysis of the DNA binding domain. Cell *51*, 1079-1090.
Kahn, S.E., Hull, R.L., and Utzschneider, K.M. (2006). Mechanisms linking obesity to insulin resistance and type 2 diabetes. Nature *444*, 840-846.
Kallio, P.J., Wilson, W.J., O'Brien, S., Makino, Y., and Poellinger, L. (1999). Regulation of the hypoxia-inducible transcription factor 1alpha by the ubiquitin-proteasome pathway. J Biol Chem *274*, 6519-6525.
Kamiryo, T., Nishikawa, Y., Mishina, M., Terao, M., and Numa, S. (1979). Involvement of long-chain acyl coenzyme A for lipid synthesis in repression of acetyl-coenzyme A carboxylase in Candida lipolytica. Proc Natl Acad Sci U S A *76*, 4390-4394.
Kang, M.J., Fujino, T., Sasano, H., Minekura, H., Yabuki, N., Nagura, H., Iijima, H., and Yamamoto, T.T. (1997). A novel arachidonate-preferring acyl-CoA synthetase is present in steroidogenic cells of the rat adrenal, ovary, and testis. Proc Natl Acad Sci U S A *94*, 2880-2884.
Karasseva, N., Tsika, G., Ji, J., Zhang, A., Mao, X., and Tsika, R. (2003). Transcription enhancer factor 1 binds multiple muscle MEF2 and A/T-rich elements during fast-to-slow skeletal muscle fiber type transitions. Mol Cell Biol *23*, 5143-5164.
Kariya, K., Farrance, I.K., and Simpson, P.C. (1993). Transcriptional enhancer factor-1 in cardiac myocytes interacts with an alpha 1-adrenergic- and beta-protein kinase C-inducible element in the rat beta-myosin heavy chain promoter. J Biol Chem *268*, 26658-26662.
Kelly, T.J., Lerin, C., Haas, W., Gygi, S.P., and Puigserver, P. (2009). GCN5-mediated transcriptional control of the metabolic coactivator PGC-1beta through lysine acetylation. J Biol Chem *284*, 19945-19952.
Keyt, B.A., Nguyen, H.V., Berleau, L.T., Duarte, C.M., Park, J., Chen, H., and Ferrara, N. (1996). Identification of vascular endothelial growth factor determinants for binding KDR and FLT-1 receptors. Generation of receptor-selective VEGF variants by site-directed mutagenesis. J Biol Chem *271*, 5638-5646.
Kim, E.S., Hong, S.Y., Lee, H.K., Kim, S.W., An, M.J., Kim, T.I., Lee, K.R., Kim, W.H., and Cheon, J.H. (2008). Guggulsterone inhibits angiogenesis by blocking STAT3 and VEGF expression in colon cancer cells. Oncol Rep *20*, 1321-1327.
Kim, H.S., Park, Y.H., Lee, J., Ahn, J.S., Kim, J., Shim, Y.M., Kim, J.H., Park, K., Han, J., and Ahn, M.J. (2010). Clinical impact of phosphorylated signal transducer and activator of transcription 3, epidermal growth factor receptor, p53, and vascular endothelial growth factor receptor 1 expression in resected adenocarcinoma of lung by using tissue microarray. Cancer *116*, 676-685.

Kim, J.K., Fillmore, J.J., Sunshine, M.J., Albrecht, B., Higashimori, T., Kim, D.W., Liu, Z.X., Soos, T.J., Cline, G.W., O'Brien, W.R*., et al.* (2004). PKC-theta knockout mice are protected from fat-induced insulin resistance. J Clin Invest *114*, 823-827.
Knight, J.F., Shepherd, C.J., Rizzo, S., Brewer, D., Jhavar, S., Dodson, A.R., Cooper, C.S., Eeles, R., Falconer, A., Kovacs, G*., et al.* (2008). TEAD1 and c-Cbl are novel prostate basal cell markers that correlate with poor clinical outcome in prostate cancer. Br J Cancer *99*, 1849-1858.
Knoll, L.J., Johnson, D.R., and Gordon, J.I. (1995). Complementation of Saccharomyces cerevisiae strains containing fatty acid activation gene (FAA) deletions with a mammalian acyl-CoA synthetase. J Biol Chem *270*, 10861-10867.
Koeppel, M., van Heeringen, S.J., Smeenk, L., Navis, A.C., Janssen-Megens, E.M., and Lohrum, M. (2009). The novel p53 target gene IRF2BP2 participates in cell survival during the p53 stress response. Nucleic Acids Res *37*, 322-335.
Krishnan, J., Ahuja, P., Bodenmann, S., Knapik, D., Perriard, E., Krek, W., and Perriard, J.C. (2008). Essential role of developmentally activated hypoxia-inducible factor 1alpha for cardiac morphogenesis and function. Circ Res *103*, 1139-1146.
Kuwahara, H., Nishizaki, M., and Kanazawa, H. (2008). Nuclear localization signal and phosphorylation of Serine350 specify intracellular localization of DRAK2. J Biochem *143*, 349-358.
Langley, E., Pearson, M., Faretta, M., Bauer, U.M., Frye, R.A., Minucci, S., Pelicci, P.G., and Kouzarides, T. (2002). Human SIR2 deacetylates p53 and antagonizes PML/p53-induced cellular senescence. EMBO J *21*, 2383-2396.
Larsen, B.D., Rampalli, S., Burns, L.E., Brunette, S., Dilworth, F.J., and Megeney, L.A. (2010). Caspase 3/caspase-activated DNase promote cell differentiation by inducing DNA strand breaks. Proc Natl Acad Sci U S A *107*, 4230-4235.
Lee, B.J., Cansizoglu, A.E., Suel, K.E., Louis, T.H., Zhang, Z., and Chook, Y.M. (2006). Rules for nuclear localization sequence recognition by karyopherin beta 2. Cell *126*, 543-558.
Lee, K.A., Lynd, J.D., O'Reilly, S., Kiupel, M., McCormick, J.J., and LaPres, J.J. (2008). The biphasic role of the hypoxia-inducible factor prolyl-4-hydroxylase, PHD2, in modulating tumor-forming potential. Mol Cancer Res *6*, 829-842.
Lennarz, W.J. (1963). A long-chain fatty acid acyl-coA synthetase in Bacillus megaterium. Biochim Biophys Acta *73*, 335-337.
Leung, D.W., Cachianes, G., Kuang, W.J., Goeddel, D.V., and Ferrara, N. (1989). Vascular endothelial growth factor is a secreted angiogenic mitogen. Science *246*, 1306-1309.
Levy, A.P., Levy, N.S., Wegner, S., and Goldberg, M.A. (1995). Transcriptional regulation of the rat vascular endothelial growth factor gene by hypoxia. J Biol Chem *270*, 13333-13340.
Levy, E., Menard, D., Delvin, E., Montoudis, A., Beaulieu, J.F., Mailhot, G., Dube, N., Sinnett, D., Seidman, E., and Bendayan, M. (2009). Localization, function and regulation of the two intestinal fatty acid-binding protein types. Histochem Cell Biol *132*, 351-367.
Lewin, T.M., Kim, J.H., Granger, D.A., Vance, J.E., and Coleman, R.A. (2001). Acyl-CoA synthetase isoforms 1, 4, and 5 are present in different subcellular membranes in rat liver and can be inhibited independently. J Biol Chem *276*, 24674-24679.

Lewis, R.E., Cao, L., Perregaux, D., and Czech, M.P. (1990). Threonine 1336 of the human insulin receptor is a major target for phosphorylation by protein kinase C. Biochemistry *29*, 1807-1813.
Li, Z., Zhao, B., Wang, P., Chen, F., Dong, Z., Yang, H., Guan, K.L., and Xu, Y. (2010). Structural insights into the YAP and TEAD complex. Genes Dev *24*, 235-240.
Lidke, D.S., Huang, F., Post, J.N., Rieger, B., Wilsbacher, J., Thomas, J.L., Pouyssegur, J., Jovin, T.M., and Lenormand, P. (2010). ERK nuclear translocation is dimerization-independent but controlled by the rate of phosphorylation. J Biol Chem *285*, 3092-3102.
Lin, J., Wu, H., Tarr, P.T., Zhang, C.Y., Wu, Z., Boss, O., Michael, L.F., Puigserver, P., Isotani, E., Olson, E.N.*, et al.* (2002). Transcriptional co-activator PGC-1 alpha drives the formation of slow-twitch muscle fibres. Nature *418*, 797-801.
Lindi, V.I., Uusitupa, M.I., Lindstrom, J., Louheranta, A., Eriksson, J.G., Valle, T.T., Hamalainen, H., Ilanne-Parikka, P., Keinanen-Kiukaanniemi, S., Laakso, M.*, et al.* (2002). Association of the Pro12Ala polymorphism in the PPAR-gamma2 gene with 3-year incidence of type 2 diabetes and body weight change in the Finnish Diabetes Prevention Study. Diabetes *51*, 2581-2586.
Liu, Y., Cox, S.R., Morita, T., and Kourembanas, S. (1995). Hypoxia regulates vascular endothelial growth factor gene expression in endothelial cells. Identification of a 5' enhancer. Circ Res *77*, 638-643.
Liu, Y., Xin, Y., Ye, F., Wang, W., Lu, Q., Kaplan, H.J., and Dean, D.C. (2010). Taz-tead1 links cell-cell contact to zeb1 expression, proliferation, and dedifferentiation in retinal pigment epithelial cells. Invest Ophthalmol Vis Sci *51*, 3372-3378.
Lluis, F., Ballestar, E., Suelves, M., Esteller, M., and Munoz-Canoves, P. (2005). E47 phosphorylation by p38 MAPK promotes MyoD/E47 association and muscle-specific gene transcription. EMBO J *24*, 974-984.
Luan, J., Browne, P.O., Harding, A.H., Halsall, D.J., O'Rahilly, S., Chatterjee, V.K., and Wareham, N.J. (2001). Evidence for gene-nutrient interaction at the PPARgamma locus. Diabetes *50*, 686-689.
Ma, R.Y., Tong, T.H., Cheung, A.M., Tsang, A.C., Leung, W.Y., and Yao, K.M. (2005). Raf/MEK/MAPK signaling stimulates the nuclear translocation and transactivating activity of FOXM1c. J Cell Sci *118*, 795-806.
Macey, M.J., and Stumpf, P.K. (1968). Fat Metabolism in Higher Plants XXXVI: Long Chain Fatty Acid Synthesis in Germinating Peas. Plant Physiol *43*, 1637-1647.
Maeda, T., Chapman, D.L., and Stewart, A.F. (2002a). Mammalian vestigial-like 2, a cofactor of TEF-1 and MEF2 transcription factors that promotes skeletal muscle differentiation. J Biol Chem *277*, 48889-48898.
Maeda, T., Gupta, M.P., and Stewart, A.F. (2002b). TEF-1 and MEF2 transcription factors interact to regulate muscle-specific promoters. Biochem Biophys Res Commun *294*, 791-797.
Mahoney, W.M., Jr., Hong, J.H., Yaffe, M.B., and Farrance, I.K. (2005). The transcriptional co-activator TAZ interacts differentially with transcriptional enhancer factor-1 (TEF-1) family members. Biochem J *388*, 217-225.
Mann, C.J., Osborn, D.P., and Hughes, S.M. (2007). Vestigial-like-2b (VITO-1b) and Tead-3a (Tef-5a) expression in zebrafish skeletal muscle, brain and notochord. Gene Expr Patterns *7*, 827-836.

Marcel, Y.L., and Suzue, G. (1972). Kinetic studies on the specificity of long chain acyl coenzyme A synthetase from rat liver microsomes. J Biol Chem *247*, 4433-4436.
Maroto, M., Reshef, R., Munsterberg, A.E., Koester, S., Goulding, M., and Lassar, A.B. (1997). Ectopic Pax-3 activates MyoD and Myf-5 expression in embryonic mesoderm and neural tissue. Cell *89*, 139-148.
Mashek, D.G., Li, L.O., and Coleman, R.A. (2006a). Rat long-chain acyl-CoA synthetase mRNA, protein, and activity vary in tissue distribution and in response to diet. J Lipid Res *47*, 2004-2010.
Mashek, D.G., McKenzie, M.A., Van Horn, C.G., and Coleman, R.A. (2006b). Rat long chain acyl-CoA synthetase 5 increases fatty acid uptake and partitioning to cellular triacylglycerol in McArdle-RH7777 cells. J Biol Chem *281*, 945-950.
Mayya, V., Lundgren, D.H., Hwang, S.I., Rezaul, K., Wu, L., Eng, J.K., Rodionov, V., and Han, D.K. (2009). Quantitative phosphoproteomic analysis of T cell receptor signaling reveals system-wide modulation of protein-protein interactions. Sci Signal *2*, ra46.
Miyamoto, Y., Imamoto, N., Sekimoto, T., Tachibana, T., Seki, T., Tada, S., Enomoto, T., and Yoneda, Y. (1997). Differential modes of nuclear localization signal (NLS) recognition by three distinct classes of NLS receptors. J Biol Chem *272*, 26375-26381.
Mole, D.R., Blancher, C., Copley, R.R., Pollard, P.J., Gleadle, J.M., Ragoussis, J., and Ratcliffe, P.J. (2009). Genome-wide association of hypoxia-inducible factor (HIF)-1alpha and HIF-2alpha DNA binding with expression profiling of hypoxia-inducible transcripts. J Biol Chem *284*, 16767-16775.
Muller, T.D., Hinney, A., Scherag, A., Nguyen, T.T., Schreiner, F., Schafer, H., Hebebrand, J., Roth, C.L., and Reinehr, T. (2008). 'Fat mass and obesity associated' gene (FTO): no significant association of variant rs9939609 with weight loss in a lifestyle intervention and lipid metabolism markers in German obese children and adolescents. BMC Med Genet *9*, 85.
Muoio, D.M., Lewin, T.M., Wiedmer, P., and Coleman, R.A. (2000). Acyl-CoAs are functionally channeled in liver: potential role of acyl-CoA synthetase. Am J Physiol Endocrinol Metab *279*, E1366-1373.
Nicklas, B.J., van Rossum, E.F., Berman, D.M., Ryan, A.S., Dennis, K.E., and Shuldiner, A.R. (2001). Genetic variation in the peroxisome proliferator-activated receptor-gamma2 gene (Pro12Ala) affects metabolic responses to weight loss and subsequent weight regain. Diabetes *50*, 2172-2176.
Nieman, K.M., Kenny, H.A., Penicka, C.V., Ladanyi, A., Buell-Gutbrod, R., Zillhardt, M.R., Romero, I.L., Carey, M.S., Mills, G.B., Hotamisligil, G.S.*, et al.* (2011). Adipocytes promote ovarian cancer metastasis and provide energy for rapid tumor growth. Nat Med *17*, 1498-1503.
Novak, E.M., Metzger, M., Chammas, R., da Costa, M., Dantas, K., Manabe, C., Pires, J., de Oliveira, A.C., and Bydlowski, S.P. (2003). Downregulation of TNF-alpha and VEGF expression by Sp1 decoy oligodeoxynucleotides in mouse melanoma tumor. Gene Ther *10*, 1992-1997.
Ockner, R.K., Burnett, D.A., Lysenko, N., and Manning, J.A. (1979). Sex differences in long chain fatty acid utilization and fatty acid binding protein concentration in rat liver. J Clin Invest *64*, 172-181.
Oh, M., Rybkin, II, Copeland, V., Czubryt, M.P., Shelton, J.M., van Rooij, E., Richardson, J.A., Hill, J.A., De Windt, L.J., Bassel-Duby, R.*, et al.* (2005). Calcineurin

is necessary for the maintenance but not embryonic development of slow muscle fibers. Mol Cell Biol *25*, 6629-6638.
Oikawa, E., Iijima, H., Suzuki, T., Sasano, H., Sato, H., Kamataki, A., Nagura, H., Kang, M.J., Fujino, T., Suzuki, H.*, et al.* (1998). A novel acyl-CoA synthetase, ACS5, expressed in intestinal epithelial cells and proliferating preadipocytes. J Biochem *124*, 679-685.
Olabisi, O.A., Soto-Nieves, N., Nieves, E., Yang, T.T., Yang, X., Yu, R.Y., Suk, H.Y., Macian, F., and Chow, C.W. (2008). Regulation of transcription factor NFAT by ADP-ribosylation. Mol Cell Biol *28*, 2860-2871.
Olfert, I.M., Howlett, R.A., Tang, K., Dalton, N.D., Gu, Y., Peterson, K.L., Wagner, P.D., and Breen, E.C. (2009). Muscle-specific VEGF deficiency greatly reduces exercise endurance in mice. J Physiol *587*, 1755-1767.
Olsen, J.V., Blagoev, B., Gnad, F., Macek, B., Kumar, C., Mortensen, P., and Mann, M. (2006). Global, in vivo, and site-specific phosphorylation dynamics in signaling networks. Cell *127*, 635-648.
Oppermann, F.S., Gnad, F., Olsen, J.V., Hornberger, R., Greff, Z., Keri, G., Mann, M., and Daub, H. (2009). Large-scale proteomics analysis of the human kinome. Mol Cell Proteomics *8*, 1751-1764.
Ota, M., and Sasaki, H. (2008). Mammalian Tead proteins regulate cell proliferation and contact inhibition as transcriptional mediators of Hippo signaling. Development *135*, 4059-4069.
Paine, P.L., Moore, L.C., and Horowitz, S.B. (1975). Nuclear envelope permeability. Nature *254*, 109-114.
Parsons, S.A., Millay, D.P., Wilkins, B.J., Bueno, O.F., Tsika, G.L., Neilson, J.R., Liberatore, C.M., Yutzey, K.E., Crabtree, G.R., Tsika, R.W.*, et al.* (2004). Genetic loss of calcineurin blocks mechanical overload-induced skeletal muscle fiber type switching but not hypertrophy. J Biol Chem *279*, 26192-26200.
Pennacchio, L.A., Olivier, M., Hubacek, J.A., Cohen, J.C., Cox, D.R., Fruchart, J.C., Krauss, R.M., and Rubin, E.M. (2001). An apolipoprotein influencing triglycerides in humans and mice revealed by comparative sequencing. Science *294*, 169-173.
Picard, F., Kurtev, M., Chung, N., Topark-Ngarm, A., Senawong, T., Machado De Oliveira, R., Leid, M., McBurney, M.W., and Guarente, L. (2004). Sirt1 promotes fat mobilization in white adipocytes by repressing PPAR-gamma. Nature *429*, 771-776.
Pisabarro, R.E., Sanguinetti, C., Stoll, M., and Prendez, D. (2004). High incidence of type 2 diabetes in peroxisome proliferator-activated receptor gamma2 Pro12Ala carriers exposed to a high chronic intake of trans fatty acids and saturated fatty acids. Diabetes Care *27*, 2251-2252.
Poirier, P., Giles, T.D., Bray, G.A., Hong, Y., Stern, J.S., Pi-Sunyer, F.X., and Eckel, R.H. (2006). Obesity and cardiovascular disease: pathophysiology, evaluation, and effect of weight loss. Arterioscler Thromb Vasc Biol *26*, 968-976.
Pollak, N., Dolle, C., and Ziegler, M. (2007). The power to reduce: pyridine nucleotides--small molecules with a multitude of functions. Biochem J *402*, 205-218.
Potente, M., Ghaeni, L., Baldessari, D., Mostoslavsky, R., Rossig, L., Dequiedt, F., Haendeler, J., Mione, M., Dejana, E., Alt, F.W.*, et al.* (2007). SIRT1 controls endothelial angiogenic functions during vascular growth. Genes Dev *21*, 2644-2658.

Prince, F.P., Hikida, R.S., Hagerman, F.C., Staron, R.S., and Allen, W.H. (1981). A morphometric analysis of human muscle fibers with relation to fiber types and adaptations to exercise. J Neurol Sci *49*, 165-179.
Raijmakers, R., Kraiczek, K., de Jong, A.P., Mohammed, S., and Heck, A.J. (2010). Exploring the human leukocyte phosphoproteome using a microfluidic reversed-phase-TiO2-reversed-phase high-performance liquid chromatography phosphochip coupled to a quadrupole time-of-flight mass spectrometer. Anal Chem *82*, 824-832.
Rajamohan, S.B., Pillai, V.B., Gupta, M., Sundaresan, N.R., Birukov, K.G., Samant, S., Hottiger, M.O., and Gupta, M.P. (2009). SIRT1 promotes cell survival under stress by deacetylation-dependent deactivation of poly(ADP-ribose) polymerase 1. Mol Cell Biol *29*, 4116-4129.
Ralston, A., Cox, B.J., Nishioka, N., Sasaki, H., Chea, E., Rugg-Gunn, P., Guo, G., Robson, P., Draper, J.S., and Rossant, J. (2010). Gata3 regulates trophoblast development downstream of Tead4 and in parallel to Cdx2. Development *137*, 395-403.
Randle, P.J., Garland, P.B., Hales, C.N., and Newsholme, E.A. (1963). The glucose fatty-acid cycle. Its role in insulin sensitivity and the metabolic disturbances of diabetes mellitus. Lancet *1*, 785-789.
Rane, S., He, M., Sayed, D., Vashistha, H., Malhotra, A., Sadoshima, J., Vatner, D.E., Vatner, S.F., and Abdellatif, M. (2009). Downregulation of miR-199a derepresses hypoxia-inducible factor-1alpha and Sirtuin 1 and recapitulates hypoxia preconditioning in cardiac myocytes. Circ Res *104*, 879-886.
Ravi, R., Mookerjee, B., Bhujwalla, Z.M., Sutter, C.H., Artemov, D., Zeng, Q., Dillehay, L.E., Madan, A., Semenza, G.L., and Bedi, A. (2000). Regulation of tumor angiogenesis by p53-induced degradation of hypoxia-inducible factor 1alpha. Genes Dev *14*, 34-44.
Reinartz, A., Ehling, J., Leue, A., Liedtke, C., Schneider, U., Kopitz, J., Weiss, T., Hellerbrand, C., Weiskirchen, R., Knuchel, R*., et al.* (2010). Lipid-induced up-regulation of human acyl-CoA synthetase 5 promotes hepatocellular apoptosis. Biochim Biophys Acta *1801*, 1025-1035.
Rhodes, S.J., and Konieczny, S.F. (1989). Identification of MRF4: a new member of the muscle regulatory factor gene family. Genes Dev *3*, 2050-2061.
Ribas, R., Moncaut, N., Siligan, C., Taylor, K., Cross, J.W., Rigby, P.W., and Carvajal, J.J. (2011). Members of the TEAD family of transcription factors regulate the expression of Myf5 in ventral somitic compartments. Dev Biol *355*, 372-380.
Roden, M., Price, T.B., Perseghin, G., Petersen, K.F., Rothman, D.L., Cline, G.W., and Shulman, G.I. (1996). Mechanism of free fatty acid-induced insulin resistance in humans. J Clin Invest *97*, 2859-2865.
Rosado, E.L., Bressan, J., Martinez, J.A., and Marques-Lopes, I. (2010). Interactions of the PPARgamma2 polymorphism with fat intake affecting energy metabolism and nutritional outcomes in obese women. Ann Nutr Metab *57*, 242-250.
Rothman, D.L., Magnusson, I., Cline, G., Gerard, D., Kahn, C.R., Shulman, R.G., and Shulman, G.I. (1995). Decreased muscle glucose transport/phosphorylation is an early defect in the pathogenesis of non-insulin-dependent diabetes mellitus. Proc Natl Acad Sci U S A *92*, 983-987.
Rothman, D.L., Shulman, R.G., and Shulman, G.I. (1992). 31P nuclear magnetic resonance measurements of muscle glucose-6-phosphate. Evidence for reduced

insulin-dependent muscle glucose transport or phosphorylation activity in non-insulin-dependent diabetes mellitus. J Clin Invest *89*, 1069-1075.
Rudnicki, M.A., Schnegelsberg, P.N., Stead, R.H., Braun, T., Arnold, H.H., and Jaenisch, R. (1993). MyoD or Myf-5 is required for the formation of skeletal muscle. Cell *75*, 1351-1359.
Ryuto, M., Ono, M., Izumi, H., Yoshida, S., Weich, H.A., Kohno, K., and Kuwano, M. (1996). Induction of vascular endothelial growth factor by tumor necrosis factor alpha in human glioma cells. Possible roles of SP-1. J Biol Chem *271*, 28220-28228.
Safdar, A., Abadi, A., Akhtar, M., Hettinga, B.P., and Tarnopolsky, M.A. (2009). miRNA in the regulation of skeletal muscle adaptation to acute endurance exercise in C57Bl/6J male mice. PLoS One *4*, e5610.
Samuel, V.T., Petersen, K.F., and Shulman, G.I. (2010). Lipid-induced insulin resistance: unravelling the mechanism. Lancet *375*, 2267-2277.
Santiago, F.S., Ishii, H., Shafi, S., Khurana, R., Kanellakis, P., Bhindi, R., Ramirez, M.J., Bobik, A., Martin, J.F., Chesterman, C.N.*, et al.* (2007). Yin Yang-1 inhibits vascular smooth muscle cell growth and intimal thickening by repressing p21WAF1/Cip1 transcription and p21WAF1/Cip1-Cdk4-cyclin D1 assembly. Circ Res *101*, 146-155.
Santra, M., Santra, S., Zhang, J., and Chopp, M. (2008). Ectopic decorin expression up-regulates VEGF expression in mouse cerebral endothelial cells via activation of the transcription factors Sp1, HIF1alpha, and Stat3. J Neurochem *105*, 324-337.
Sawada, A., Kiyonari, H., Ukita, K., Nishioka, N., Imuta, Y., and Sasaki, H. (2008). Redundant roles of Tead1 and Tead2 in notochord development and the regulation of cell proliferation and survival. Mol Cell Biol *28*, 3177-3189.
Schafer, G., Cramer, T., Suske, G., Kemmner, W., Wiedenmann, B., and Hocker, M. (2003). Oxidative stress regulates vascular endothelial growth factor-A gene transcription through Sp1- and Sp3-dependent activation of two proximal GC-rich promoter elements. J Biol Chem *278*, 8190-8198.
Schroder, K., Schutz, S., Schloffel, I., Batz, S., Takac, I., Weissmann, N., Michaelis, U.R., Koyanagi, M., and Brandes, R.P. (2010). Hepatocyte growth factor induces a pro-angiogenic phenotype and mobilizes endothelial progenitor cells by activating Nox2. Antioxid Redox Signal.
Semenza, G.L., Nejfelt, M.K., Chi, S.M., and Antonarakis, S.E. (1991). Hypoxia-inducible nuclear factors bind to an enhancer element located 3' to the human erythropoietin gene. Proc Natl Acad Sci U S A *88*, 5680-5684.
Shalaby, F., Rossant, J., Yamaguchi, T.P., Gertsenstein, M., Wu, X.F., Breitman, M.L., and Schuh, A.C. (1995). Failure of blood-island formation and vasculogenesis in Flk-1-deficient mice. Nature *376*, 62-66.
Shen, X., Park, J.S., Qiu, Y., Sugar, J., and Yue, B.Y. (2009). Effects of Sp1 overexpression on cultured human corneal stromal cells. Genes Cells *14*, 1133-1139.
Sheng, T., Chi, S., Zhang, X., and Xie, J. (2006). Regulation of Gli1 localization by the cAMP/protein kinase A signaling axis through a site near the nuclear localization signal. J Biol Chem *281*, 9-12.
Shie, J.L., Wu, G., Wu, J., Liu, F.F., Laham, R.J., Oettgen, P., and Li, J. (2004). RTEF-1, a novel transcriptional stimulator of vascular endothelial growth factor in hypoxic endothelial cells. J Biol Chem *279*, 25010-25016.

Shulman, G.I., Rothman, D.L., Jue, T., Stein, P., DeFronzo, R.A., and Shulman, R.G. (1990). Quantitation of muscle glycogen synthesis in normal subjects and subjects with non-insulin-dependent diabetes by 13C nuclear magnetic resonance spectroscopy. N Engl J Med *322*, 223-228.
Sierra-Honigmann, M.R., Nath, A.K., Murakami, C., Garcia-Cardena, G., Papapetropoulos, A., Sessa, W.C., Madge, L.A., Schechner, J.S., Schwabb, M.B., Polverini, P.J.*, et al.* (1998). Biological action of leptin as an angiogenic factor. Science *281*, 1683-1686.
Skerjanc, I.S., and McBurney, M.W. (1994). The E box is essential for activity of the cardiac actin promoter in skeletal but not in cardiac muscle. Dev Biol *163*, 125-132.
Son, N.H., Yu, S., Tuinei, J., Arai, K., Hamai, H., Homma, S., Shulman, G.I., Abel, E.D., and Goldberg, I.J. (2010). PPARgamma-induced cardiolipotoxicity in mice is ameliorated by PPARalpha deficiency despite increases in fatty acid oxidation. J Clin Invest *120*, 3443-3454.
Spinner, D.S., Liu, S., Wang, S.W., and Schmidt, J. (2002). Interaction of the myogenic determination factor myogenin with E12 and a DNA target: mechanism and kinetics. J Mol Biol *317*, 431-445.
Stefan, N., Fritsche, A., Haring, H., and Stumvoll, M. (2001). Effect of experimental elevation of free fatty acids on insulin secretion and insulin sensitivity in healthy carriers of the Pro12Ala polymorphism of the peroxisome proliferator--activated receptor-gamma2 gene. Diabetes *50*, 1143-1148.
Stewart, A.F., Larkin, S.B., Farrance, I.K., Mar, J.H., Hall, D.E., and Ordahl, C.P. (1994). Muscle-enriched TEF-1 isoforms bind M-CAT elements from muscle-specific promoters and differentially activate transcription. J Biol Chem *269*, 3147-3150.
Stewart, A.F., Richard, C.W., 3rd, Suzow, J., Stephan, D., Weremowicz, S., Morton, C.C., and Adra, C.N. (1996). Cloning of human RTEF-1, a transcriptional enhancer factor-1-related gene preferentially expressed in skeletal muscle: evidence for an ancient multigene family. Genomics *37*, 68-76.
Stewart, A.F., Suzow, J., Kubota, T., Ueyama, T., and Chen, H.H. (1998). Transcription factor RTEF-1 mediates alpha1-adrenergic reactivation of the fetal gene program in cardiac myocytes. Circ Res *83*, 43-49.
Sudarsan, V., Anant, S., Guptan, P., VijayRaghavan, K., and Skaer, H. (2001). Myoblast diversification and ectodermal signaling in Drosophila. Dev Cell *1*, 829-839.
Suzuki, H., Kawarabayasi, Y., Kondo, J., Abe, T., Nishikawa, K., Kimura, S., Hashimoto, T., and Yamamoto, T. (1990). Structure and regulation of rat long-chain acyl-CoA synthetase. J Biol Chem *265*, 8681-8685.
Szabo, G., Bahrle, S., Stumpf, N., Sonnenberg, K., Szabo, E.E., Pacher, P., Csont, T., Schulz, R., Dengler, T.J., Liaudet, L.*, et al.* (2002). Poly(ADP-Ribose) polymerase inhibition reduces reperfusion injury after heart transplantation. Circ Res *90*, 100-106.
Tajbakhsh, S., Rocancourt, D., Cossu, G., and Buckingham, M. (1997). Redefining the genetic hierarchies controlling skeletal myogenesis: Pax-3 and Myf-5 act upstream of MyoD. Cell *89*, 127-138.
Takayama, S., White, M.F., and Kahn, C.R. (1988). Phorbol ester-induced serine phosphorylation of the insulin receptor decreases its tyrosine kinase activity. J Biol Chem *263*, 3440-3447.

Teng, A.C.T., Kuraitis, D., Deeke, S.A., Ahmadi, A., Dugan, S.G., Cheng, B.L., Crowson, M.G., Burgon, P.G., Suuronen, E.J., Chen, H.H., *et al.* (2010). IRF2BP2 is a skeletal and cardiac muscle-enriched ischemia-inducible activator of VEGFA expression. Faseb J *24*, 4825-4834.
Teodoro, J.G., Parker, A.E., Zhu, X., and Green, M.R. (2006). p53-mediated inhibition of angiogenesis through up-regulation of a collagen prolyl hydroxylase. Science *313*, 968-971.
Termin, A., Staron, R.S., and Pette, D. (1989). Myosin heavy chain isoforms in histochemically defined fiber types of rat muscle. Histochemistry *92*, 453-457.
Tinnikov, A.A., Yeung, K.T., Das, S., and Samuels, H.H. (2009). Identification of a novel pathway that selectively modulates apoptosis of breast cancer cells. Cancer Res *69*, 1375-1382.
Tsai, C.F., Wang, Y.T., Chen, Y.R., Lai, C.Y., Lin, P.Y., Pan, K.T., Chen, J.Y., Khoo, K.H., and Chen, Y.J. (2008). Immobilized metal affinity chromatography revisited: pH/acid control toward high selectivity in phosphoproteomics. J Proteome Res *7*, 4058-4069.
Tsika, R.W., Herrick, R.E., and Baldwin, K.M. (1987). Subunit composition of rodent isomyosins and their distribution in hindlimb skeletal muscles. J Appl Physiol *63*, 2101-2110.
Tsika, R.W., Ma, L., Kehat, I., Schramm, C., Simmer, G., Morgan, B., Fine, D.M., Hanft, L.M., McDonald, K.S., Molkentin, J.D., *et al.* (2010). TEAD-1 overexpression in the mouse heart promotes an age-dependent heart dysfunction. J Biol Chem *285*, 13721-13735.
Tsika, R.W., Schramm, C., Simmer, G., Fitzsimons, D.P., Moss, R.L., and Ji, J. (2008). Overexpression of TEAD-1 in transgenic mouse striated muscles produces a slower skeletal muscle contractile phenotype. J Biol Chem *283*, 36154-36167.
Ueyama, T., Zhu, C., Valenzuela, Y.M., Suzow, J.G., and Stewart, A.F. (2000). Identification of the functional domain in the transcription factor RTEF-1 that mediates alpha 1-adrenergic signaling in hypertrophied cardiac myocytes. J Biol Chem *275*, 17476-17480.
Van Hoof, D., Munoz, J., Braam, S.R., Pinkse, M.W., Linding, R., Heck, A.J., Mummery, C.L., and Krijgsveld, J. (2009). Phosphorylation dynamics during early differentiation of human embryonic stem cells. Cell Stem Cell *5*, 214-226.
Van Horn, C.G., Caviglia, J.M., Li, L.O., Wang, S., Granger, D.A., and Coleman, R.A. (2005). Characterization of recombinant long-chain rat acyl-CoA synthetase isoforms 3 and 6: identification of a novel variant of isoform 6. Biochemistry *44*, 1635-1642.
Vassilev, A., Kaneko, K.J., Shu, H., Zhao, Y., and DePamphilis, M.L. (2001). TEAD/TEF transcription factors utilize the activation domain of YAP65, a Src/Yes-associated protein localized in the cytoplasm. Genes Dev *15*, 1229-1241.
Vaudin, P., Delanoue, R., Davidson, I., Silber, J., and Zider, A. (1999). TONDU (TDU), a novel human protein related to the product of vestigial (vg) gene of Drosophila melanogaster interacts with vertebrate TEF factors and substitutes for Vg function in wing formation. Development *126*, 4807-4816.
Vaziri, H., Dessain, S.K., Ng Eaton, E., Imai, S.I., Frye, R.A., Pandita, T.K., Guarente, L., and Weinberg, R.A. (2001). hSIR2(SIRT1) functions as an NAD-dependent p53 deacetylase. Cell *107*, 149-159.

Visconti, R.P., Richardson, C.D., and Sato, T.N. (2002). Orchestration of angiogenesis and arteriovenous contribution by angiopoietins and vascular endothelial growth factor (VEGF). Proc Natl Acad Sci U S A *99*, 8219-8224.
Vyas, D.R., McCarthy, J.J., Tsika, G.L., and Tsika, R.W. (2001). Multiprotein complex formation at the beta myosin heavy chain distal muscle CAT element correlates with slow muscle expression but not mechanical overload responsiveness. J Biol Chem *276*, 1173-1184.
Wang, G.L., Jiang, B.H., Rue, E.A., and Semenza, G.L. (1995). Hypoxia-inducible factor 1 is a basic-helix-loop-helix-PAS heterodimer regulated by cellular O2 tension. Proc Natl Acad Sci U S A *92*, 5510-5514.
Wang, G.L., and Semenza, G.L. (1993). Characterization of hypoxia-inducible factor 1 and regulation of DNA binding activity by hypoxia. J Biol Chem *268*, 21513-21518.
Weintraub, H., Davis, R., Lockshon, D., and Lassar, A. (1990). MyoD binds cooperatively to two sites in a target enhancer sequence: occupancy of two sites is required for activation. Proc Natl Acad Sci U S A *87*, 5623-5627.
Williams, J.A., and Bell, J.B. (1988). Molecular organization of the vestigial region in Drosophila melanogaster. EMBO J *7*, 1355-1363.
Williams, J.A., Paddock, S.W., Vorwerk, K., and Carroll, S.B. (1994). Organization of wing formation and induction of a wing-patterning gene at the dorsal/ventral compartment boundary. Nature *368*, 299-305.
Willig, T.N., Carlier, L., Legrand, M., Riviere, H., and Navarro, J. (1993). Nutritional assessment in Duchenne muscular dystrophy. Dev Med Child Neurol *35*, 1074-1082.
Wright, W.E., Sassoon, D.A., and Lin, V.K. (1989). Myogenin, a factor regulating myogenesis, has a domain homologous to MyoD. Cell *56*, 607-617.
Wunderlich, M.T., Hanhoff, T., Goertler, M., Spener, F., Glatz, J.F., Wallesch, C.W., and Pelsers, M.M. (2005). Release of brain-type and heart-type fatty acid-binding proteins in serum after acute ischaemic stroke. J Neurol *252*, 718-724.
Xiao, J.H., Davidson, I., Matthes, H., Garnier, J.M., and Chambon, P. (1991). Cloning, expression, and transcriptional properties of the human enhancer factor TEF-1. Cell *65*, 551-568.
Xu, M., Jin, Y., Song, Q., Wu, J., Philbrick, M.J., Cully, B.L., An, X., Guo, L., Gao, F., and Li, J. (2011). The endothelium-dependent effect of RTEF-1 in pressure overload cardiac hypertrophy: role of VEGF-B. Cardiovasc Res.
Xu, Q., Briggs, J., Park, S., Niu, G., Kortylewski, M., Zhang, S., Gritsko, T., Turkson, J., Kay, H., Semenza, G.L.*, et al.* (2005). Targeting Stat3 blocks both HIF-1 and VEGF expression induced by multiple oncogenic growth signaling pathways. Oncogene *24*, 5552-5560.
Yagi, R., Kohn, M.J., Karavanova, I., Kaneko, K.J., Vullhorst, D., DePamphilis, M.L., and Buonanno, A. (2007). Transcription factor TEAD4 specifies the trophectoderm lineage at the beginning of mammalian development. Development *134*, 3827-3836.
Yamakawa, M., Liu, L.X., Date, T., Belanger, A.J., Vincent, K.A., Akita, G.Y., Kuriyama, T., Cheng, S.H., Gregory, R.J., and Jiang, C. (2003). Hypoxia-inducible factor-1 mediates activation of cultured vascular endothelial cells by inducing multiple angiogenic factors. Circ Res *93*, 664-673.
Yamashita, Y., Kumabe, T., Cho, Y.Y., Watanabe, M., Kawagishi, J., Yoshimoto, T., Fujino, T., Kang, M.J., and Yamamoto, T.T. (2000). Fatty acid induced glioma cell

growth is mediated by the acyl-CoA synthetase 5 gene located on chromosome 10q25.1-q25.2, a region frequently deleted in malignant gliomas. Oncogene *19*, 5919-5925.
Yeung, K.T., Das, S., Zhang, J., Lomniczi, A., Ojeda, S.R., Xu, C.F., Neubert, T.A., and Samuels, H.H. (2011). A Novel Transcription Complex That Selectively Modulates Apoptosis of Breast Cancer Cells through Regulation of FASTKD2. Mol Cell Biol *31*, 2287-2298.
Yoshida, T. (2008). MCAT elements and the TEF-1 family of transcription factors in muscle development and disease. Arterioscler Thromb Vasc Biol *28*, 8-17.
Young, R.M., Wang, S.J., Gordan, J.D., Ji, X., Liebhaber, S.A., and Simon, M.C. (2008). Hypoxia-mediated selective mRNA translation by an internal ribosome entry site-independent mechanism. J Biol Chem *283*, 16309-16319.
Yu, C., Chen, Y., Cline, G.W., Zhang, D., Zong, H., Wang, Y., Bergeron, R., Kim, J.K., Cushman, S.W., Cooney, G.J.*, et al.* (2002). Mechanism by which fatty acids inhibit insulin activation of insulin receptor substrate-1 (IRS-1)-associated phosphatidylinositol 3-kinase activity in muscle. J Biol Chem *277*, 50230-50236.
Yuan, A., Lin, C.Y., Chou, C.H., Shih, C.M., Chen, C.Y., Cheng, H.W., Chen, Y.F., Chen, J.J., Chen, J.H., Yang, P.C.*, et al.* (2011). Functional and Structural Characteristics of Tumor Angiogenesis in Lung Cancers Overexpressing Different VEGF Isoforms Assessed by DCE- and SSCE-MRI. PLoS One *6*, e16062.
Zanta, M.A., Belguise-Valladier, P., and Behr, J.P. (1999). Gene delivery: a single nuclear localization signal peptide is sufficient to carry DNA to the cell nucleus. Proc Natl Acad Sci U S A *96*, 91-96.
Zeng, X., Tamai, K., Doble, B., Li, S., Huang, H., Habas, R., Okamura, H., Woodgett, J., and He, X. (2005). A dual-kinase mechanism for Wnt co-receptor phosphorylation and activation. Nature *438*, 873-877.
Zhang, F., White, R.L., and Neufeld, K.L. (2000). Phosphorylation near nuclear localization signal regulates nuclear import of adenomatous polyposis coli protein. Proc Natl Acad Sci U S A *97*, 12577-12582.
Zhang, L., Jin, M., Margariti, A., Wang, G., Luo, Z., Zampetaki, A., Zeng, L., Ye, S., Zhu, J., and Xiao, Q. (2010). Sp1-dependent activation of HDAC7 is required for platelet-derived growth factor-BB-induced smooth muscle cell differentiation from stem cells. J Biol Chem *285*, 38463-38472.
Zhang, X., Milton, C.C., Humbert, P.O., and Harvey, K.F. (2009). Transcriptional output of the Salvador/warts/hippo pathway is controlled in distinct fashions in Drosophila melanogaster and mammalian cell lines. Cancer Res *69*, 6033-6041.
Zhao, B., Ye, X., Yu, J., Li, L., Li, W., Li, S., Lin, J.D., Wang, C.Y., Chinnaiyan, A.M., Lai, Z.C.*, et al.* (2008). TEAD mediates YAP-dependent gene induction and growth control. Genes Dev *22*, 1962-1971.
Zhong, Z., Wen, Z., and Darnell, J.E., Jr. (1994). Stat3: a STAT family member activated by tyrosine phosphorylation in response to epidermal growth factor and interleukin-6. Science *264*, 95-98.
Zhou, Y., Abidi, P., Kim, A., Chen, W., Huang, T.T., Kraemer, F.B., and Liu, J. (2007). Transcriptional activation of hepatic ACSL3 and ACSL5 by oncostatin m reduces hypertriglyceridemia through enhanced beta-oxidation. Arterioscler Thromb Vasc Biol *27*, 2198-2205.
Zhuang, Y., Kim, C.G., Bartelmez, S., Cheng, P., Groudine, M., and Weintraub, H. (1992). Helix-loop-helix transcription factors E12 and E47 are not essential for

skeletal or cardiac myogenesis, erythropoiesis, chondrogenesis, or neurogenesis. Proc Natl Acad Sci U S A *89*, 12132-12136.

CONTRIBUTION OF COLLABORATORS

This thesis is composed of some experiments that require the expertise of our collaborators. Without their inputs, this thesis would not have been possible. This section of the thesis is dedicated to acknowledge their contributions in depth. In chapter 2, Dr. Adamo and Dr. Tesson provided the pGL3-ACSL5 constructs that contained either a C- or T-allele. In chapter 3, Dr. Stephan Dugon contributed to the manuscript by performing yeast-two hybrid assays under the guidance of Dr. Patrick Burgon. Ms. Shelley Deeke contributed to this chapter with IRF2BP2 immunohistology of mouse embryo. Mr. Kuraitis and Mr. Ahmadi both contributed to this chapter by performing femoral artery ligation and transverse aortic restriction, respectively, under the guidance of Dr. Erik Suuronen. Finally, Dr. Chen provided scientific knowledge and invaluable critics for all manuscripts. I am very much in debt to the scientific contributions of all collaborators.

STATEMENT

I hereby declare myself, Allen Chun-Tien Teng, has faithfully performed all experiments, excluding those mentioned in the section of **CONTRIBUTION OF COLLABORATORS**, and has written all published manuscript and this thesis under the supervision of Dr. Alexandre F. R. Stewart and in accordance with the guidelines of the Department of Biochemistry, of the Faculty of Graduate and Postgraduate Studies, and of the University of Ottawa.